Title
Developmental genetic basis of stickleback evolved tooth gain

Author
Ellis, Nicholas

Publication Date
2016

Peer reviewed|Thesis/dissertation

Developmental genetic basis of stickleback evolved tooth gain

by

Nicholas Alexander Ellis

A dissertation submitted in partial satisfaction of the

requirements for the degree of

Doctor of Philosophy

in

Molecular and Cell Biology

in the

Graduate Division

of the

University of California, Berkeley

Committee in charge:

Professor Craig T. Miller, Chair
Professor Richard Harland
Professor Iswar Hariharan
Professor Marvalee Wake

Spring 2016

Developmental genetic basis of stickleback evolved tooth gain

Abstract

Developmental genetic basis of stickleback evolved tooth gain

by

Nicholas Alexander Ellis

Doctor of Philosophy in Molecular and Cell Biology

University of California, Berkeley

Professor Craig T. Miller, Chair

An abundance of morphological diversity is seen across nature yet we know little of the mechanistic underpinnings of these evolved changes. Developmental patterning is achieved by relatively few signaling pathways, which have been modified throughout evolution to give rise to the various forms we see today. Despite extensive studies characterizing mutant phenotypes under laboratory settings, we still know little about the developmental and genetic mechanisms underlying evolved phenotypes in nature. Outstanding questions include: How have developmental mechanisms been modified? When the same phenotype evolves, are the genetic bases the same or different? And in cases with continuously regenerating morphology, how are these phenotypes maintained over time and what signaling pathways play a role? In this dissertation I address these questions using the teeth of the threespine stickleback fish, *Gasterosteus aculeatus*, as a model.

Teeth have long served as a model system to study basic questions about vertebrate organogenesis, morphogenesis, and evolution. In most non-mammalian vertebrates, teeth regenerate throughout adult life. New model systems that undergo continuous tooth replacement are sorely needed to complement developmental studies of tooth formation in mice, which do not replace their teeth. Fish have evolved a tremendous amount of diversity in dental patterning in both their oral and pharyngeal dentitions, offering numerous opportunities to study how morphology develops, regenerates, and evolves in different lineages.

Threespine stickleback fish have emerged as a new system to study how morphology evolves, and provide a particularly powerful system to study the development and evolution of dental morphology. Sticklebacks have undergone an adaptive radiation, with oceanic marine populations repeatedly colonizing and rapidly adapting to freshwater lakes and creeks throughout the northern hemisphere. Colonization of freshwater environments is accompanied by a variety of changes to the head skeleton, many of which are likely adaptive for the major shift in diet from small zooplankton in the ocean to larger prey in freshwater. Natural variation in dental patterning exists between stickleback fish populations providing an opportunity to dissect the developmental genetic basis of tooth formation and replace-

ment. Marine and freshwater sticklebacks can be intercrossed and their F1 hybrids are fertile, allowing forward genetic mapping of genomic regions controlling evolved differences.

In chapter 1, I introduce the oral and pharyngeal dentition in sticklebacks and provide morphological, histological, and molecular evidence for homology of oral and pharyngeal teeth. Next, using a dense developmental time-course of lab-reared animals, the temporal and spatial sequence of early tooth formation for the ventral pharyngeal dentition is described. This sequence is highly stereotypical allowing the characterization of the first tooth replacement event and providing a guide for future phenotyping. Finally, the early sequence of tooth development is compared to that described in other fish, revealing that major changes to how dental morphology arises and regenerates have evolved across different fish lineages.

In chapter 2, I focus on how the variation in dental patterning manifests during development. Previous work had identified a freshwater population with increased tooth number arising late in development, however the mechanism of how teeth were gained over time remained elusive. Here, using a vital dye pulse-chase method, we showed increased tooth number results from an increased tooth replacement rate. We also identified a second freshwater population which has convergently evolved tooth gain allowing us to study whether the developmental and genetic bases underlying this phenotype are the same or different. Despite the similar evolved phenotype of more teeth and an accelerated adult replacement rate, the timing of tooth number divergence and the spatial patterns of newly formed teeth are different in the two freshwater populations, suggesting distinct developmental mechanisms underlie the evolved changes. Using genome-wide linkage mapping in marine-freshwater F2 genetic crosses, we found largely non-overlapping genomic regions controlling tooth patterning in the two high-toothed populations. This work represents one of the first demonstrations of distinct developmental genetic bases underlying evolved changes in morphology in vertebrates.

In chapter 3, I test the role of BMP signaling on stickleback tooth formation and replacement. Although distinct genomic regions underlying evolved tooth gain in two freshwater populations were identified, the reoccurrence of BMP pathway members (ex. *Bmp6*, *Msxe*, *Bmp7a*) appearing as candidates in loci underlying evolved tooth gain suggests the hypothesis that changes in different components of the BMP signaling pathway underlies convergent evolution of tooth gain. Using the small molecule BMP signaling inhibitor LDN-193189, we showed BMP signaling plays both positive and negative roles in tooth development and replacement. BMP knockdown results in failure to initiate late forming primary positions while premature replacement occurs at early, established tooth positions. Notably, this accelerated tooth replacement is independent of tooth shedding and may be a mechanism used to evolved gains in tooth number. Late in development at a stage after individual tooth positions can be tracked, BMP knockdown in marine fish increased the number of newly forming teeth, likely due to increased tooth replacement. Collectively these data suggest that during stickleback tooth formation and replacement, BMPs positively regulate tooth development while negatively regulating tooth replacement and suggest this pathway has been modified during freshwater adaptation to achieve evolved tooth gain.

In chapter 4, I provide a protocol demonstrating how to dissect and flat-mount the internal branchial skeleton. By mounting this complex three-dimensional skeleton into largely two-dimensions, one can easily phenotype a variety of internal traits including pharyngeal tooth patterning. This method is a fast and relatively inexpensive way to study variation of trophic traits and is also applicable to a wide variety of fish species. In sticklebacks, we have used this method to visualize and precisely measure skeletal morphology in genetic crosses to map genomic regions controlling craniofacial patterning.

Together this dissertation makes significant progress toward understanding the developmental genetic basis of evolved tooth gain in stickleback fish. These results have broad implications for understanding the repeatability of evolution, mechanisms of evolved gain traits, the process and signaling pathways of tooth replacement, and how signaling pathways can be modulated to produce morphological variation.

"The important thing is to not stop questioning. Curiosity has its own reason for existence. One cannot help but be in awe when he contemplates the mysteries of eternity, of life, of the marvelous structure of reality. It is enough if one tries merely to comprehend a little of this mystery each day."
-Albert Einstein

Acknowledgments

"Art is I; science is we" - Claude Bernard

I would like to express my sincere gratitude to my advisor Craig for providing continuous support both in and outside of the lab. I am a better scientist and writer having spent time with you. I look back on my time in the Miller lab fondly, though I'm still eagerly awaiting that pufferfish room. I would also like to extend my appreciation to each of my committee members; Richard Harland, Iswar Hariharan, and Marvalee Wake for their helpful suggestions along this journey.

I'd also like to thank Steven Vogler for first getting me seriously interested in Biology. David Olson, my first science mentor, for cultivating that initial excitement and teaching me how to think like a scientist (and do molecular biology). To Seth Blair for allowing me the opportunity to become a lab rat and for showing me PIs can still do science. And to Janet Branchaw for her continued support and guidance in my pursuit of higher education.

To the current and former Miller lab members, thanks for the helpful discussions and for keeping the lab lively. Thanks to Andrew for his countless helpful suggestions and lessons over the years, to Phil for always being excited about the science, to Priscilla for being my comrade in arms and a molecular biology guru, I will miss our morning talks, to James for his computational prowess and knowing how to do all the analyses I asked for in words, to Chris for his perspective and general geeking out over fish with me, and to Emily for teaching me R, UNIX, and that "less is more." May the Miller lab 'Atlas' exchange live on.

To our honorary Miller lab members Miles and Jim. Miles, thanks for your special flavor of humor and spot on graduation advice. Jim, thank you for computationally bailing me out on many occasions and for always lightening the mood.

To Nick Donde and Siegen McKellar, it has been a distinct pleasure training and watching you both grow into independent scientists. I have learned far more from you than you have from me.

To my in-laws, Bob and Diana Ziegler, thanks for your kind encouragement and tolerance of our moving across the country. To my parents, Chris and Tammy Ellis, who always ranked education highly. Thanks for reading me my favorite animal encyclopedia as a toddler, ultimately ensuring I'd end up as a Biologist, for always indulging my big ideas, and making me feel like I could accomplish anything. Thank you for always believing in me.

To my son Lincoln, thank you for teaching me what is important in life, for forcing a work life balance upon me that I failed to attain for years, for strategically shutting off my computer at the most comically inopportune times, and for always being happy to see me.

To my wife Alisha, thank you for your constant love and support through this arduous journey and still having a smile on your face; for helping label tubes, feed fish, listen to endless practice talks, and take an interest in my work. I couldn't have done this without you.

Nick Ellis
In Berkeley, 2016

Contents

Contents **iii**

List of Figures **v**

List of Tables **vii**

1 Early development and replacement of the stickleback pharyngeal dentition **1**
1.1 Abstract . . . 2
1.2 Introduction . . . 2
1.3 Materials and Methods . . . 4
1.4 Results . . . 5
1.5 Discussion . . . 14
1.6 Acknowledgments . . . 20
1.7 References . . . 20

2 Distinct developmental and genetic mechanisms underlie convergently evolved tooth gain in sticklebacks **26**
2.1 Abstract . . . 27
2.2 Introduction . . . 27
2.3 Materials and Methods . . . 29
2.4 Results . . . 32
2.5 Discussion . . . 47
2.6 Acknowledgments . . . 52
2.7 References . . . 53

3 Opposing roles for BMP signaling in tooth formation and replacement in sticklebacks **59**
3.1 Abstract . . . 60
3.2 Introduction . . . 60
3.3 Materials and Methods . . . 62
3.4 Results/Discussion . . . 65
3.5 Acknowledgments . . . 78

3.6 References 79

4 Appendix: Dissection and flat-mounting of the stickleback branchial skeleton 85

4.1 Abstract 86
4.2 Introduction 86
4.3 Protocol 88
4.4 Results 94
4.5 Discussion 95
4.6 Acknowledgments 96
4.7 References 96

List of Figures

1.1 **Stickleback oral and pharyngeal jaws.** . . . 6
1.2 **Oral and pharyngeal jaw morphology.** . . . 7
1.3 **Oral and pharyngeal teeth are morphologically indistinguishable.** . . . 8
1.4 **Oral and pharyngeal teeth have similar gene expression patterns during development.** . . . 9
1.5 ***Pitx2* and *Bmp6* tooth expression in section and whole mount.** . . . 10
1.6 **Developmental time course of pharyngeal tooth formation.** . . . 11
1.7 **Dorsal pharyngeal tooth plates develop on pharyngobranchial cartilage templates.** . . . 12
1.8 **Sequence of pharyngeal tooth development.** . . . 13
1.9 **Histological sections of tooth replacement.** . . . 15
1.10 **Replacement teeth form deep but with invaginated epithelia that is continuous with lumenal pharyngeal epithelium.** . . . 16

2.1 **Description and location of independent stickleback populations.** . . . 33
2.2 **Two freshwater stickleback populations exhibit evolved tooth gain.** . . . 34
2.3 **Tooth number for dorsal tooth plate 1, but not 2, differs between populations.** . . . 35
2.4 **In both freshwater populations, evolved tooth gain manifests late in development.** . . . 36
2.5 **Previously published PAXB and RABS data points.** . . . 37
2.6 **Tooth germ number, but not area, differs between marine and freshwater fish late in development.** . . . 38
2.7 **Adult marine and freshwater teeth vary in width, but not height.** . . . 39
2.8 **Pulse-chase reveals that both freshwater populations have elevated rates of new tooth formation.** . . . 40
2.9 **Early pulse-chase reveals tooth gain rates are relatively fixed early in marine and freshwater sticklebacks.** . . . 41
2.10 **Distinct spatial patterns of new teeth in two high-toothed freshwater populations.** . . . 42
2.11 **Largely distinct genetic bases underlie evolved tooth gain in two high-toothed freshwater populations.** . . . 44

2.12 **Correlation of tooth number, tooth plate area, and intertooth spacing phenotypes in F2 cross.** . . . 45
2.13 **Genome wide QTL scans for tooth number, area, and intertooth spacing.** 46
2.14 **Genome wide QTL scans for dorsal pharyngeal tooth number.** . . . 47
2.15 **Model for convergent evolution of tooth gain in two freshwater populations.** . . . 49

3.1 **BMP knockdown reduces pharyngeal tooth number in marine and freshwater populations.** . . . 66
3.2 **BMP signaling is required for proper jaw and hyoid dermal skeletal development.** . . . 67
3.3 ***Smad5* mutant fish exhibit reduced tooth number.** . . . 69
3.4 **Principal component analysis for LDN RNAseq.** . . . 70
3.5 **Expression of *Ids*, *Msxs*, and BMP ligands and receptors.** . . . 71
3.6 **BMP knockdown results in up-regulation of tooth development markers.** 73
3.7 **BMP knockdown inhibits formation of primary positions, but stimulates early tooth replacement.** . . . 74
3.8 **Examples of mis-patterned LDN-193189 treated tooth plates.** . . . 75
3.9 **BMP knockdown induces early replacements independent of tooth shedding at the first tooth position.** . . . 76
3.10 **Effects on tooth number and replacement are dose dependent with replacement events independent of tooth shedding.** . . . 77
3.11 **Low level BMP knockdown late in development increases replacement in marine sticklebacks.** . . . 78

4.1 **Stickleback head skeletal morphology.** . . . 89
4.2 **Stickleback branchial skeleton dissection.** . . . 90
4.3 **Flat mounting the branchial skeleton.** . . . 93
4.4 **Representative stickleback branchial skeleton.** . . . 95

List of Tables

2.1 **Tooth cycling dynamics.** 41
2.2 **Spatial location of teeth by population.** 42
2.3 **Summary of CERC tooth patterning QTL.** 43
2.4 **CERC QTL interval details.** 48

3.1 **LDN treatment causes reduced tooth number in both marine and freshwater populations.** 68
3.2 **Mapped reads for RNAseq of individual DMSO control and LDN treated fish.** 72
3.3 **Increasing LDN dosage decreases tooth number without affecting size.** 72

Chapter 1

Early development and replacement of the stickleback pharyngeal dentition

> "If the ichthyologist have reason to complain of the monotony which unavoidably pervades his descriptions of the external characters of the objects of his study, the anatomist in treating of the dental system of fishes, finds, on the contrary, his difficulty in obtaining the command of language sufficiently varied to pourtray the singular diversity and beauty, and the interesting physiological relations which are manifested in that part of their organization. The teeth of fishes, in fact, in whatever relation they are considered, whether in regard to number, form, substance, structure, situation, or mode of attachment, offer more various and striking modifications than do those of any other class of animals."
> -Richard Owen, *Odontography*

The following chapter was originally published as an article: *Journal of Morphology* 2016

Nicholas A. Ellis, Nikunj N. Donde and Craig T. Miller

Department of Molecular and Cell Biology, University of California-Berkeley, Berkeley CA, 94720, USA

1.1 Abstract

Teeth have long served as a model system to study basic questions about vertebrate organogenesis, morphogenesis, and evolution. In non-mammalian vertebrates, teeth typically regenerate throughout adult life. Fish have evolved a tremendous diversity in dental patterning in both their oral and pharyngeal dentitions, offering numerous opportunities to study how morphology develops, regenerates, and evolves in different lineages. Threespine stickleback fish (*Gasterosteus aculeatus*) have emerged as a new system to study how morphology evolves, and provide a particularly powerful system to study the development and evolution of dental morphology. Here we describe the oral and pharyngeal dentitions of stickleback fish, providing additional morphological, histological, and molecular evidence for homology of oral and pharyngeal teeth. Focusing on the ventral pharyngeal dentition in a dense developmental time course of lab-reared fish, we describe the temporal and spatial consensus sequence of early tooth formation. Early in development, this sequence is highly stereotypical and consists of seventeen primary teeth forming the early tooth field, followed by the first tooth replacement event. Comparing this detailed morphological and ontogenetic sequence to that described in other fish reveals that major changes have evolved to how dental morphology arises and regenerates across different fish lineages.

Keywords: Teeth, Tooth patterning, Polyphyodonty, Regeneration, Stickleback

1.2 Introduction

Teeth are a classic model system for understanding vertebrate development and evolution. Mice, a monophyodont (no tooth replacement) rodent, have served as the primary model for understanding tooth formation (Jernvall and Thesleff, 2000; Tucker and Sharpe, 2004; Bei, 2009; Tummers and Thesleff, 2009; OConnell et al., 2012; Lan et al., 2014). Complementary systems are needed to understand tooth replacement in polyphyodonts (vertebrates with life-long tooth replacement, the primitive jawed vertebrate condition; Reif, 1982; Fraser et al., 2010; Brazeau and Friedman, 2014). Dental patterning has been studied in a variety of polyphyodonts in the context of comparative morphology, development, ecology, and evolution for decades (e.g. Owen, 1845; Osborn, 1971; Wake, 1976). Polyphyodonty has been variously modified in different extant gnathostome lineages and recent work in snakes (Buchtov et al., 2008; Handrigan and Richman, 2010; Gaete and Tucker, 2013), geckos (Handrigan et al., 2010), alligators (Wu et al., 2013), and other reptiles (Juuri et al., 2013) has begun to investigate the cellular and molecular mechanisms of tooth replacement. Fish offer a powerful system to study these mechanisms due to high numbers of offspring, external fertilization, rapid development, and rich diversity in tooth patterning (Evans and Deubler, 1955; Berkovitz, 1977; Wakita et al., 1977; Motta, 1984; Nakajima, 1987; Trapani and Schaefer, 2001; Bemis et al., 2005).

Teeth in fish can be located in the oral jaw (oral teeth) and/or internally in the branchial

skeleton (pharyngeal teeth). The branchial skeleton, comprised of posterior segmental homologs of the mandibular and hyoid skeletons, is located in the throat of a fish and functions as an interface between fish and their food (Sibbing, 1991). Prey mastication and manipulation is typically performed by the pharyngeal jaw while oral teeth are primarily used to capture prey (Lauder, 1983; Hulsey et al., 2005; Wainwright, 2006). Oral and pharyngeal teeth have long been thought to be developmentally homologous (Owen, 1845), and have recently been shown to form via similar mechanisms involving similar gene expression patterns (Fraser et al., 2009). Furthermore, similar signaling pathways control tooth development in both fish and mammals (Fraser et al., 2013). For example, genes encoding the Ectodysplasin ligand and receptor, *Eda* and *Edar*, are required for oral and pharyngeal teeth in fish (Harris et al., 2008; Atukorala et al., 2011), and for oral teeth in mice and humans (Mikkola and Thesleff, 2003). While mammalian teeth are restricted to a single row along the dental arcade (Mikkola, 2009; Zhang et al., 2009), in non-mammalian vertebrates the tooth field is often much larger and contains multiple rows of teeth.

Numerous fish species have been used to study tooth patterning and replacement including zebrafish (Huysseune and Thesleff, 2004; Huysseune, 2006), cichlids (Huysseune, 1983; Fraser et al., 2013), trout (Fraser, Berkovitz, et al., 2006; Smith, Fraser, et al., 2009), medaka (Abduweli et al., 2014; Mantoku et al., 2015), and many others (Trapani and Schaefer, 2001; Smith, Okabe, et al., 2009; Moriyama et al., 2010; Fraser et al., 2012; Vandenplas et al., 2014; Underwood et al., 2015). These studies have uncovered differences in the location of tooth fields, the arrangement and number of teeth in tooth families, and the positioning and modes of tooth replacement. The spatiotemporal pattern of early tooth positioning within developing tooth fields has also been studied in many of these models (Huysseune et al., 1998; Van der heyden and Huysseune, 2000; Debiais-Thibaud et al., 2007; Stock, 2007; Le Pabic et al., 2009; Atukorala and Franz-Odendaal, 2014) with major differences found in the sequence and pattern of early tooth formation. Collectively, these studies highlight the diversity of tooth patterning and replacement mechanisms among teleosts.

The threespine stickleback fish, *Gasterosteus aculeatus*, offers an excellent model system to study the developmental and genetic basis of tooth development and replacement. Sticklebacks have undergone an adaptive radiation, with oceanic marine populations repeatedly colonizing and rapidly adapting to freshwater lakes and creeks throughout the northern hemisphere (Bell and Foster, 1994). A suite of morphological changes has evolved including a substantial increase in pharyngeal tooth number in some freshwater populations (Cleves et al., 2014; Miller et al., 2014; Ellis et al., 2015), likely adaptive to a shift in diet towards larger prey (Hynes, 1950; Lemmetyinen and Mankki, 1975). Evolved tooth gain arises late during larval development in two freshwater populations, and is associated with an increased tooth replacement rate in both populations (Cleves et al., 2014; Ellis et al., 2015). The natural variation present in dental patterning and replacement rates provides an entry point to study the developmental genetic basis of tooth regeneration. However, a detailed understanding of the early sequence of tooth formation and replacement is required to interpret the evolved changes arising later in development. Here we present a careful description of early stickleback pharyngeal tooth development and replacement to test three hypotheses

about tooth formation and replacement. First, we find morphological and molecular support for the hypothesis of homology of oral and pharyngeal teeth. Second, focusing on the ventral pharyngeal tooth plate, we find support for the hypothesis that the early spatiotemporal pattern of tooth formation and replacement is stereotypical. Third, comparing this early sequence of tooth formation to that described for other species of fish supports the hypothesis that several changes in tooth field patterning have evolved in different fish lineages.

1.3 Materials and Methods

Stickleback husbandry

Threespine stickleback fish, *Gasterosteus aculeatus* (Linnaeus, 1758) were all lab-reared in brackish water (3.5 g/l Instant Ocean salt, 0.217 ml/l 10% sodium bicarbonate) at 18°C in 110 l aquaria. All freshwater fish were from the Paxton benthic population (British Columbia) (Schluter and McPhail, 1992) and marine fish were from either the Rabbit Slough (Alaska) or Little Campbell River (British Columbia) populations. Fish were fed live Artemia as fry, Artemia and frozen Daphnia as juveniles, and frozen bloodworms and Mysis shrimp as adults. All experiments were performed with approval of the Institutional Animal Care and Use Committee of the University of California-Berkeley (protocol # R330).

Skeletal staining and visualization

For skeletal staining, fish were fixed in 10% neutral buffered formalin overnight at 4°C, and washed in water. Juveniles and adults were stained in 0.008% Alizarin Red S in 1% KOH for 24 h. Early time course fish (8-23 days post fertilization) were stained with an acid-free Alizarin Red S and Alcian Blue two color protocol as described (Walker and Kimmel, 2007). Fish were rinsed in water and cleared in 50% glycerol, 0.25% KOH. Dissection and mounting was performed as previously described (Miller et al., 2014; Ellis and Miller, 2016). Bright-field images were taken on a Leica DM2500 except Fig. 1.1B which was taken on a Leica M165 stereomicroscope. Fluorescent images were taken on a Leica M165 using a rhodamine filter.

To determine tooth positioning and the order of eruption, bilateral tooth plates in 53 Alizarin and Alcian stained (see above) freshwater fish ranging from 8-23 days post fertilization (dpf) were scored. To generate the consensus pattern, each tooth position was scored in individual fish. If at least 50% of the fish had the position filled, it was included for that time point. For two later time points (16 and 18dpf) with more variable standard lengths, fish ± one day were also considered to determine the consensus.

Histology

Tissue was processed and sectioned as previously described (Ellis et al., 2015). Briefly, samples were fixed overnight in 10% neutral buffered formalin (NBF) at 4°C and decalcified using Humasons formic acid A (Humason, 1962) at a working concentration of 6% formic acid and 2.5% NBF (~1% formaldehyde). Histoclear (National Diagnostics) was used in the place of

xylene as a clearing agent. Tissue was embedded in Paraplast (Fisher), sectioned with a Microm HM340E (Thermo Scientific), baked overnight at 50°C, stained with hematoxylin and eosin, and cover-slipped with Permount (Fisher). The number of samples was: n=5 26 dpf marine specimens to image and compare oral and pharyngeal teeth; n=14 freshwater (5 15 millimeters standard length (mm), 5 25 mm, and 4 40 mm) and n=15 marine (5 15 mm, 6 25 mm, and 4 40 mm) specimens to characterize tooth replacement.

In situ hybridization

In situ hybridization was performed essentially as described (Xu et al., 1994; Fraser et al., 2008) with the following exceptions: samples were fixed overnight in 4% paraformaldehyde in 1X PBS with 1% DMSO at 4°C, digested with 20 μg/mL proteinase K for 30 minutes at room temperature, and blocked with 20% sheep serum, 2% Boehringer blocking reagent in maleic acid buffer with Tween-20. For sections, whole-mount in situs were embedded in gelatin-albumin cross-linked with 1.75% glutaraldehyde and sectioned at 40 μm on a Pelco 101 Vibratome Series 1000. Pitx2 and Bmp6 riboprobes have been published (Cleves et al., 2014). For each probe, at least four fish were analyzed and representative results presented.

1.4 Results

Location and homology of teeth in the threespine stickleback

Two sets of jaws are present in threespine stickleback fish, one oral jaw and another at the posterior of the branchial skeleton, the pharyngeal jaw (Fig. 1.1A, B, Fig. 1.2A) (Swinnerton, 1902; Anker, 1974). In the oral jaw, teeth are restricted to the premaxilla (upper jaw, Fig. 1.2D) and the dentary (lower jaw, Fig 1.2E). No teeth are present on the maxilla early in development (Fig 1.2H) or late (Fig. 1.1A). Pharyngeal teeth are restricted ventrally to the fifth ceratobranchial (Fig. 1.2C), hereafter referred to as the ventral tooth plate (VTP), and dorsally to the 2nd and fused 3rd/4th pharyngobranchials (Fig. 1.2B), hereafter referred to as dorsal tooth plate 1 (DTP1) and dorsal tooth plate 2 (DTP2) respectively. These tooth fields are specified during embryonic development, and then teeth are added continuously from early larval pre-hatching stages throughout adult stages (compare Fig. 1.2F to 1.2B, 1.2G to 1.2C, and 1.2H to 1.2D,E).

To test whether pharyngeal and oral teeth have similar cellular morphologies, we compared histological sections through both sets of jaws. Detailed comparisons of sections revealed pharyngeal and oral teeth are morphologically similar across the ventral tooth plate (Fig. 1.3A-C), dorsal tooth plate (Fig 1.3D), dentary (Fig. 1.3E-F), and premaxilla (Fig. 1.3G-J) with each tooth mostly embedded in a mucosal layer and consisting of an inner dental pulp containing odontoblasts, a mineralized dentine cone, and an enameloid cap covering the tip (apparent in whole mount as yellow tinted tips in Fig. 1.2B-E). In section, pharyngeal and oral teeth appear morphologically indistinguishable.

To test the hypothesis that similar gene expression patterns occur during stickleback pharyngeal and oral tooth development, we performed in situ hybridization with two known

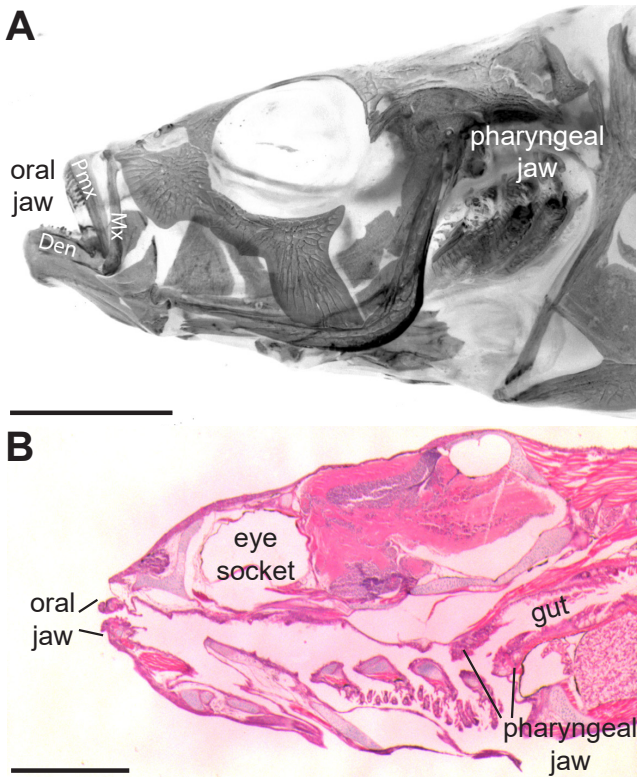

Figure 1.1: **Stickleback oral and pharyngeal jaws.**
(A) Adult 6-month-old freshwater stickleback head (anterior to the left) stained with Alizarin red in whole-mount, imaged under fluorescence (color inverted) after removal of the opercle and subopercle. (B) Hematoxylin and eosin 6 μm sagittal section of 26 days post fertilization marine stickleback. Two sets of toothed jaws are present, the oral jaw in the mouth and the pharyngeal jaw at the back of the branchial skeleton, anterior to the gut. Mx = maxilla, Pmx = premaxilla, Den = dentary bone. Scale bars = 5 mm (A) and 500 μm (B).

markers of tooth development. Pitx2, a marker of the inner and outer dental epithelium (Fraser et al., 2004, 2008; Fraser, Graham, et al., 2006), is expressed in both domains in all developing pharyngeal (Fig. 1.4A,C, Fig. 1.5A, B, B′), and oral teeth (Fig. 1.4E, Fig. 1.5A′, A″, B″). Bmp6, a marker dynamically expressed in both the inner dental epithelium and odontogenic mesenchyme of early developing tooth germs, but restricted to the dental mesenchyme in later stage tooth germs (Cleves et al., 2014), is also expressed in a similar pattern across all teeth (Fig. 1.4B, D, F, Fig. 1.5C, C′, D, D′). Thus, as was found in trout (Fraser et al., 2004) and cichlids (Fraser et al., 2009), similar gene expression patterns are seen in developing stickleback oral and pharyngeal teeth.

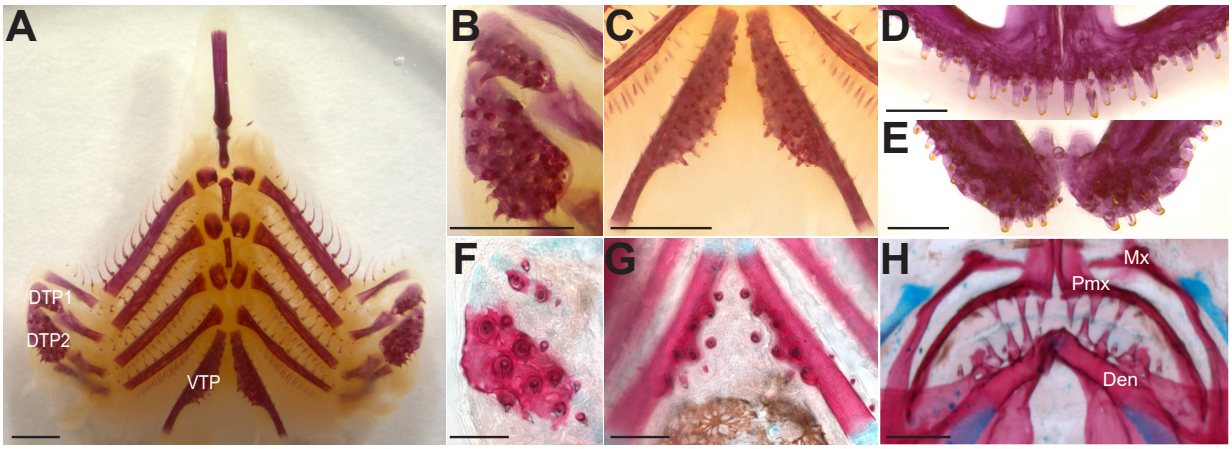

Figure 1.2: **Oral and pharyngeal jaw morphology.**
(A-E) Alizarin red stained, flat-mounted branchial skeleton (A-C) and oral jaw (D-E) from a 6-month-old freshwater adult stickleback. (B-C) Magnified view of left dorsal pharyngeal tooth plate 1 and 2 (B) and the ventral pharyngeal tooth plates (C). (D) Premaxilla (upper or dorsal oral jaw) dentition. (E) Dentary (lower or ventral oral jaw) dentition. (F-H) Tooth plates from Alizarin red and Alcian blue stained 20 days post fertilization freshwater larval stickleback. (F) Left dorsal pharyngeal tooth plate 1 and 2. (G) Ventral pharyngeal tooth plates. (H) Oral jaw containing both premaxillary and dentary dentition. DTP1= dorsal tooth plate 1, DTP2= dorsal tooth plate 2, VTP= ventral tooth plate, Mx= maxilla, Pmx=premaxilla, Den= dentary bone. Scale bars = 1 mm (A-C), = 500 μm (D-E), and 100 μm (F-H).

Spatial and temporal development of pharyngeal teeth

Tooth development begins prior to hatching with a pioneer tooth germ specified on VTP and DTP2 by 6 days post fertilization (dpf). Upon hatching at 8 dpf, both of these teeth are calcified and are flanked by two developing tooth germs (Fig. 1.6A, B). At 10 dpf, the first developing DTP1 tooth germ is visible and medial positions are added to both VTP and DTP2 (Fig. 1.6C, D). By 12 dpf, the first DTP1 tooth is calcified and individual teeth on VTP and DTP2 further ossify around the base of the tooth, forming the tooth plate (Fig. 1.6E,F). Both DTPs form juxtaposed and immediately ventral to the pharyngobranchial cartilages (Fig. 1.7A-B, white arrowhead). In contrast, VTP teeth form posterior and medial to chondrocytes of the fifth ceratobranchial (Fig. 1.7B). By 18 dpf, many teeth are calcified and the underlying tooth plate has formed by fusing the extended ossification around the base of teeth together (Fig. 1.6G, H). Notably, the DTP2 tooth plate extends medially past the field of developing teeth (Fig. 1.6H).

To test the hypothesis that the early sequence of tooth formation is hard-wired and stereotypical during early development, we scored each tooth position across a dense developmental time course of freshwater fish. Each position was ordered numerically by when a

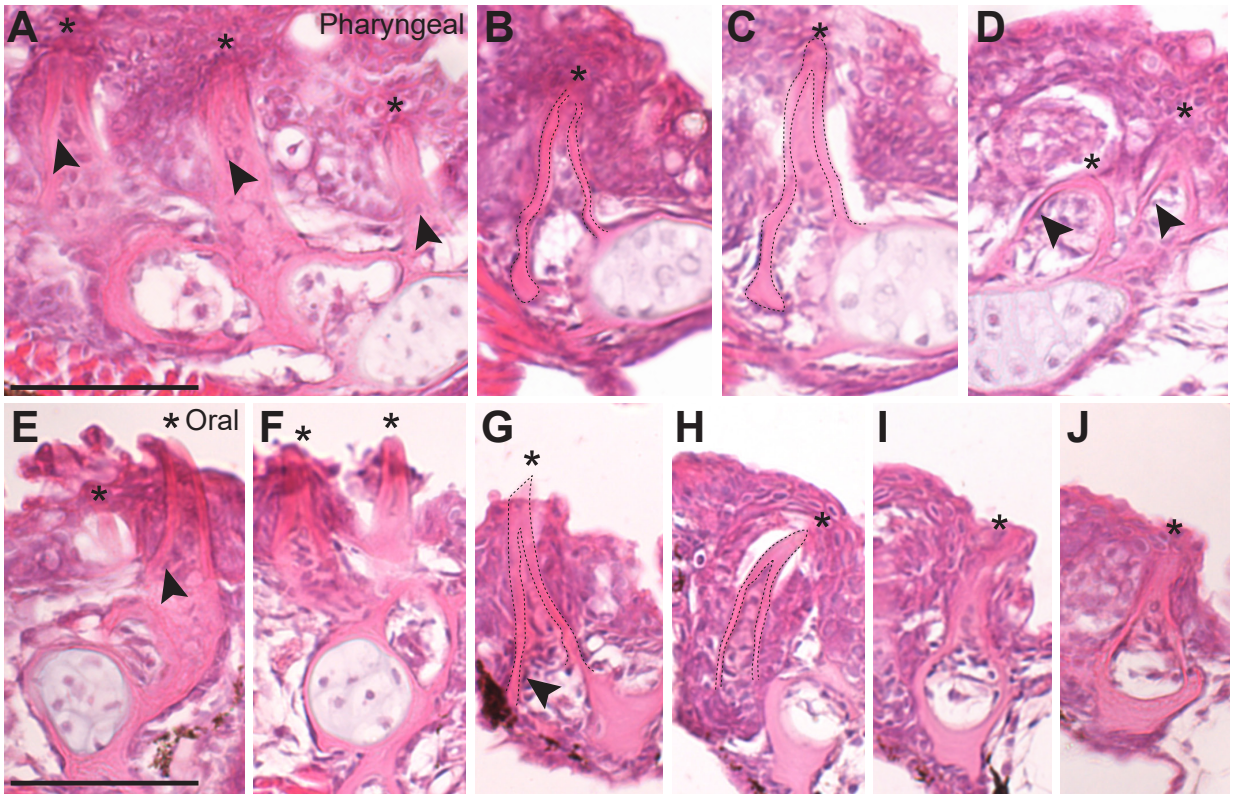

Figure 1.3: **Oral and pharyngeal teeth are morphologically indistinguishable.** Hematoxylin and eosin stained 6 μm sagittal sections of pharyngeal (A-D) and oral (E-J) teeth on the ventral pharyngeal tooth plate (A-C), dorsal pharyngeal tooth plate 1 (D), dentary (E-F) and premaxilla (G-J). Asterisks mark the tips of teeth, all of which are unicuspid cones (dashed lines in B,C and G,H). Cells in the pulp cavity likely include presumptive odontoblasts (arrowheads). All sections are from a 26 days post fertilization marine fish. Scale bars = 50 μm.

tooth typically arises in that position and scored as absent, developing germ (present, but un-calcified), calcified, or ankylosed (attached to the tooth plate). The pioneer tooth on each tooth plate was numbered as one. We generated a diagram summarizing the consensus sequence of tooth formation, with teeth shown as circles with colors ranging from dark red to light yellow correspond to the day the individual tooth typically calcifies. For example, the pioneer tooth on VTP and DTP2 calcified at 8 dpf and is colored dark red while the DTP1 pioneer tooth did not calcify until 12 dpf and is colored lighter red (Fig. 1.8A).

The order of teeth developing on the tooth plate was highly stereotypical early and became more variable with later positions. Focusing on the VTP, the order of tooth formation and ankylosing to the tooth plate was invariant through position 7. However, here position 6 arose and calcified before position 7, but position 7 ankylosed to the tooth plate first, sug-

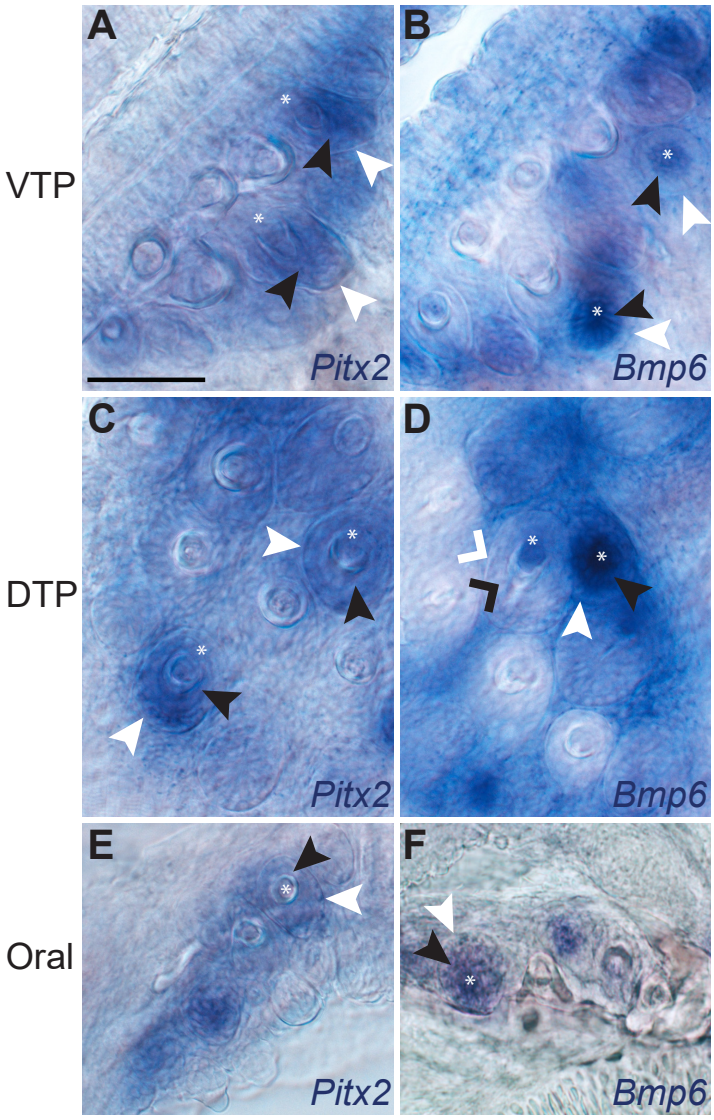

Figure 1.4: **Oral and pharyngeal teeth have similar gene expression patterns during development.**
Whole-mount in situ hybridization of *Pitx2* (A,C,E) and *Bmp6* (B,D,F) expression in the ventral pharyngeal tooth plate (VTP) (A,B), dorsal pharyngeal tooth plate (DTP) (C,D), and in the oral jaw (E,F) in 15 day post fertilization freshwater larvae. *Pitx2* expression is detected in the inner and outer dental epithelium and not in dental mesenchyme. *Bmp6* is detected in the inner (but not outer) dental epithelium and condensing dental mesenchyme in early tooth germs. After calcification begins, *Bmp6* expression is only detected in dental mesenchyme (see panel D). Expression of both genes is detected in similar patterns in developing oral and pharyngeal tooth germs. Inner dental epithelium = black arrowheads (black caret on late stage), outer dental epithelium = white arrowheads (white caret on late stage), dental mesenchyme = black caret. Also see Fig. 1.5. Scale bar = 50 μm.

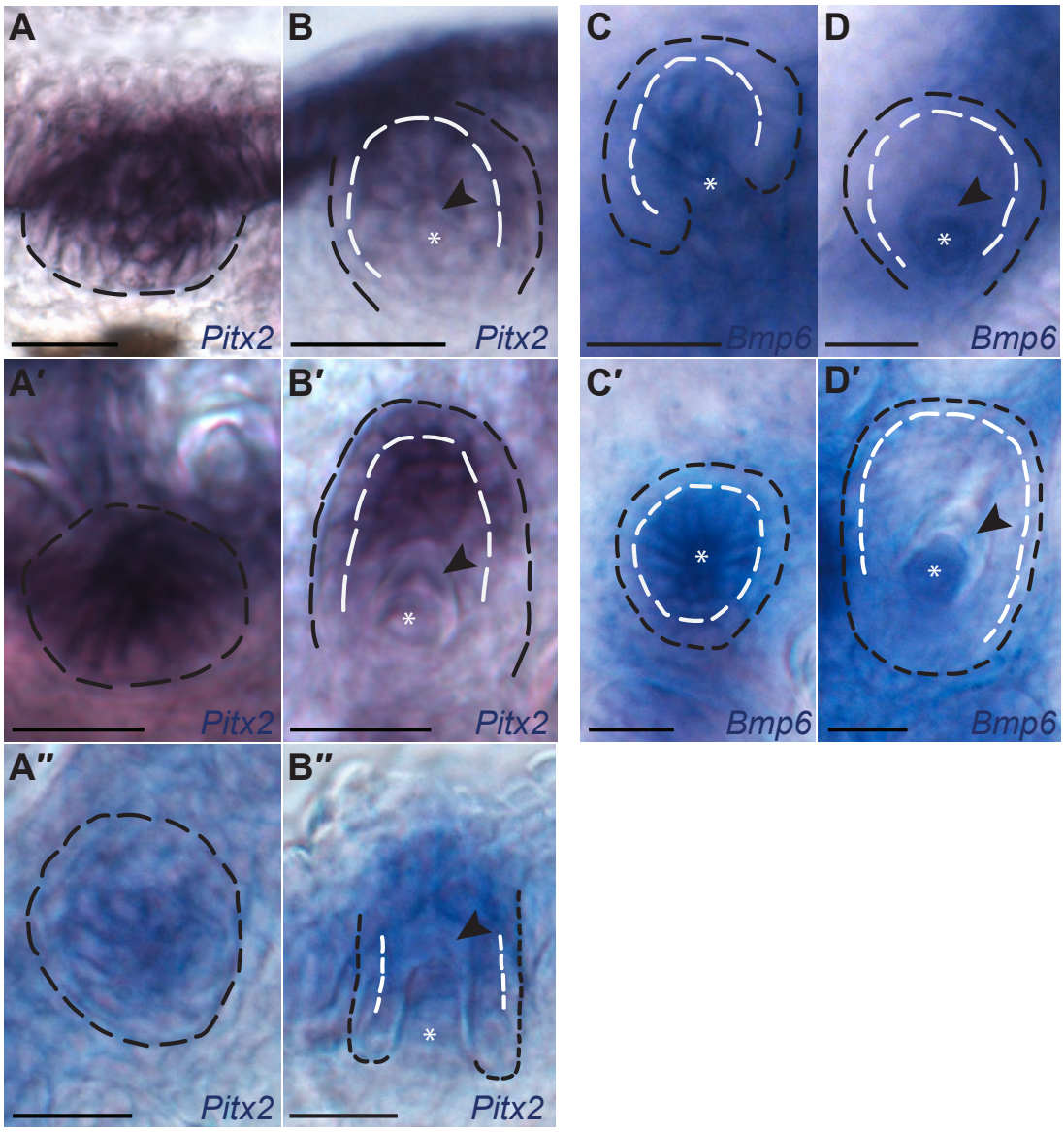

Figure 1.5: ***Pitx2* and *Bmp6* tooth expression in section and whole mount.** In situ hybridization for *Pitx2* (A-A″, B-B″) and *Bmp6* (C, C′, D, D′) in section (A-D) and whole mount (A′-D′, A″, B″). Tooth developmental stages are vertically matched for early germs (A, A′, C, C′) and late germs (B, B′, D, D′) for pharyngeal (A-D, A′-D′) and oral (A″, B″) teeth. *Pitx2* expression is detected in the dental epithelium (A-B, A′-B′, A″-B″) while *Bmp6* expression is detected in the inner dental epithelium and mesenchyme early (C, C′), and appears restricted to the mesenchyme only late (D, D′). The black dotted line outlines the developing tooth germ while the white dotted line separates the inner and outer dental epithelium (when discernable). Black arrowheads denote mineralized teeth and white asterisks denote mesenchyme. Scale bar = 15 μm.

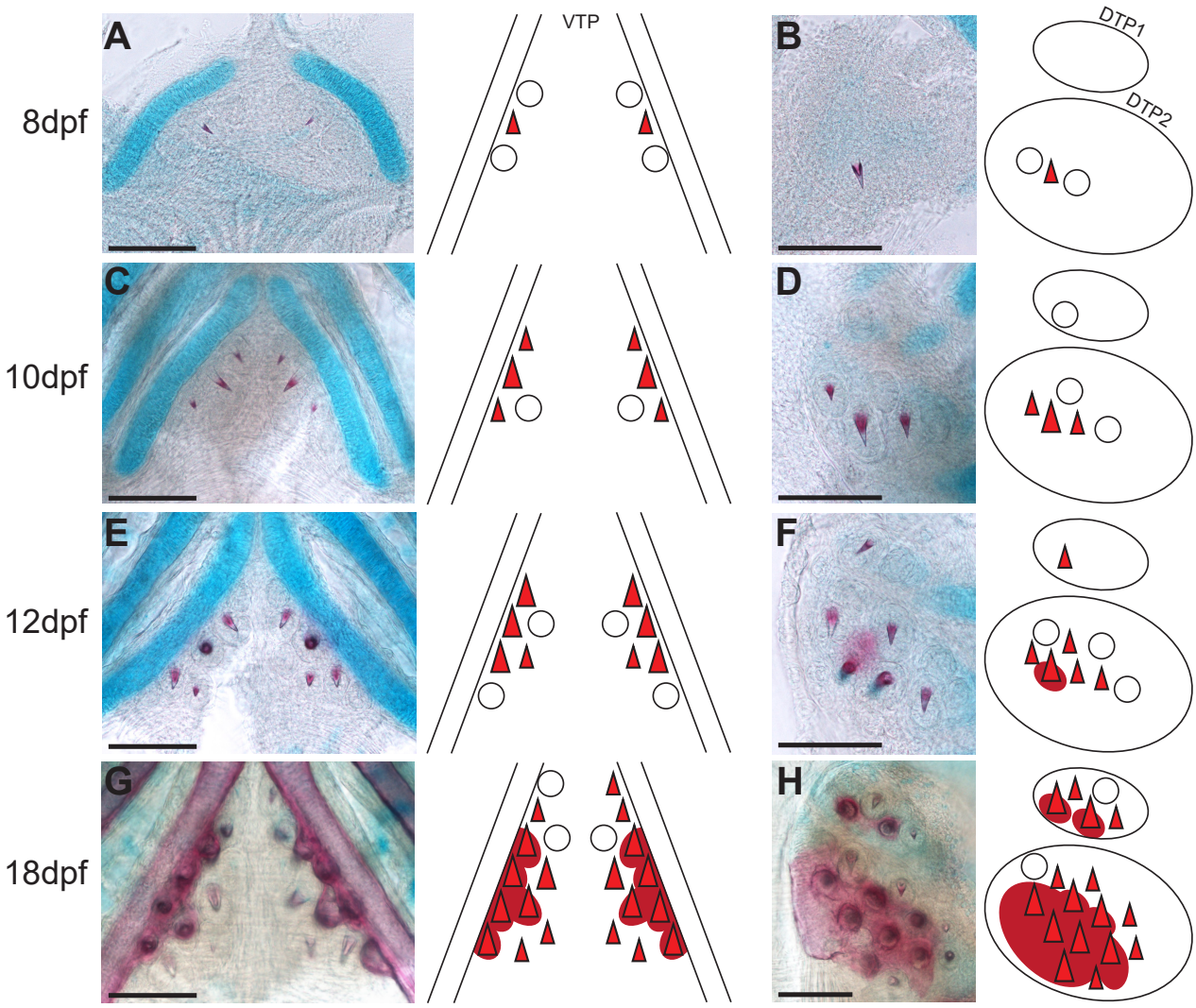

Figure 1.6: **Developmental time course of pharyngeal tooth formation.** In each panel, bilateral ventral pharyngeal tooth plates (A, C, E, G) or unilateral dorsal pharyngeal tooth plates 1 and 2 (B, D, F, H) of freshwater larvae are shown on the left, and a diagram depicting the tooth positions at each stage on the right. In all panels, anterior is towards the top. (A, B) 8 days post fertilization (dpf), (C, D) 10 dpf, (E, F) 12 dpf, and (G, H) 18 dpf tooth plates stained with Alizarin red and Alcian blue to label bone and cartilage, respectively. Open circles depict developing, but un-calcified tooth germs. Red triangles depict calcified, developing teeth and dark red circles beneath depict ossification of the tooth plate. Scale bars = 100 μm.

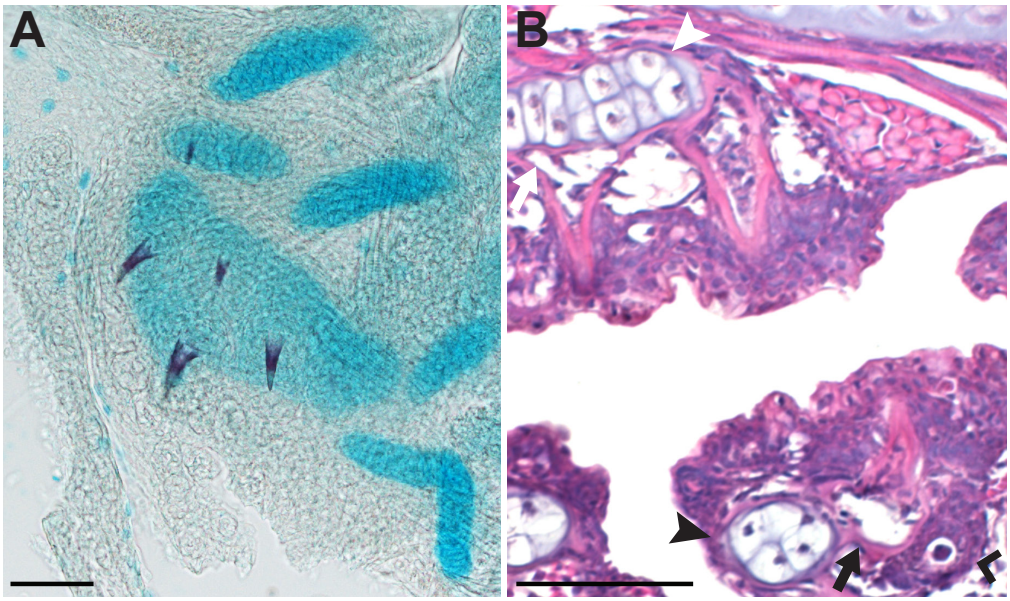

Figure 1.7: **Dorsal pharyngeal tooth plates develop on pharyngobranchial cartilage templates.**
(A) Alizarin red (bone) and Alcian blue (cartilage) stained 11 days post fertilization (dpf) marine dorsal pharyngeal tooth plates. The pharyngobranchial cartilages chondrify before dorsal pharyngeal teeth form adjacently. (B) Transverse H&E sections of 20 dpf marine dorsal and ventral pharyngeal tooth plates. The dorsal pharyngeal tooth plate contains chondrocytes (white arrowhead) and teeth ossify directly on the thin layer of perichondral bone surrounding them (white arrow). The fifth ceratobranchial contains chondrocytes (black arrowhead), but the ventral pharyngeal tooth plate does not (black arrow), instead forming from subsequent ossification ventral to individual teeth. Note the medial tooth germ not surrounded by bone (black caret). Scale bars = 50 μm.

gesting the sequences of tooth calcification and ankylosing to the tooth plate are different. Also at this stage, around 12 dpf, symmetry broke down between the left and right tooth plates where each side occasionally had a different number of calcified teeth. After 12 dpf and after position 7, the order of teeth arising had more variation. However, by scoring an additional 35 fish at time points between 13 and 23 dpf, a consensus emerged (Figure. 1.8B). For example, position 10 generally formed before position 11, but this was not always the case and the sequence of later positions was even more variable. Qualitatively, an early marine time course appears similar in patterning through 20dpf (pers. obs.)

Pharyngeal tooth replacement in sticklebacks
To examine the histological basis of tooth replacement, we cut serial sections through developing tooth plates and focused on the VTP. We used four histological criteria to distinguish

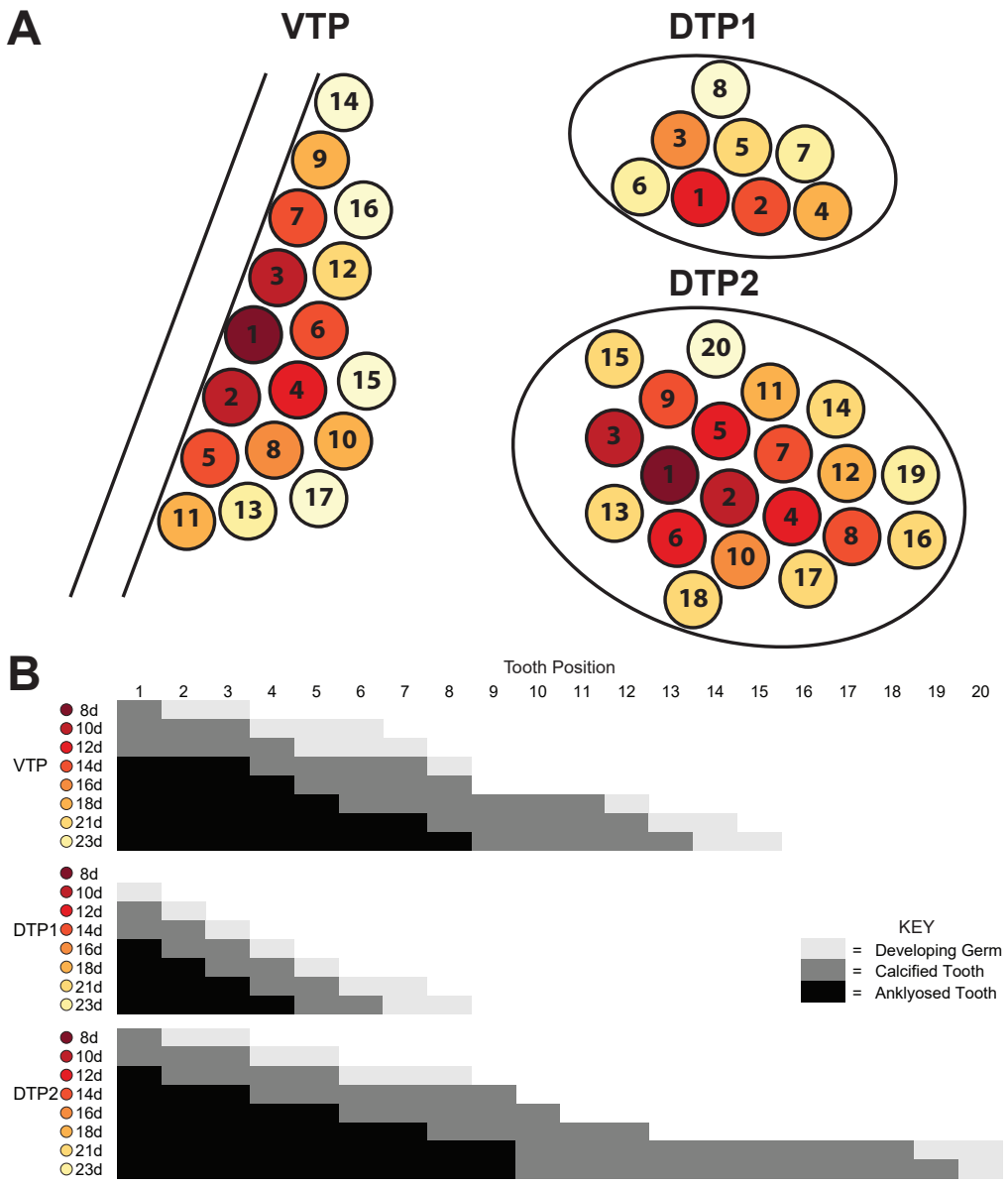

Figure 1.8: **Sequence of pharyngeal tooth development.**
(A) Unilateral (left side) tooth plate diagrams following the flat-mounted orientation from Fig. 2A. Each circle indicates the position where a tooth will form and each number corresponds to the order in which that position typically arises on each tooth plate. The color scheme follows the consensus sequence (B) and is color-coded dark red to light yellow for each day of development. Circles are colored according to the day they typically first ossify. (B) Consensus sequence of the number of teeth present across early development. Each position is scored as no tooth (white), developing germ (light gray), calcified tooth (dark gray), and ankylosed tooth (black) for each day. Note that the VTP diagram is a dorsal view and the DTP diagrams are a ventral view, as the tooth plates appear in flat-mounts (as in Figures 1.2 and 1.6).

primary from replacement teeth. First, replacement teeth appear at the base of an existing tooth, and asymmetrically erode bone away from the base of the primary tooth they are replacing (Wakita et al., 1977). Second, primary teeth form superficially, near the buccal cavity, while replacement teeth form deeper in the tooth plate tissue. Third, primary teeth form extraosseously (outside of bone; Trapani and Schaefer, 2001), while replacement teeth form intraosseously in sticklebacks (Huysseune and Witten, 2006). Fourth, the epithelium of replacement teeth appears locally connected to the epithelium of the tooth they are replacing, and extends deep into the tooth plate tissue (Huysseune and Thesleff, 2004; Huysseune, 2006).

Using these criteria, seventeen primary teeth typically form on the tooth plate before the first replacement tooth forms laterally to position one (Fig. 1.9A). In section, this replacement tooth formed intraosseously within the fifth ceratobranchial and immediately adjacent to position one. The base of the tooth located at position one was eroded on the side of the new replacement tooth (Fig 1.9B), a phenomenon also seen in adult stage tooth replacement events (Fig. 1.9C, D). Other late stage replacement teeth also form intraosseously (Fig. 1.9F, G). While primary teeth form at the interface of the epithelium and mesenchyme (Fig. 7E), replacement teeth formed deep in the mesenchyme (Fig. 1.9E, E′). However, the epithelium of all replacement teeth was continuous with the lumenal pharyngeal epithelium in adjacent serial sections (see Fig. 1.10). The first replacement tooth on VTP erupted between ~25-30 dpf while the first DTP2 replacement tooth erupted between ~20-24 dpf.

1.5 Discussion

Location and use of stickleback teeth

Fish retain the primitive jawed vertebrate condition of constant tooth regeneration (Reif, 1982; Fraser et al., 2010; Brazeau and Friedman, 2014) and provide model systems to study tooth replacement. Toothed locations are highly modular and variable across teleosts. While some fish have teeth covering most bones of their branchial skeletons (Liem and Greenwood, 1981), others, such as zebrafish, have lost all oral and dorsal pharyngeal teeth and rely solely on the ventral pharyngeal tooth plate attached to the fifth ceratobranchial (Stock, 2007). As previously described (Swinnerton, 1902; Anker, 1974) sticklebacks have teeth on the premaxilla and dentary in the oral jaw, and on the fifth ceratobranchial and the 2nd and fused 3rd/4th pharyngobranchials in the branchial skeleton.

Variation in tooth number has been identified in the oral premaxillary (upper jaw) (Caldecutt et al., 2001), ventral pharyngeal (Cleves et al., 2014; Miller et al., 2014; Ellis et al., 2015), and dorsal pharyngeal (Ellis et al., 2015) dentitions in sticklebacks. Variation in pharyngeal tooth number is heritable, and appears to correlate with trophic niche, as benthic lake and creek freshwater populations are higher toothed than oceanic populations (Cleves et al., 2014; Ellis et al., 2015). Stickleback feeding kinematics suggest the oral jaw is primarily used for prey capture and suction feeding (McGee et al., 2013). Instead, food mastication

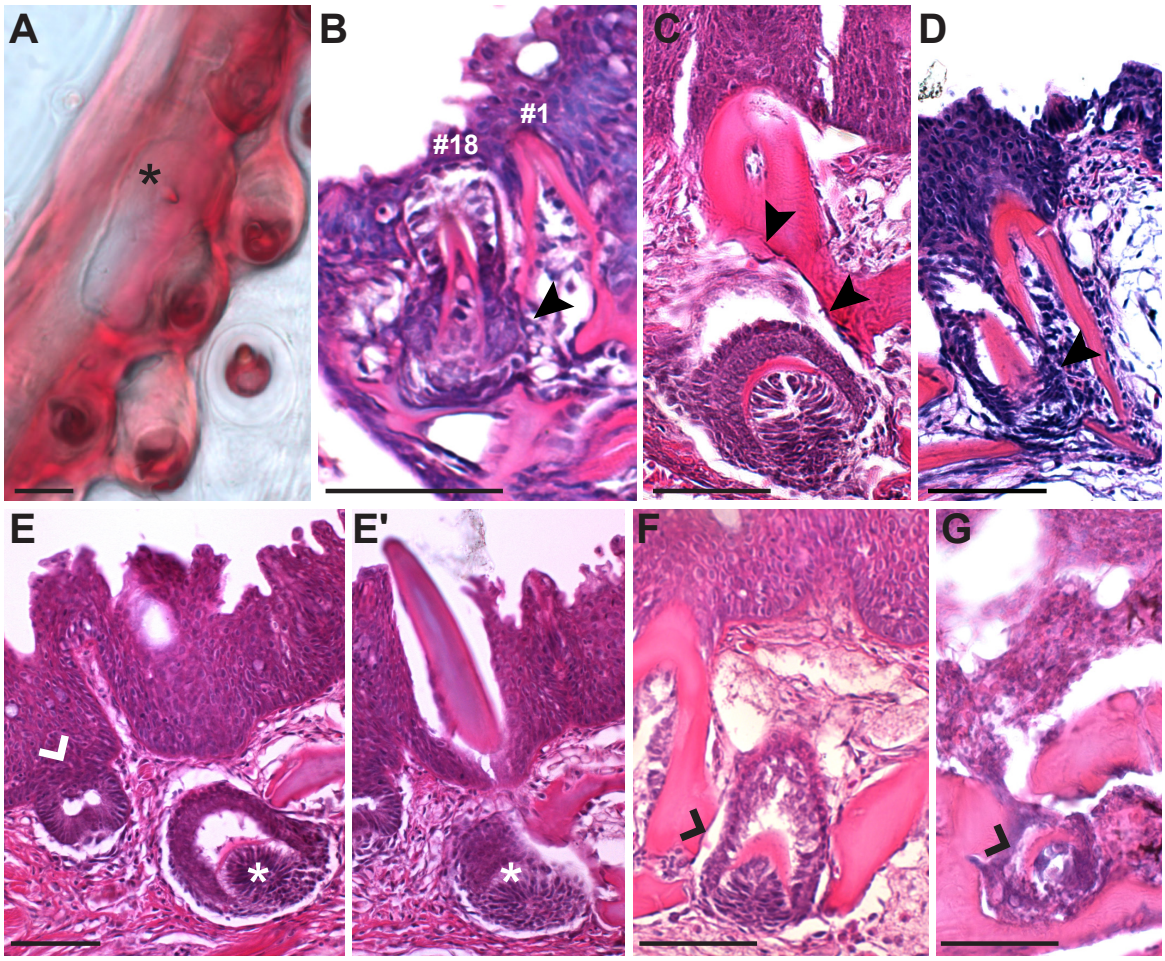

Figure 1.9: **Histological sections of tooth replacement.**
(A) Whole-mount 29 days post fertilization Alizarin red stained freshwater ventral pharyngeal tooth plate with position #1 and position #2 shed and the first replacement tooth arising (black asterisk). (B) Hematoxylin and eosin section through the first ventral pharyngeal tooth replacement event in a 30 day marine larvae. The eighteenth tooth to form is the replacement of the initial pioneer tooth forming lateral to and at the base of position one, within the fifth ceratobranchial bone. Bone resorption (black arrowheads) has occurred at the base of position one adjacent to the replacement tooth. (C,D) Examples of adult tooth replacement occurring similarly. Bone resorption is present on the side with the replacement tooth (black arrowheads). (E) Primary tooth germs form at the interface of the epithelium and the mesenchyme (left tooth germ, white caret), replacement teeth form deep in the mesenchyme (right germ, white asterisks), but with deeply invaginating epithelium that is continuous with the lumenal pharyngeal epithelium (see Fig. 1.10). (E′) Adjacent serial section showing the adult tooth above the replacement germ (white asterisks). (F,G) Stickleback replacement teeth form intraosseously, though not completely encased in bone (tooth germs marked with black caret). (C-F) Adult freshwater, (G) adult marine. Scale bars = 50 μm.

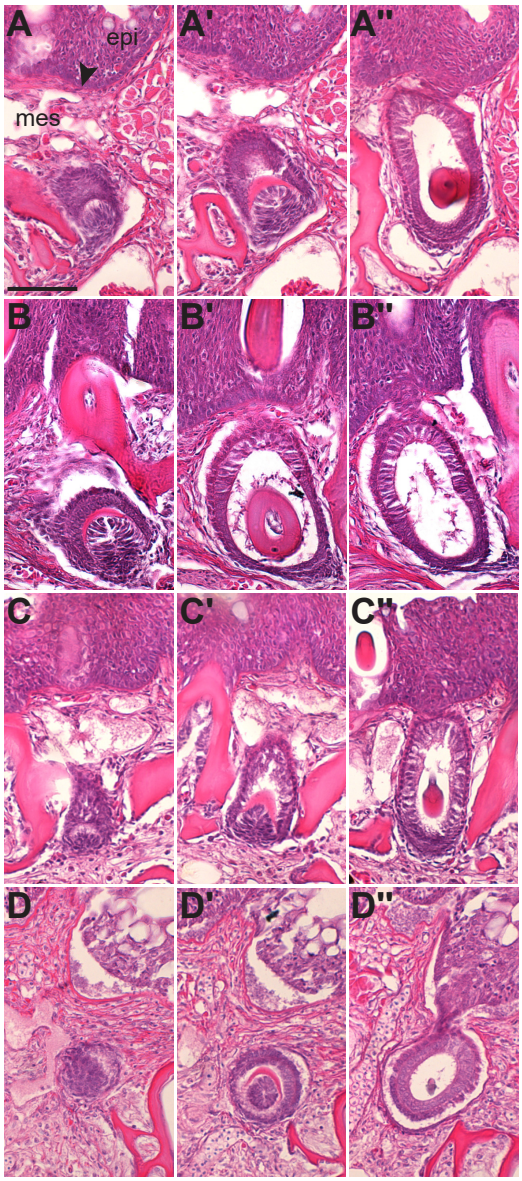

Figure 1.10: **Replacement teeth form deep but with invaginated epithelia that is continuous with lumenal pharyngeal epithelium.**
H&E stained 6 μm serial sections from adult sticklebacks showing pharyngeal teeth forming deep in the mesenchyme with an epithelial connection to the lumenal pharyngeal epithelium. (A-A$''$, B-B$''$, C-C$''$, D-D$''$) Each series indicates an individual tooth germ forming deep in the mesenchyme (A, B ,C, D), yet with a clear epithelial connection to the lumenal pharyngeal epithelium in subsequent serial sections (A$'$, A$''$, B$'$, B$''$, C$'$, C$''$, D$'$, D$''$). (A) Arrowhead indicates the stratum compactum, the boundary between the pharyngeal epithelium and the underlying connective tissue. Scale bar is 50 μm and applies to all panels. (A-C) Adult freshwater, (D) adult marine. Note B and C$'$ appear in Fig. 1.9C and Fig. 1.9F respectively.

likely involves the pharyngeal jaw and teeth. In cichlid fish, evolved changes in pharyngeal jaw morphology (Meyer, 1990; Huysseune, 1995) also correlate with trophic niche (Muschick et al., 2012), suggesting pharyngeal jaw patterning is likely an important ecological trait. Tooth number in cichlids has a phenotypically plastic component in response to diet (Huysseune, 1995). It remains to be determined whether shifts in diet can result in phenotypically plastic changes in tooth patterning in sticklebacks.

Oral and pharyngeal tooth homology

Stickleback pharyngeal teeth resemble oral teeth morphologically in whole-mount and in histological sections, and molecularly by gene expression patterns. These morphological and molecular parallels further support the classically proposed homology between oral and pharyngeal teeth (Owen, 1845), also supported by recent developmental genetic studies. For example, both oral and pharyngeal tooth formation require Ectodysplasin signaling (reviewed in Sadier et al., 2014). Furthermore, ectopic expression of *Ectodysplasin* is remarkably sufficient to restore dorsal pharyngeal tooth formation in zebrafish (Aigler et al., 2014). A previous study found evidence for the conservation of a dental gene network between oral and pharyngeal teeth in two species of cichlids, *M. zebra* and *L. fuelleborni* (Fraser et al., 2009). In sticklebacks, *Pitx2*, *Bmp6*, and *Shh* are expressed in developing pharyngeal teeth (Cleves et al., 2014). Here we show *Pitx2* and *Bmp6* are also expressed in similar patterns in developing stickleback oral teeth. *Pitx2* and *Shh* are also expressed in epithelia of developing pharyngeal teeth in zebrafish (Jackman et al., 2004, 2010) and in developing oral teeth in Mexican tetra (Stock et al., 2006). Interestingly, two transcriptional enhancers have been identified which drive expression in all developing oral and pharyngeal teeth. A 4 kb enhancer of the zebrafish *dlx2b* gene drives expression in teeth in both sets of jaws in tetras, despite zebrafish not having oral teeth (Jackman and Stock, 2006). Similarly, in sticklebacks, a 190 bp *Bmp6* enhancer drives expression in all teeth in both sets of jaws (Erickson et al., 2015). In axolotls, oral tooth epithelia have been shown to be derived from the ectoderm, endoderm, or even mixed ecto/endoderm origin within a single tooth, suggesting the embryonic source of the dental epithelium can be either ectoderm or endoderm, and further supporting homology of oral and pharyngeal teeth (Soukup et al., 2008). Collectively the current and these former studies strongly support developmental homology between oral and pharyngeal teeth.

Initial patterning of pharyngeal dentition

Compared to other fish such as medaka where adult teeth are in a regular array (Debiais-Thibaud et al., 2007; Abduweli et al., 2014) the adult pharyngeal dentition seems relatively unorganized in sticklebacks. However, the early sequence of tooth formation follows a highly stereotypical pattern. Initially, a pioneer tooth arises on each pharyngeal tooth plate. Subsequent teeth then form in a stereotypical sequence around this pioneer tooth. The pioneer tooth is calcified by 8 dpf on VTP and DTP2 while DTP1 calcifies by 12 dpf. The second tooth forms posterior and lateral to position one with the third tooth forming anterior and medial to position one in quick succession. This initial pattern of three teeth is conserved across all three pharyngeal tooth plates with a slight shift of position 3 on DTP1. After the

fourth tooth forms, each tooth plate follows a unique pattern with no two consecutive teeth forming next to one another. Several similarities in extended positions are shared between DTP1 and DTP2. Notably, position 1-5, and 7 all are generally conserved while position 6 and 8 form in a different spatial location (see Fig. 1.8). As tooth number and complexity of the pattern increases, more variation is present in the order of eruption of teeth, however each discrete position is present. Variation in eruption times in humans also increases at later developmental stages (Parner et al., 2001; Woodroffe et al., 2010).

Comparing the stickleback early tooth formation sequence in the ventral pharyngeal dentition to the sequence described in other fish reveals some significant evolved differences in how the tooth field in different fish arises. In zebrafish (D. rerio), the first four teeth follow the same spatial pattern as sticklebacks (Van der heyden and Huysseune, 2000). However in this system, the fourth tooth to form (termed $4V_3$) is described as a replacement of the pioneer tooth (termed $4V_1$). Additionally, the first row to form is the medially most row (termed ventral) and subsequent primary positions form 2 distinct rows lateral to the pioneer tooth in zebrafish (termed mediodorsal and dorsal rows) (Van der heyden and Huysseune, 2000; Huysseune and Witten, 2006) (see Nakajima, 1984, 1987; Stock, 2007 for discussion of other cypriniform patterns). In stark contrast, all stickleback subsequent primary positions form medially to the pioneer tooth. The only teeth that form lateral to the pioneer tooth in sticklebacks are replacements for the primary teeth adjacent to the fifth ceratobranchial. Compared to the Mexican tetra (*A. mexicanus*), the first 2 positions match. However, the third tooth in Mexican tetra instead forms medially and all subsequent teeth form medially or posteriorly to the pioneer tooth (Atukorala and Franz-Odendaal, 2014) whereas sticklebacks continue to add teeth anteriorly as well. Medaka (*O. latipes*) early pharyngeal tooth patterning is quite similar to the early stickleback positions. Positions 1-5 are spatially identical but temporally different, with positions 2 and 3 having opposite sequence of formation relative to sticklebacks. Despite this early similarity, the medaka pharyngeal dentition resolves into discrete rows late in development (Debiais-Thibaud et al., 2007), which is not seen in sticklebacks. Thus, within the ventral pharyngeal jaw, different fish species have evolved changes in (1) the number of primary teeth that form before replacement occurs, (2) the spatial sequence of tooth addition in both the mediolateral and anteroposterior directions, (3) the temporal sequence of early tooth position formation, and (4) the regularity of tooth row formation.

Early tooth patterning data for the dorsal pharyngeal tooth plates is more rare, likely in part due to their absence in many cypriniforms (Stock, 2007). In medaka, the first four dorsal teeth form in the same spatial pattern as the first four teeth in stickleback DTP2. The fifth medaka tooth, referred to as the 'second tooth ridge' forms more medially, but in close proximity to the fifth stickleback position. The next few medaka positions continue these two mediolateral 'ridges' or rows of teeth, while the next few stickleback positions form across the tooth field in an anteroposterior direction as well (Debiais-Thibaud et al., 2007). Compared to the Mexican tetra, the first two dorsal positions again match the stickleback positions with the next few tetra positions all forming posteriorly (Atukorala and Franz-Odendaal, 2014) while sticklebacks add tooth positions anteriorly as well. In one species

of cichlid (*Astatotilapia elegans*) with the dorsal tooth pattern recorded, positions after the pioneer tooth form anterolateral through 20 dpf (Huysseune, 1983), the opposite direction of the tetra. These early similarities yet late differences highlight the diversity of developmental programs governing teleost pharyngeal tooth patterning. Future studies will address the underlying molecular genetic and cellular bases of these programs, and how evolved changes in establishing and replacing these tooth fields arise.

Tooth replacement

Similar to cichlids (Huysseune, 1995; Fraser et al., 2013) and rainbow trout (Fraser, Berkovitz, et al., 2006), stickleback tooth replacement appears to occur on a one-for-one basis, where a replacement tooth directly replaces a primary tooth and is not connected to an extended tooth family with other replacement teeth already forming. A new epithelial down growth, termed the successional dental lamina, forms for each replacement tooth, budding off the reduced enamel organ of the predecessor tooth (Huysseune, 2006). The dental lamina in sticklebacks appears discontinuous (separate invagination for each tooth family) and non-permanent (reforms for each individual replacement tooth; after the definitions in Reif, 1982): some but not all positions have a detectable dental lamina at a given time point. This pattern of replacement is dissimilar to other teleosts such as zebrafish and medaka where multiple replacements have been proposed to be present for a single position (Van der heyden and Huysseune, 2000; Abduweli et al., 2014).

First generation teeth form extraosseously (outside the bone) in teleosts, while replacement teeth can from either extraosseously or intraosseously (reviewed in Trapani and Schaefer, 2001). First generation teeth arise individually from the pharyngeal epithelium in zebrafish, while replacement teeth form in crypts associated with the erupted primary tooth (Huysseune et al., 1998; Huysseune and Thesleff, 2004; Huysseune, 2006; Stock, 2007). These replacement teeth form extraosseously in zebrafish, but intraosseously in cichlids (Huysseune et al., 1994; Huysseune and Witten, 2006; Fraser et al., 2013). In sticklebacks, primary teeth form extraosseously at the interface of the epithelium and the mesenchyme. Replacement teeth in sticklebacks form intraosseously, surrounded by a bony crypt, though rarely fully encased on all sides (see Fig. 1.9F, G and Fig. 1.10). Replacement teeth form deep in the tooth plate, connected to but several cell diameters away from the pharyngeal epithelium, below or adjacent to the predecessor tooth. While stickleback replacement teeth share an epithelium with the tooth they will replace (see Fig. 1.9), this epithelium extends directly to the lumenal pharyngeal epithelium (see Fig. 1.10). The replacement may displace or arise next to the original tooth. The pattern of tooth replacement appears to initially follow the primary tooth eruption pattern with position one generally replacing first and positions 2 and 3 following. The early sequence and pattern of stickleback tooth development and replacement described here will facilitate future developmental genetic studies of tooth formation and replacement, as well as provide another comparison for understanding how dental morphology forms and is regenerated throughout development, and is modified during evolution.

1.6 Acknowledgments

We thank Priscilla Erickson and Phillip Cleves for generating and dissecting a subset of fish, Marvalee Wake for sectioning and decalcification suggestions, the He lab for assistance staining slides, and Gareth Fraser for advice on in situ hybridization.

This work was supported by the National Institutes of Health (NIH) [R01-DE021475 to C.T.M.]; National Science Foundation (NSF) Graduate Research Fellowship (N.A.E.) and an Achievement Rewards for College Scientists (ARCS) Fellowship (N.A.E.).

1.7 References

Abduweli D, Baba O, Tabata MJ, Higuchi K, Mitani H, Takano Y. 2014. Tooth replacement and putative odontogenic stem cell niches in pharyngeal dentition of medaka (*Oryzias latipes*). *Microscopy* 113.

Aigler SR, Jandzik D, Hatta K, Uesugi K, Stock DW. 2014. Selection and constraint underlie irreversibility of tooth loss in cypriniform fishes.*Proc Natl Acad Sci U S A* 111:77077712.

Anker GC. 1974. Morphology and kinetics of the head of the stickleback, *Gasterosteus aculeatus*. *Trans Zool Soc London* 32:311416.

Atukorala ADS, Franz-Odendaal TA. 2014. Spatial and temporal events in tooth development of *Astyanax mexicanus*. *Mech Dev* 134:4254.

Atukorala ADS, Inohaya K, Baba O, Tabata MJ, Ratnayake RARK, Abduweli D, Kasugai S, Mitani H, Takano Y. 2011. Scale and tooth phenotypes in medaka with a mutated *ectodysplasin-A* receptor: implications for the evolutionary origin of oral and pharyngeal teeth. *Arch Histol Cytol* 73:139148.

Bei M. 2009. Molecular genetics of tooth development. *Curr Opin Genet Dev* 19:504510.

Bell M, Foster S. 1994. *The Evolutionary Biology of the Threespine Stickleback*. New York: Oxford University Press.

Bemis WE, Giuliano A, McGuire B. 2005. Structure, attachment, replacement and growth of teeth in bluefish, *Pomatomus saltatrix* (Linnaeus, 1776), a teleost with deeply socketed teeth. *Zoology* 108:317327.

Berkovitz B. 1977. The order of tooth development and eruption in the rainbow trout (*Salmo gairdneri*). *J Exp Zool* 221225.

Brazeau MD, Friedman M. 2014. The characters of Palaeozoic jawed vertebrates. *Zool J Linn Soc* 170:779821.

Buchtov M, Handrigan GR, Tucker AS, Lozanoff S, Town L, Fu K, Diewert VM, Wicking C, Richman JM. 2008. Initiation and patterning of the snake dentition are dependent on Sonic hedgehog signaling. *Dev Biol* 319:132145.

Caldecutt WJ, Bell MA, Buckland-Nicks JA. 2001. Sexual dimorphism and geographic variation in dentition of threespine stickleback, *Gasterosteus aculeatus*. *Copeia* 4:936944.

Cleves PA, Ellis NA, Jimenez MT, Nunez SM, Schluter D, Kingsley DM, Miller CT. 2014. Evolved tooth gain in sticklebacks is associated with a *cis*-regulatory allele of *Bmp6*. *Proc Natl Acad Sci* 111:1391213917.

Debiais-Thibaud M, Borday-Birraux V, Germon I, Bourrat F, Metcalfe CJ, Casane D, Laurenti P. 2007. Development of oral and pharyngeal teeth in the medaka (*Oryzias latipes*): comparison of morphology and expression of *eve1* gene. *J Exp Zool* 708:693708.

Ellis NA, Glazer AM, Donde NN, Cleves PA, Agoglia RM, Miller CT. 2015. Distinct developmental and genetic mechanisms underlie convergently evolved tooth gain in sticklebacks. *Development* 142:24422451.

Ellis NA, Miller CT. 2016. Dissection and flat-mounting of the threespine stickleback branchial skeleton. *J Vis Exp* e54056.

Erickson PA, Cleves PA, Ellis NA, Schwalbach KT, Hart JC, Miller CT. 2015. A 190 base pair, TGF- responsive tooth and fin enhancer is required for stickleback *Bmp6* expression. *Dev Biol* 401:310323.

Evans HE, Deubler EE. 1955. Pharyngeal tooth replacement in *Semotilus atromaculatus* and *Clinostomus elongatus*, two species of cyprinid fishes. *Copeia* 1:3141.

Fraser G, Graham A, Smith M. 2006. Developmental and evolutionary origins of the vertebrate dentition: molecular controls for spatiotemporal organisation of tooth sites in osteichthyans. *J Exp Zool* 306:183203.

Fraser GJ, Berkovitz BK, Graham A, Smith MM. 2006. Gene deployment for tooth replacement in the rainbow trout (*Oncorhynchus mykiss*): a developmental model for evolution of osteichthyan dentition. *Evol Dev* 8:446457.

Fraser GJ, Bloomquist RF, Streelman JT. 2008. A periodic pattern generator for dental diversity. *BMC Biol* 6:32.

Fraser GJ, Bloomquist RF, Streelman JT. 2013. Common developmental pathways link tooth shape to regeneration. *Dev Biol* 377:399414.

Fraser GJ, Britz R, Hall A, Johanson Z, Smith MM. 2012. Replacing the first-generation dentition in pufferfish with a unique beak. *Proc Natl Acad Sci U S A* 27.

Fraser GJ, Cerny R, Soukup V, Bronner-Fraser M, Streelman JT. 2010. The odontode explosion: The origin of tooth-like structures in vertebrates. *BioEssays* 32:808817.

Fraser GJ, Graham A, Smith MM. 2004. Conserved deployment of genes during odontogenesis across osteichthyans. *Proc Biol Sci* 271:23112317.

Fraser GJ, Hulsey CD, Bloomquist RF, Uyesugi K, Manley NR, Streelman JT. 2009. An ancient gene network is co-opted for teeth on old and new jaws. *PLoS Biol* 7:e1000031.

Gaete M, Tucker AS. 2013. Organized emergence of multiple-generations of teeth in snakes is dysregulated by activation of Wnt/beta-catenin signalling. *PLoS One* 8:e74484.

Handrigan GR, Leung KJ, Richman JM. 2010. Identification of putative dental epithelial stem cells in a lizard with life-long tooth replacement. *Development* 137:35453549.

Handrigan GR, Richman JM. 2010. A network of Wnt, hedgehog and BMP signaling pathways regulates tooth replacement in snakes. *Dev Biol* 348:130141.

Harris MP, Rohner N, Schwarz H, Perathoner S, Konstantinidis P, Nsslein-Volhard C. 2008. Zebrafish *eda* and *edar* mutants reveal conserved and ancestral roles of Ectodysplasin signaling in vertebrates. *PLoS Genet* 4:e1000206.

Hulsey CD, Fraser GJ, Streelman JT. 2005. Evolution and development of complex biomechanical systems: 300 million years of fish jaws. *Zebrafish* 2:243257.

Humason G. 1962. *Animal Tissue Techniques*. San Francisco: W. H. Freeman and Company.

Huysseune A. 1983. Observations on tooth development and implantation in the upper pharyngeal jaws in *Astatotilapia elegans* (Teleostei, Cichlidae). *J Morphol* 175:217234.

Huysseune A. 1995. Phenotypic plasticity in the lower pharyngeal jaw dentition of *Astatoreochromis alluaudi* (Teleostei: Cichlidae). *Arch Oral Biol* 40:10051014.

Huysseune A. 2006. Formation of a successional dental lamina in the zebrafish (*Danio rerio*): support for a local control of replacement tooth initiation. *Int J Dev Biol* 50:637643.

Huysseune A, Sire JY, Meunier FJ. 1994. Comparative-study of lower pharyngeal jaw structure in two phenotypes of *Astatoreochromis alluaudi* (Teleostei, Cichlidae). *J Morphol* 221:2543.

Huysseune A, Thesleff I. 2004. Continuous tooth replacement: the possible involvement of epithelial stem cells. *Bioessays* 26:665671.

Huysseune A, Van der heyden C, Sire J-Y. 1998. Early development of the zebrafish (*Danio rerio*) pharyngeal dentition (Teleostei, Cyprinidae). *Anat Embryol* (Berl) 198:289305.

Huysseune A, Witten PE. 2006. Developmental mechanisms underlying tooth patterning in continuously replacing osteichthyan dentitions. *J Exp Zool Part B Mol Dev Evol* 306:204215.

Hynes HBN. 1950. The food of fresh-water sticklebacks (*Gasterosteus aculeatus* and *Pygosteus pungitius*), with a review of methods used in studies of the food of fishes. *J Anim Ecol* 19:3658.

Jackman WR, Draper BW, Stock DW. 2004. Fgf signaling is required for zebrafish tooth development. *Dev Biol* 274:139157.

Jackman WR, Stock DW. 2006. Transgenic analysis of *dlx* regulation in fish tooth development reveals evolutionary retention of enhancer function despite organ loss. *Proc Natl Acad Sci U S A* 103:1939019395.

Jackman WR, Yoo JJ, Stock DW. 2010. Hedgehog signaling is required at multiple stages of zebrafish tooth development. *BMC Dev Biol* 10:119.

Jernvall J, Thesleff I. 2000. Reiterative signaling and patterning during mammalian tooth morphogenesis. *Mech Dev* 92:1929.

Juuri E, Jussila M, Seidel K, Holmes S, Wu P, Richman J, Heikinheimo K, Chuong C-M, Arnold K, Hochedlinger K, Klein O, Michon F, Thesleff I. 2013. *Sox2* marks epithelial competence to generate teeth in mammals and reptiles. *Development* 140:14241432.

Lan Y, Jia S, Jiang R. 2014. Molecular patterning of the mammalian dentition. *Semin Cell Dev Biol* 25-26:6170.

Lauder G. 1983. Functional design and evolution of the pharyngeal jaw apparatus in euteleostean fishes. *Zool J Linn Soc* 77:138.

Le Pabic P, Stellwag EJ, Scemama JL. 2009. Embryonic development and skeletogenesis of the pharyngeal jaw apparatus in the cichlid Nile tilapia (*Oreochromis niloticus*). *Anat Rec* 292:17801800.

Lemmetyinen R, Mankki J. 1975. The three-spined stickleback (*Gasterosteus aculeatus*) in the food chains of the northern Baltic. *Merentutkimuslait Julk/Havsforskningsinst* 239:155161.

Liem K, Greenwood P. 1981. A functional approach to the phylogeny of the pharyngognath teleosts. *Am Zool* 21:83101.

Mantoku A, Chatani M, Aono K, Inohaya K, Kudo A. 2015. Osteoblast and osteoclast behaviors in the turnover of attachment bones during medaka tooth replacement. *Dev Biol* 112.

McGee MD, Schluter D, Wainwright PC. 2013. Functional basis of ecological divergence in sympatric stickleback. *BMC Evol Biol* 13:277.

Meyer A. 1990. Morphometrics and allometry in the trophically polymorphic cichlid fish, *Cichlusomu citrinelfum*: alternative adaptations and ontogenetic changes in shape. *J Zool, Lond* 221:237260.

Mikkola ML. 2009. Controlling the number of tooth rows. *Sci Signal 2*:pe53.

Mikkola ML, Thesleff I. 2003. Ectodysplasin signaling in development. *Cytokine Growth Factor Rev* 14:211224.

Miller CT, Glazer AM, Summers BR, Blackman BK, Norman AR, Shapiro MD, Cole BL, Peichel CL, Schluter D, Kingsley DM. 2014. Modular skeletal evolution in sticklebacks is controlled by additive and clustered quantitative trait loci. *Genetics* 197:405420.

Moriyama K, Watanabe S, Iida M, Sahara N. 2010. Plate-like permanent dental laminae of upper jaw dentition in adult gobiid fish, *Sicyopterus japonicus*. *Cell Tissue Res* 340:189200.

Motta PJ. 1984. Tooth attachment, replacement, and growth in the butterfly fish, *Chaetodon miliaris* (Chaetodontidae, Perciformes). *Can J Zool* 62:183189.

Muschick M, Indermaur A, Salzburger W. 2012. Convergent evolution within an adaptive radiation of cichlid fishes. *Curr Biol* 22:23622368.

Nakajima T. 1984. Larval vs. adult pharyngeal dentition in some Japanese cyprinid fishes. *J Dent Res* 63:11401146.

Nakajima T. 1987. Development of pharyngeal dentition in the cobitid fishes, *Misgurnus anguillicaudatus* and *Cobitis biwae*, with a consideration of evolution of cypriniform. *Copeia* 1987:208213.

OConnell DJ, Ho JWK, Mammoto T, Turbe-Doan A, OConnell JT, Haseley PS, Koo S, Kamiya N, Ingber DE, Park PJ, Maas RL. 2012. A Wnt-Bmp feedback circuit controls intertissue signaling dynamics in tooth organogenesis. *Sci Signal* 5:110.

Osborn J. 1971. The ontogeny of tooth succession in *Lacerta vivipara Jacquin* (1787). *Proc R Soc London Ser B*, Biol Sci 179:261289.

Owen R. 1845. *Odontography; a treatise on the comparative anatomy of the teeth.* Vol. 1. ed. London: Hippolyte Bailliere. 1-178 p.

Parner ET, Heidmann JM, Vath M, Poulsen S. 2001. A longitudinal study of time trends in the eruption of permanent teeth in Danish children. *Arch Oral Biol* 46:425431.

Reif W. 1982. Evolution of dermal skeleton and dentition in vertebrates. In: Hecht MK, editor. *Evol. Biol.* New York: Plenum Press. p. 287368.

Sadier A, Viriot L, Pantalacci S, Laudet V. 2014. The ectodysplasin pathway: from diseases to adaptations. *Trends Genet* 30:2431.

Schluter D, McPhail JD. 1992. Ecological character displacement and speciation in sticklebacks. *Am Nat* 140:85108.

Sibbing F. 1991. Food capture and oral processing. In: Winfield IJ,, Nelson JS, editors. *Cyprinid Fishes* Chapman and Hall. p. 377412.

Smith MM, Fraser GJ, Mitsiadis TA. 2009. Dental lamina as source of odontogenic stem cells: evolutionary origins and developmental control of tooth generation in gnathostomes. *J Exp Zool B Mol Dev Evol* 312B:260280.

Smith MM, Okabe M, Joss J. 2009. Spatial and temporal pattern for the dentition in the Australian lungfish revealed with *sonic hedgehog* expression profile. *Proc Biol Sci* 276:623631.

Soukup V, Epperlein H-H, Horcek I, Cerny R. 2008. Dual epithelial origin of vertebrate oral teeth. *Nature* 455:795798.

Stock D. 2007. Zebrafish dentition in comparative context. *J Exp Zool B Mol Dev Evol* 308B:523549.

Stock DW, Jackman WR, Trapani J. 2006. Developmental genetic mechanisms of evolutionary tooth loss in cypriniform fishes. *Development* 133:31273137.

Swinnerton HH. 1902. A contribution to the morphology of the Teleostean head skeleton, based upon a study of the developing skull of the three-spined stickleback (*Gasterosteus aculeatus*). *Q J Microsc Sci* 45:503601.

Trapani J, Schaefer S. 2001. Position of developing replacement teeth in teleosts. *Copeia* 2001:3551.

Tucker A, Sharpe P. 2004. The cutting-edge of mammalian development; how the embryo makes teeth. *Nat Rev Genet* 5:499508.

Tummers M, Thesleff I. 2009. The importance of signal pathway modulation in all aspects of tooth development. *J Exp Zool B Mol Dev Evol* 312B:309319.

Underwood CJ, Johanson Z, Welten M, Metscher B, Rasch LJ, Fraser GJ, Smith MM. 2015. Development and evolution of dentition pattern and tooth order in the skates And rays (Batoidea; Chondrichthyes). *PLoS One* 10:e0122553.

Van der heyden C, Huysseune A. 2000. Dynamics of tooth formation and replacement in the zebrafish (*Danio rerio*) (Teleostei, Cyprinidae). *Dev Dyn* 219:486496.

Vandenplas S, De Clercq A, Huysseune A. 2014. Tooth replacement without a dental lamina: the search for epithelial stem cells in *Polypterus senegalus*. *J Exp Zool B Mol Dev Evol* 322:281293.

Wainwright P. 2006. Functional morphology of the pharyngeal jaw apparatus. In: Shadwick RE,, Lauder G V., editors. *Fish Physiology: Fish Biomechanics* Academic Press. p. 77102.

Wake M. 1976. The development and replacement of teeth in viviparous caecilians. *J Morphol* 148:33-64.

Wakita M, Itoh K, Kobayashi S. 1977. Tooth replacement in the teleost fish *Prionurus microlepidotus Lacpde. J Morphol* 153:129141.

Walker MB, Kimmel CB. 2007. A two-color acid-free cartilage and bone stain for zebrafish larvae. *Biotech Histochem* 82:2328.

Woodroffe S, Mihailidis S, Hughes T, Bockmann M, Seow WK, Gotjamanos T, Townsend GC. 2010. Primary tooth emergence in Australian children: timing, sequence and patterns of asymmetry. *Aust Dent J* 55:245251.

Wu P, Wu X, Jiang T-X, Elsey RM, Temple BL, Divers SJ, Glenn TC, Yuan K, Chen M-H, Widelitz RB, Chuong C-M. 2013. Specialized stem cell niche enables repetitive renewal of alligator teeth. *Proc Natl Acad Sci* 110.

Xu Q, Holder N, Patient R, Wilson SW. 1994. Spatially regulated expression of three receptor tyrosine kinase genes during gastrulation in the zebrafish. *Development* 120:287299.

Zhang Z, Lan Y, Chai Y, Jiang R. 2009. Antagonistic actions of *Msx1* and *Osr2* pattern mammalian teeth into a single row. *Science* 323:12321234.

Chapter 2

Distinct developmental and genetic mechanisms underlie convergently evolved tooth gain in sticklebacks

> "Not everything that can be counted counts, and not everything that counts can be counted."
> -Albert Einstein

The following chapter was originally published as an article: *Development* 2015 142, 2442-2451

Nicholas A. Ellis, Andrew M. Glazer, Nikunj N. Donde, Phillip A. Cleves, Rachel M. Agoglia and Craig T. Miller

Department of Molecular and Cell Biology, University of California-Berkeley, Berkeley CA, 94720, USA

2.1 Abstract

Teeth are a classic model system of organogenesis, as repeated and reciprocal epithelial and mesenchymal interactions pattern placode formation and outgrowth. Less is known about the developmental and genetic bases of tooth formation and replacement in polyphyodonts, which are vertebrates with continual tooth replacement. Here, we leverage natural variation in the threespine stickleback fish *Gasterosteus aculeatus* to investigate the genetic basis of tooth development and replacement. We find that two derived freshwater stickleback populations have both convergently evolved more ventral pharyngeal teeth through heritable genetic changes. In both populations, evolved tooth gain manifests late in development. Using pulse-chase vital dye labeling to mark newly forming teeth in adult fish, we find that both high-toothed freshwater populations have accelerated tooth replacement rates relative to low-toothed ancestral marine fish. Despite the similar evolved phenotype of more teeth and an accelerated adult replacement rate, the timing of tooth number divergence and the spatial patterns of newly formed adult teeth are different in the two populations, suggesting distinct developmental mechanisms. Using genome-wide linkage mapping in marine-freshwater F2 genetic crosses, we find that the genetic basis of evolved tooth gain in the two freshwater populations is largely distinct. Together, our results support a model whereby increased tooth number and an accelerated tooth replacement rate have evolved convergently in two independently derived freshwater stickleback populations using largely distinct developmental and genetic mechanisms.

Keywords: Convergent evolution, Odontogenesis, Stickleback, Polyphyodonty, Tooth replacement

2.2 Introduction

Teeth are a classic model system for studying organogenesis in vertebrates, as repeated epithelial-mesenchymal interactions orchestrate odontogenesis (Ahn, 2015; Biggs and Mikkola, 2014; Jernvall and Thesleff, 2012). The developmental genetic basis of tooth formation has been most intensively studied in the mouse (Tucker and Sharpe, 2004), which has revealed detailed genetic networks that specify primary tooth formation and placement (Bei, 2009; Jernvall and Thesleff, 2000; Lan et al., 2014; OConnell et al., 2012; Tummers and Thesleff, 2009). However, since mice are monophyodont rodents that do not replace their teeth, other vertebrate models are needed to study the developmental basis of tooth replacement. The ancestral vertebrate dental phenotype is polyphyodonty, or continuous tooth replacement, a trait retained in sharks, fish and reptiles (Jernvall and Thesleff, 2012; Tucker and Fraser, 2014). These replacement teeth may appear adjacent or beneath primary teeth and are often retained in the tooth field before the primary tooth is shed. In sharks, up to 200 teeth can develop as replacements for a single position (Reif, 1984).

Recent studies on tooth replacement have supported the hypothesis that genetic net-

works controlling primary tooth formation are redeployed during tooth replacement in both polyphyodont vertebrates (Fraser et al., 2006, 2013; Handrigan and Richman, 2010) and diphyodont mammals (which have two successive sets of teeth) (Jussila et al., 2014). Genetic studies in humans also demonstrate that shared genetic networks pattern primary and replacement teeth (Nieminen, 2009; van den Boogaard et al., 2012). Induction of tooth replacement has been proposed to be regulated by odontogenic stem cells, and candidate pathways, stem cell niches and markers have been proposed (Abduweli et al., 2014; Gaete and Tucker, 2013; Handrigan et al., 2010; Huysseune and Thesleff, 2004; Juuri et al., 2013; Smith et al., 2009b; Wu et al., 2013).

Fish retain the polyphyodont mode of tooth replacement and offer several advantages for developmental genetic studies, including external development and large numbers of offspring per mating. Many fish also have two sets of tooth-covered jawsan oral jaw in their mandibular arch primarily for grasping prey, as well as a pharyngeal jaw in the posterior branchial segments in their throat for manipulation and mastication (Hulsey et al., 2005; Lauder, 1983; Sibbing, 1991; Wainwright, 2006). Oral and pharyngeal teeth form via highly similar developmental genetic mechanisms and are developmentally homologous (Fraser et al., 2009). For example, the Eda/Edar pathway is required for the proper formation of oral teeth in mammals (Mikkola and Thesleff, 2003), both oral and pharyngeal teeth in medaka fish (Atukorala et al., 2011), and for the only teeth that form in zebrafish ventral pharyngeal teeth (Harris et al., 2008).

To study the developmental genetic basis of tooth formation and replacement, we leveraged natural variation in dental patterning in threespine stickleback fish (*Gasterosteus aculeatus*). Sticklebacks have undergone a dramatic adaptive radiation in which ancestral marine populations have repeatedly colonized and rapidly adapted to thousands of freshwater lakes and creeks throughout the Northern Hemisphere (Bell and Foster, 1994). Colonization of freshwater environments is accompanied by a variety of adaptations to the head skeleton, many of which are likely to be due to a major shift in diet from small zooplankton in the ocean to larger prey in freshwater (Schluter and McPhail, 1992). Recent studies (Miller et al., 2014; Cleves et al., 2014) have identified a major dental patterning polymorphism: a near twofold increase in ventral pharyngeal tooth number in a derived freshwater benthic (adapted to live on the bottom of a lake) population from Paxton Lake in Canada, possibly adaptive for crushing larger prey in the benthic niche. The increase in tooth number is accomplished by both expanding the size of the tooth field and by decreasing intertooth spacing (Cleves et al., 2014). Marine and freshwater sticklebacks can be intercrossed and their F1 hybrids are fertile, allowing forward genetic mapping of genomic regions controlling morphological differences. Genetic mapping revealed that tooth plate area (field size) and intertooth spacing are genetically separable, being controlled by largely non-overlapping genomic regions (Cleves et al., 2014). One genomic region with the largest effects on tooth number, tooth plate area and intertooth spacing maps to chromosome 21 and contains a cis-regulatory allele of the *Bone morphogenetic protein 6* (*Bmp6*) gene (Cleves et al., 2014).

Little is known about the developmental mechanisms underlying this evolved tooth gain. Additionally, whether increased tooth number has evolved in other freshwater populations

and, if so, whether similar or different developmental genetic mechanisms are used remain open questions. Here we identify a second derived freshwater stickleback population with convergently evolved tooth gain. In both freshwater populations, increased tooth number arises late in development and is associated with increased rates of new tooth formation in adults. However, the two freshwater populations have different timing of tooth number divergence, strikingly different spatial patterns of tooth addition in adults, and mostly non-overlapping genomic regions controlling tooth number. Thus, convergently evolved tooth gain in the two freshwater populations arises via largely distinct underlying developmental and genetic bases.

2.3 Materials and Methods

Stickleback husbandry

Fish were raised at 18°C in 110 l aquaria in a common brackish salinity (3.5 g/l Instant Ocean salt, 0.217 ml/l 10% sodium bicarbonate). Fish were fed a common diet of live Artemia as young fry, live Artemia and frozen Daphnia as juveniles and frozen bloodworms and Mysis shrimp as adults. All experiments were performed with approval of the Institutional Animal Care and Use Committees of the University of California-Berkeley (protocol # R330).

Skeletal staining and visualization

Laboratory-reared fish were fixed in 10% neutral buffered formalin (NBF) overnight at 4°C, washed in water, and stained with 0.008% (>20 mm) or 0.004% (<20 mm) Alizarin Red S in 1% KOH for 24 h. Fish were rinsed again in water and cleared in 50% glycerol and 0.25% KOH. Branchial skeletons were dissected and mounted as described (Miller et al., 2014). Tooth number was scored on a Leica DM2500 under a TX2 filter (with PAXB adult tooth number in Fig. 1D from Cleves et al., 2014). Area and spacing measurements were performed as described (Cleves et al., 2014). Phenotype quantifications are left and right combined for tooth number and the average of left and right for area and spacing. Representative tooth plate z-stack projections were collected on a Zeiss 700 confocal microscope. See supplementary material Methods for details of statistical analysis and phenotype corrections.

Live vital dye bone staining was adapted from Kimmel et al. (2010) and performed by pulsing fish with 100 μg/ml Alizarin Red S buffered with 1 mM HEPES (pH 7.0) in tank water for 12 h in the dark. After replacing Alizarin with clean tank water, fish were returned to tanks for 14 days, and then chased with 50 μg/ml Calcein buffered with 1 mM sodium phosphate (pH 8.0) in tank water for 12 h in the dark. After replacing Calcein with clean tank water, fish were fixed overnight in 10% NBF at 4°C and stored in 100% ethanol in the dark at 4°C until dissection and clearing as described above. Preparations were phenotyped on a Leica DM2500 using GFP and TX2 filter sets. Two month pulse-chase was performed as described above with 50 μg/ml Alizarin Red S, 25 μg/ml Calcein, and 6 h dye soaks.

Histology

Fish were fixed in 10% NBF overnight at 4°C, dissected, and decalcified as required in Humasons formic acid A (Humason, 1962). Tissue was processed pre-embedding as described (Schulte-Merker, 2002) using Histoclear (National Diagnostics) in place of xylene. Tissue was transferred, oriented, and embedded in Paraplast (Fisher) using plastic molds. Serial sections were collected using a Microm HM340E (Thermo Scientific). Sections were baked on slides overnight at 50°C then stained with Hematoxylin and Eosin using a Varistain Gemini ES automated stainer (Thermo Scientific) and cover-slipped with Permount (Fisher) mounting media. Stained sections were imaged under brightfield optics on a Leica DM2500. Germ number was quantified by counting un-erupted developing teeth on the ventral pharyngeal tooth plate in 6 μm serial sections of 4-6 individuals for each population and time point. Germs were sorted by stage (bud, cap, early to mid-bell, late bell) and germ area obtained by tracing the outer diameter of the outer dental epithelium (ODE) in ImageJ (Schneider et al., 2012). Torn or rippled germ sections were omitted from area measurements. Adult tooth width was measured by using the basement membrane of the epithelium (stratum compactum) as a landmark. Height was measured along a line perpendicular to the width measurement to the tip of the tooth in ImageJ.

Heat maps

Small, newly erupted teeth that (1) were in a deeper focal plane than adult teeth, (2) had a translucent enameloid cap and (3) had a clearly visible dental pulp (i.e. a cone within a cone visible with DIC optics) were counted and their position marked on an idealized tooth plate in ImageJ (Schneider et al., 2012). A custom R script generated bins across the tooth plate and assigned a color score based on the number of teeth within each bin per population using color schemes from ColorBrewer (http://colorbrewer2.org). Individual teeth were scored as off the tooth plate if >90% of the base of the tooth failed to overlap with the underlying tooth plate.

Preparation of Genotyping-by-Sequencing (GBS) libraries

DNA was isolated by phenol-chloroform extraction or with a DNeasy 96 Blood and Tissue Kit (Qiagen). Genomic DNA concentration was assessed using a NanoDrop 1000 spectrophotometer (Thermo Scientific) and by Quant-iT PicoGreen Assay (Invitrogen). GBS Illumina sequencing libraries were constructed as described (Elshire et al., 2011; Glazer et al., 2015). Briefly, genomic DNA was digested with ApeKI, ligated to Y-shaped adapters, and PCR amplified. Libraries were analyzed on an Agilent 2100 Bioanalyzer High-Sensitivity Chip for quality control and sequenced with 100 base pair, paired-end sequencing on an Illumina HiSeq 2000 sequencer. 174 F2 fish were barcoded into a single lane of Illumina sequencing together with 190 samples not used in this study.

Processing reads from grandparent resequencing and F2 GBS libraries

The Cerrito Creek (CERC) grandfather of the CERC x marine (Little Campbell River, LITC) F2 cross was sequenced using a Nextera DNA Sample Preparation kit (Illumina) followed by sequencing to ~6X coverage with 100 base, paired-end sequencing on an Illumina

HiSeq 2000 sequencer (SRA accession # SRS951365). Reads were mapped to the reference genome with BWA (www.bio- bwa.sourceforge.net), SNPs were called with SAMtools (www.samtools.sourceforge.net), and these SNPs were filtered for positions homozygous for an alternate allele. Genotyping-by-Sequencing (GBS) was performed as previously described (Glazer et al., 2015) with the exception that only one grandparent was used for phasing F2 genotypes and phasing was performed separately in two half sibling families. First, SNP positions that were homozygous alternate in the CERC grandparent were phased in each family (n=7,606 and n=13,477 respectively), pooled into bins, and genotypes were calculated for each bin of SNPs. Bins did not span scaffold boundaries and scaffolds were equally divided into bins with a maximum size of 500kb (see Glazer et al., 2015). Second, these genotypes were used to further phase additional SNPs in the F2s. SNP positions that correlated above 80% with called genotypes were phased and included in the pooled genotypes. Three rounds of this phasing were repeated resulting in a total of 28,283 phased SNPs binned into 761 markers in family one and 50,000 phased SNPs binned into 999 markers in family two. Three fish that had missing data for over 50% of markers were removed from the analysis. Thirty markers with missing data for more than 40% of fish were removed from the analysis. This resulted in 974 markers and 171 fish in the merged data set with over 91% of all possible genotypes present. Genetic linkage maps were created with JoinMap 4.0 (Kyazma) with regression mapping and default settings. Markers with skewed genotypes were determined based on high confidence genotypes (determined from a minimum of 10x coverage). Genotype ratios that deviated significantly from the expected 1:2:1 ratio using a chi-squared test were dropped ($P < 0.01$) except in cases where multiple linked adjacent markers significantly deviated. Twenty-three markers were dropped as chi-squared outliers and 21 markers did not fit into the linkage map resulting in a map with 930 markers.

Quantitative trait loci (QTL) mapping

QTL mapping was initially performed with stepwiseqtl using Haley-Knott regressions in R/qtl (Broman and Sen, 2009). Scantwo penalty scores for tooth number, area and spacing were 3.9, determined via 1000 permutations at α=0.05. The top three models for each phenotype were identified and further explored using scanone and addqtl adjusting for QTL found using stepwise scanning. Genome-wide LOD (logarithm of the odds) significance thresholds for each phenotype were determined with scanone via 10,000 permutations at α=0.05 resulting in a median threshold of 3.9. QTL peaks, LOD scores and percent variance explained were calculated with refineqtl and fitqtl. PAXBmarine QTL were previously identified and included for comparison (Miller et al., 2014; Cleves et al., 2014).

Statistical analysis and phenotype corrections

Data were analyzed using R and Prism 5. For comparing tooth phenotypes between populations, one way analysis of variance (ANOVA) using a Tukey-Kramer post hoc test was performed for statistical analysis between greater than 2 groups unless otherwise noted. Total length (TL), tip of snout to end of tail, measurements were used in datasets where fish were <15mm, while standard length (SL), tip of snout to base of caudal peduncle, measure-

ments were used when fish were >15mm. Phenotypes were size and/or sex corrected when appropriate.

Adult (~6 month old) lab-reared ventral pharyngeal tooth number, tooth plate area, and intertooth spacing phenotypes were all corrected for fish size (i.e. phenotypes were back transformed residuals for a regression to standard length for a mean standard length of 37 mm). Neither dorsal pharyngeal tooth plate tooth numbers correlated with standard length, so these were not size corrected. CERC x marine F2 cross phenotypes were regressed to standard length and/or corrected for sex and/or log-transformed when the transformation equalized variances by Levenes test for equality of variances and/or normalized the residuals by an Anderson-Darling test of normality when appropriate. Final corrected phenotypes for mapping QTL were ventral tooth number (raw), ventral tooth plate area and intertooth spacing (both log transformed and corrected for fish standard length), dorsal tooth plate 1 tooth number (raw), and dorsal tooth plate 2 tooth number (corrected for fish standard length).

2.4 Results

Two freshwater stickleback populations exhibit evolved tooth gain

To test the hypothesis that independently derived freshwater stickleback populations have repeatedly evolved increases in pharyngeal tooth number, we compared pharyngeal tooth morphology of three adult laboratory-reared stickleback populations: a marine population from Rabbit Slough (RABS) in Alaska, USA; a freshwater benthic population from Paxton Lake (PAXB) in British Columbia, Canada [previously shown to have evolved tooth gain (Cleves et al., 2014)]; and a second freshwater population from Cerrito Creek (CERC) in California, USA (Fig. 2.1).

Sticklebacks have three sets of bilateral pharyngeal tooth plates near the back of the throat (Fig. 2.2A) (Anker, 1974): a ventral pair on the fifth ceratobranchials, hereafter referred to as ventral tooth plates (VTP); a small dorsal pair on the anterior pharyngobranchials, hereafter referred to as dorsal tooth plates 1 (DTP1); and a large dorsal pair on the posterior pharyngobranchials, hereafter referred to as dorsal tooth plates 2 (DTP2). Relative to ancestral marine fish, both freshwater populations have evolved increased ventral and dorsal DTP1 pharyngeal tooth number (Fig. 2.2B,D; Fig. 2.3A-C). By contrast, no significant differences in DTP2 tooth number were found. As increased tooth number could result from a larger field of teeth and/or reduced intertooth spacing (Cleves et al., 2014), we quantified tooth plate area and intertooth spacing on the ventral pharyngeal tooth plate, which is the tooth plate with the largest magnitude difference in tooth number (Fig. 2.2C). Both freshwater populations have also evolved increased tooth plate area and decreased intertooth spacing compared with ancestral marine fish (Fig. 2.2E,F). Thus, both derived freshwater populations have convergently evolved increased ventral pharyngeal tooth number, increased tooth plate area and decreased intertooth spacing.

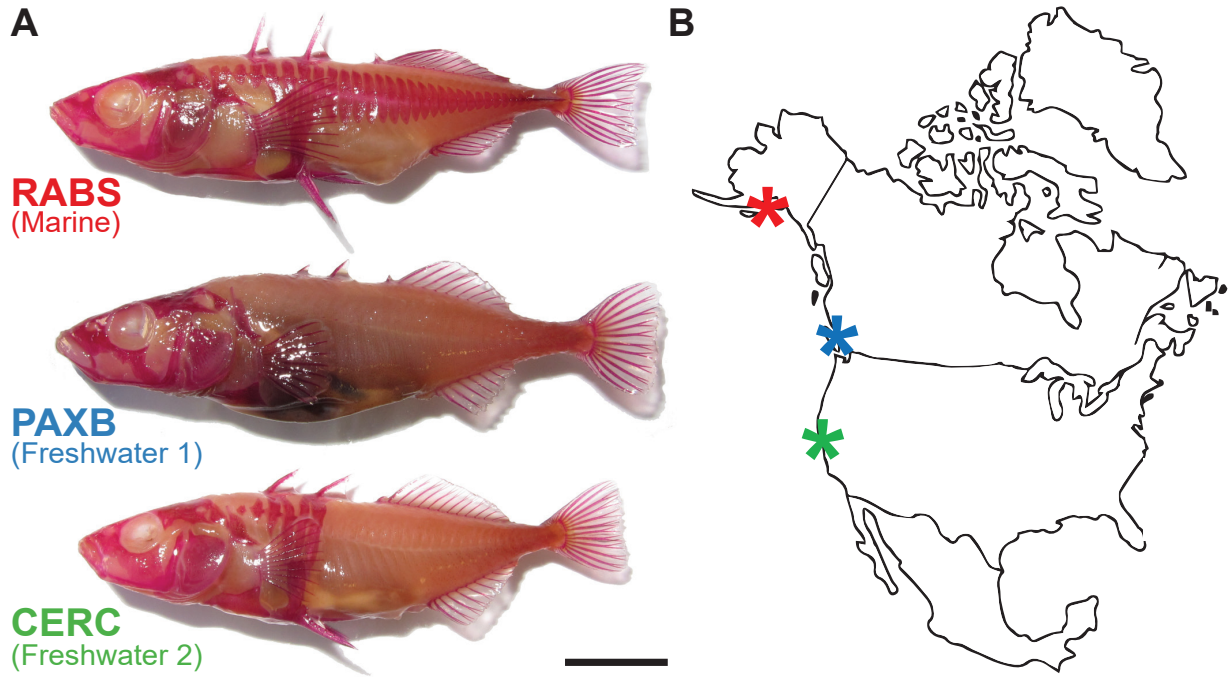

Figure 2.1: **Description and location of independent stickleback populations.** (A) Representative example adult male from each population stained with Alizarin Red S marking bone. Scale bar is 10 mm. (B) Source of each population on a map of North America denoted by color coded asterisks. RABS (marine) is from Rabbit Slough, Alaska, PAXB (freshwater 1) is from Paxton Lake, British Colombia, CERC (freshwater 2) is from Cerrito Creek, California.

Evolved tooth gain manifests late in development

Previous work showed that, compared with marine tooth number, the increased tooth number in PAXB fish manifests late in development (Cleves et al., 2014). We hypothesized that the independently derived freshwater population CERC also gains an increase in tooth number late in development. In support of this hypothesis, in sets of laboratory-reared developmental timecourse fish, both freshwater populations had similar tooth numbers to marine fish early in development. Later in development, however, CERC diverges earliest by ~10-15 mm, whereas PAXB diverges slightly later than CERC at ~20-25 mm (Fig. 2.4). Post 25 mm, both freshwater populations continue to increase total tooth number while marine tooth number plateaus.

As fish replace their teeth continuously, the differences in tooth number could result from an increase in new tooth formation and/or from a difference in tooth shedding dynamics. We hypothesized that the increased tooth number in freshwater fish results from a developmentally late increase in the tooth replacement rate, with more newly forming replacement teeth retained on the tooth plate. This model predicts that tooth germ number would differ

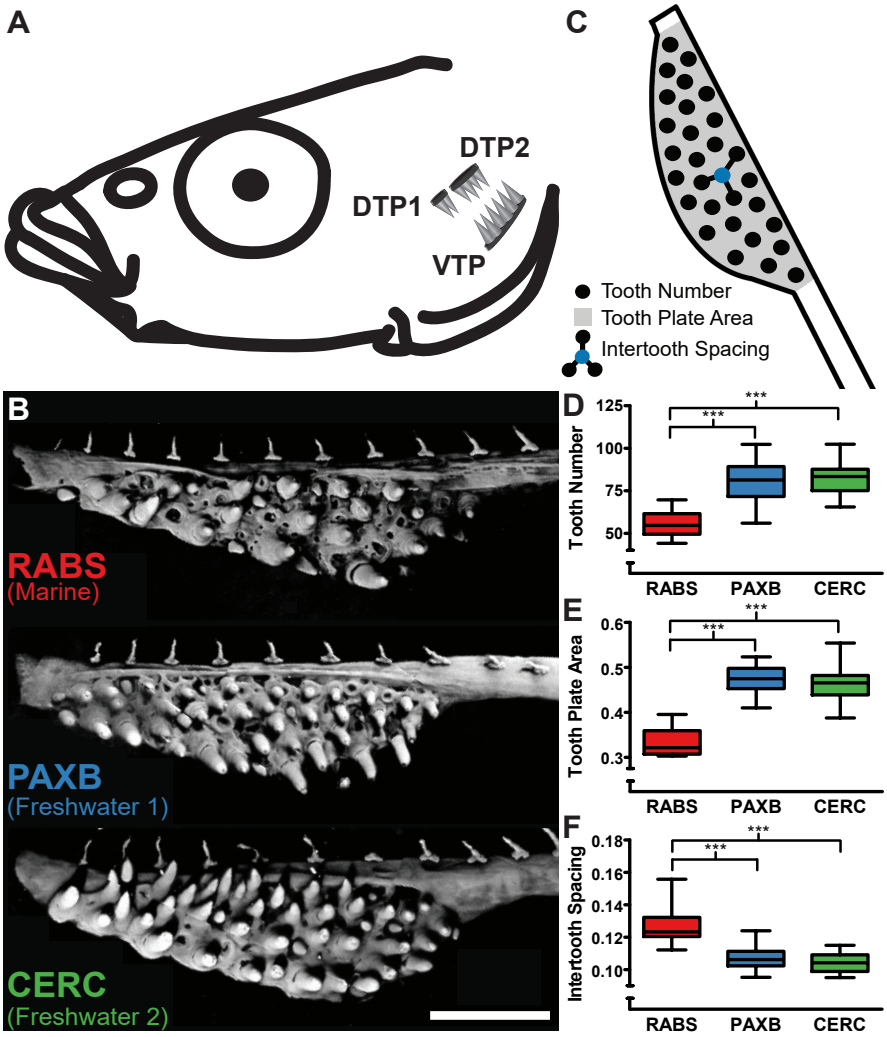

Figure 2.2: **Two freshwater stickleback populations exhibit evolved tooth gain.** (A) Location of three pharyngeal tooth plates in the stickleback head: VTP, ventral tooth plate on the fifth ceratobranchial; DTP1, dorsal tooth plate 1 (on the anterior pharyngobranchial); DTP2, dorsal tooth plate 2 (on the posterior pharyngobranchial); all three are bilaterally paired (only a unilateral set is shown). (B) Representative 3D projections of adult stickleback unilateral ventral tooth plates from three populations. Scale bar: 500 μm. (C) Depiction of tooth number, tooth plate area and intertooth spacing phenotypes. (D-F) Quantification of size-corrected total tooth number (D), tooth plate area (mm^2) (E), and intertooth spacing (mm) (F) in ventral pharyngeal tooth plates of laboratory-reared adults.***P<0.001 (one-way ANOVA using a Tukey-Kramer post-hoc test). (D-F) Respective sample size for each trait: RABS, n=19, 18, 18; PAXB, n=35, 32, 33; CERC, n=29, 29, 30.

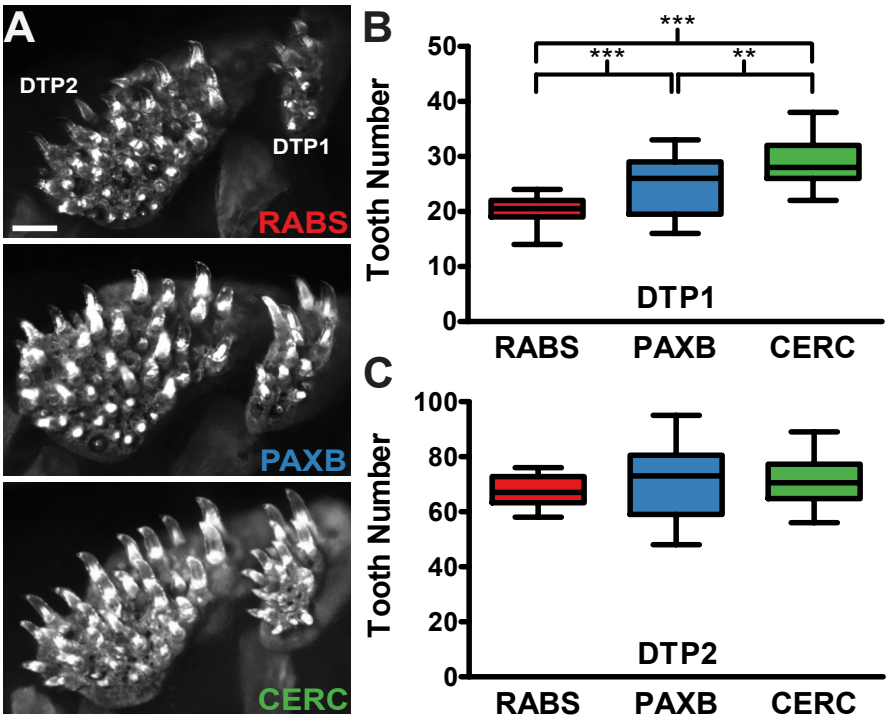

Figure 2.3: **Tooth number for dorsal tooth plate 1, but not 2, differs between populations.**
(A) Representative unilateral dorsal tooth plates. Scale bar is 200 μm. (B) Quantification of total DTP1 tooth number. (C) Quantification of total DTP2 tooth number. (B-C) Respective sample size for each trait: n=20 RABS, n=37 PAXB, n=25,26 CERC. ***P<0.001, **P<0.01 (one-way ANOVA using a Tukey-Kramer post hoc test).

at late but not early developmental stages. To test this hypothesis, we cut serial sections across different time points of each population to compare developing tooth germs over time. Similar to other vertebrates, stickleback teeth form at the interface of the epithelium and mesenchyme following stereotypic tooth development stages (these stages are reviewed by Thesleff, 2003) (Fig. 2.6A). At 15 mm and 25 mm, the populations do not have significantly different germ numbers, but by 25 mm both freshwater populations are trending towards having more developing germs. By 40 mm, both freshwater populations had significantly more tooth germs than marine fish, showing that both high-toothed freshwater populations form more teeth late in development and that the change in tooth number cannot only be attributed to differential tooth loss rates (Fig. 2.6B).

During the development of teeth and other epithelial appendages that develop from placodes, lateral signals from placodal cells inhibit interplacodal cells from adopting placode fates (Chuong et al., 2013; Jung et al., 1998; Mou et al., 2011; Noramly and Morgan, 1998). We hypothesized that the derived increase in tooth number in freshwater fish might result

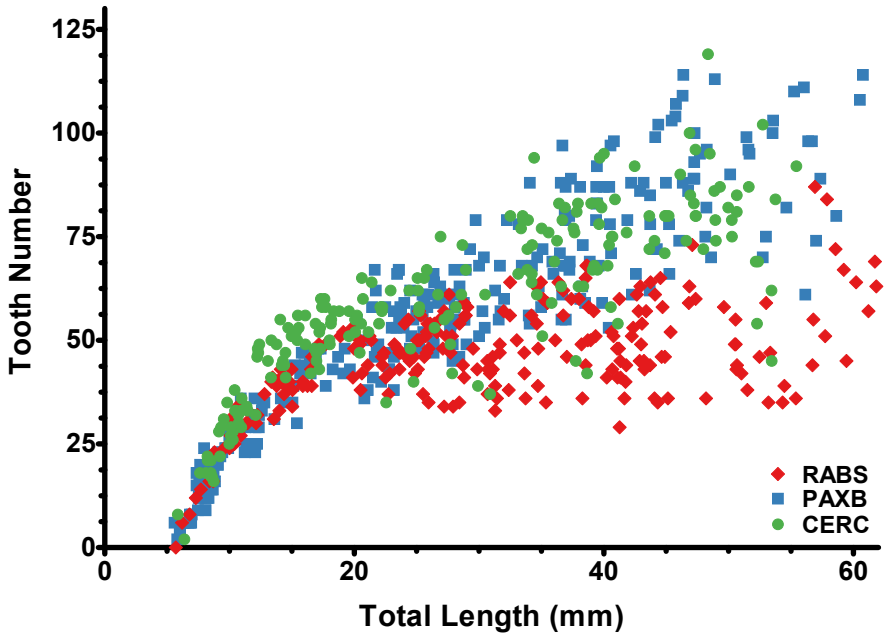

Figure 2.4: **In both freshwater populations, evolved tooth gain manifests late in development.**
Developmental timecourse of total ventral pharyngeal tooth number in the marine (RABS) and two freshwater (PAXB and CERC) populations. Total length is used as a proxy for age. CERC tooth number diverges at ~10-15 mm [binned CERC versus PAXB, and CERC versus RABS: $P<0.01$; PAXB versus RABS: not significant (ns); one-way ANOVA using a Tukey-Kramer post-hoc test], whereas PAXB tooth number diverges at ~20-25 mm (PAXB versus RABS, and CERC versus RABS: $P<0.01$; PAXB versus CERC: ns). Previously published points for RABS and PAXB are shown in gray in Fig. 2.5.

from smaller tooth germs, which may generate a reduced lateral inhibition signal, resulting in smaller intertooth spaces and more teeth. To test this, we measured tooth germ size by quantifying the area of individual developing tooth germs at early to mid-bell stage between populations at three time points: 15, 25 and 40 mm. Contrary to this hypothesis, tooth germ area was not significantly different between populations at each time point, although CERC trended towards exhibiting smaller germ size (Fig. 2.6C). Alternatively, the increase in tooth number could result from an additional wave of late-forming primary teeth, which would predict a shift towards younger germ stages in the freshwater populations. However, comparing the distribution of germ stages in all three populations revealed no significant differences (Fig. 2.6D), arguing against a model in which an additional single wave of teeth is added late, but instead suggesting differential replacement dynamics.

We further tested the hypothesis that tooth size might differ between populations, and

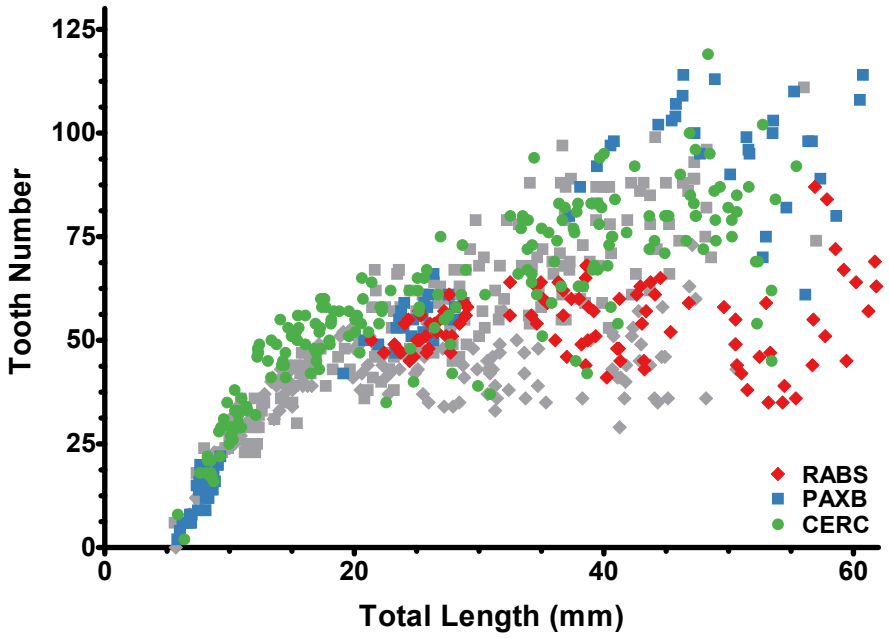

Figure 2.5: **Previously published PAXB and RABS data points.**
Points denoted in gray were previously published in Cleves et al., 2014 and included for comparison to CERC and later time points.

that smaller teeth in freshwater fish might result in a smaller zone of lateral inhibition (Osborn, 1971, 1978), by comparing tooth size from serial sections of erupted adult functional teeth. We found the adult teeth in both freshwater populations to be significantly narrower, but not shorter, than marine teeth (Fig. 2.7). In addition to possibly creating a smaller zone of lateral inhibition, decreased tooth width might indicate reduced time retained on the tooth plate in freshwater fish, further suggesting a difference in tooth cycling dynamics.

Increased rate of new tooth formation late in development underlies evolved tooth gain

To further test the hypothesis that increased tooth number in freshwater fish results from increased replacement rates, we quantified the rate of tooth replacement in adult fish using a pulse-chase method with vital dyes to mark new tooth formation. By pulsing first with Alizarin, waiting 2 weeks, then chasing with Calcein, ossifying teeth are marked at two points in time with red and green fluorescence, respectively, allowing the visualization of new teeth that formed between the two dye soaks (Calcein-positive, Alizarin-negative teeth; Fig. 2.8A). Using this method, we found that both freshwater populations have an increased number of new teeth compared with marine fish (Fig. 2.8B). To account for the total difference in tooth number between populations, we divided the number of new teeth by the total tooth number

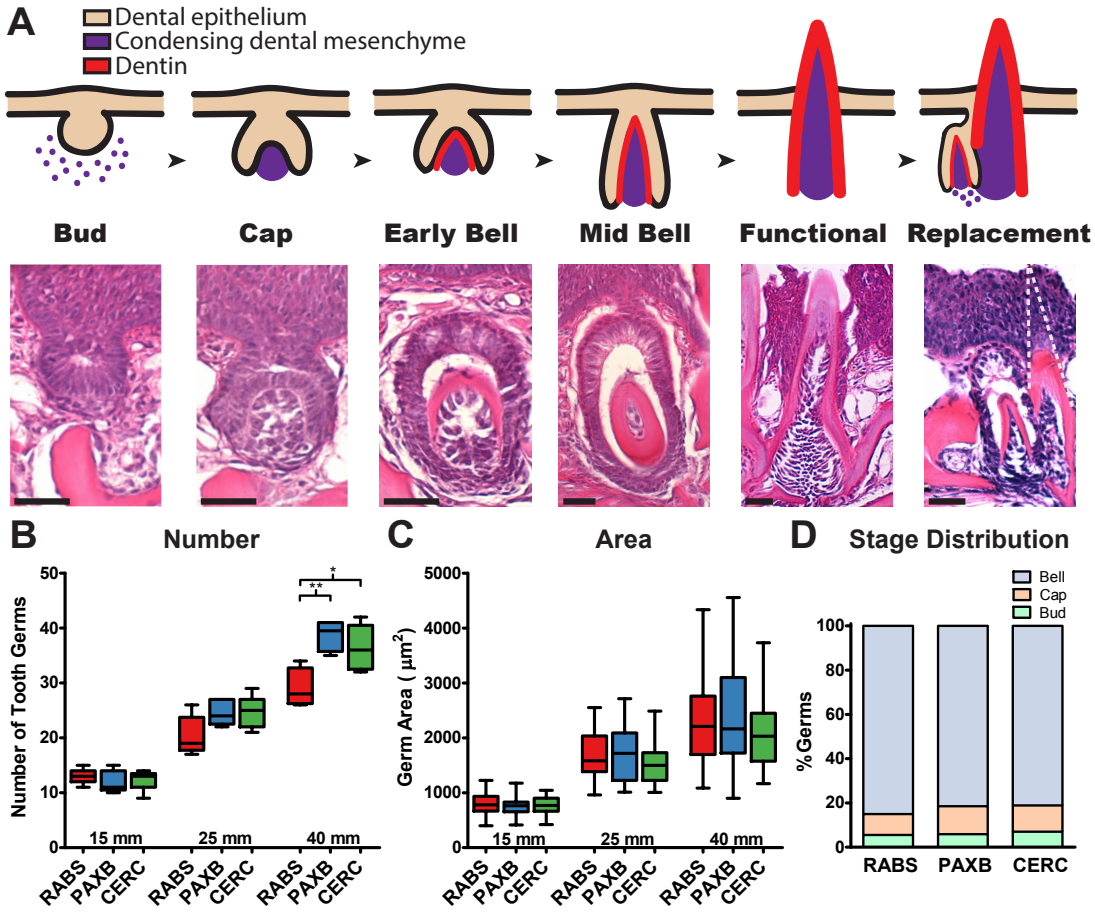

Figure 2.6: **Tooth germ number, but not area, differs between marine and freshwater fish late in development.**
(A) Stereotypic stages of tooth development from initial budding to tooth replacement, with schematic representations above and 6 μm stickleback sections beneath. Scale bars: 25 μm. The white dotted line outlines the adult tooth in an adjacent section. (B) Number of developing tooth germs from serially sectioned animals at 15, 25 and 40 mm across populations. n=5 for each population, except n=6 for 25 mm RABS and n=4 for 40 mm RABS and PAXB. (C) Tooth germ area at early to mid-bell stage. 15 mm: n=37 RABS, n=23 PAXB, n=28 CERC; 25 mm: n=33 RABS, n=36 PAXB, n=44 CERC; 40 mm: n=70 RABS, n=85 PAXB, n=72 CERC. No pairwise comparisons are significant. Average germ size for each animal between populations was also not significant. (D) Distribution of tooth germs by developmental stage from post tooth number divergence. Pooled 25 and 40 mm; n=200 RABS, n=254 PAXB, n=244 CERC. $^{**}P<0.01$, $^{*}P<0.05$ (one-way ANOVA using a Tukey-Kramer post-hoc test).

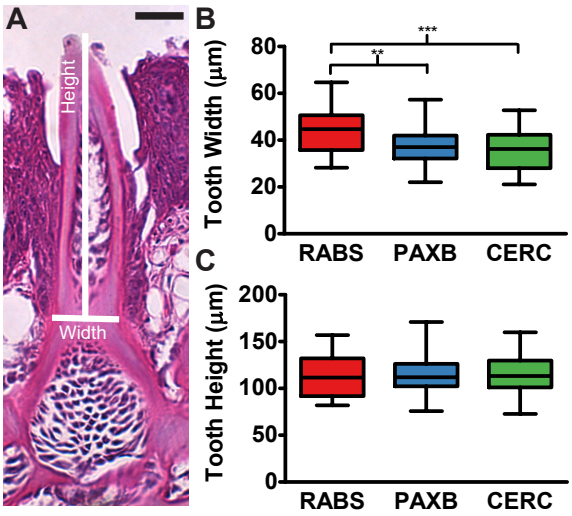

Figure 2.7: **Adult marine and freshwater teeth vary in width, but not height.** (A) Phenotyping example of adult teeth. Scale bar is 25 μm. (B) Tooth width. (C) Tooth height. (B-C) Sample Size: n=29 RABS, n=44 PAXB, n=37 CERC. ***P<0.001, **P<0.01 (one-way ANOVA using a Tukey-Kramer post hoc test).

to quantify a normalized rate of tooth gain. Both freshwater populations have a similarly increased normalized rate of tooth gain as compared with marine fish, both in adults and in 20 mm juveniles (Fig. 2.8C; Fig. 2.9).

As tooth loss rates during replacement could also affect tooth number, we tested the hypothesis that freshwater fish also have differential tooth shedding rates. Because we quantified the number of teeth observed in the developmental timecourses, as well as the new tooth gain rates quantified by pulse-chase experiments at both early and late stages, the number of teeth shed in each population could be inferred. We found that tooth shedding rates also differ between marine and freshwater populations (Table 1). These data show that two freshwater populations not only gain teeth late at an increased rate, but also shed teeth at a different rate, suggesting that the entire tooth replacement program has been sped up.

Localization of new teeth varies between freshwater populations

To examine whether marine and freshwater populations add new teeth in similar spatial patterns, we marked the position of newly formed teeth in adults. Surprisingly, we found that adult PAXB fish preferentially form new teeth on the medial edge or off the tooth plate medially, whereas CERC fish and marine RABS fish form most new teeth on the tooth plate, without an apparent medial bias (Fig. 2.10A). Comparing the number of new teeth off the tooth plate medially, PAXB is significantly different to CERC (Fig. 2.10B). However, the number of new teeth on the tooth plate is not significantly different between the two freshwater populations (Fig. 2.10C). Comparing total numbers of teeth on and off the tooth

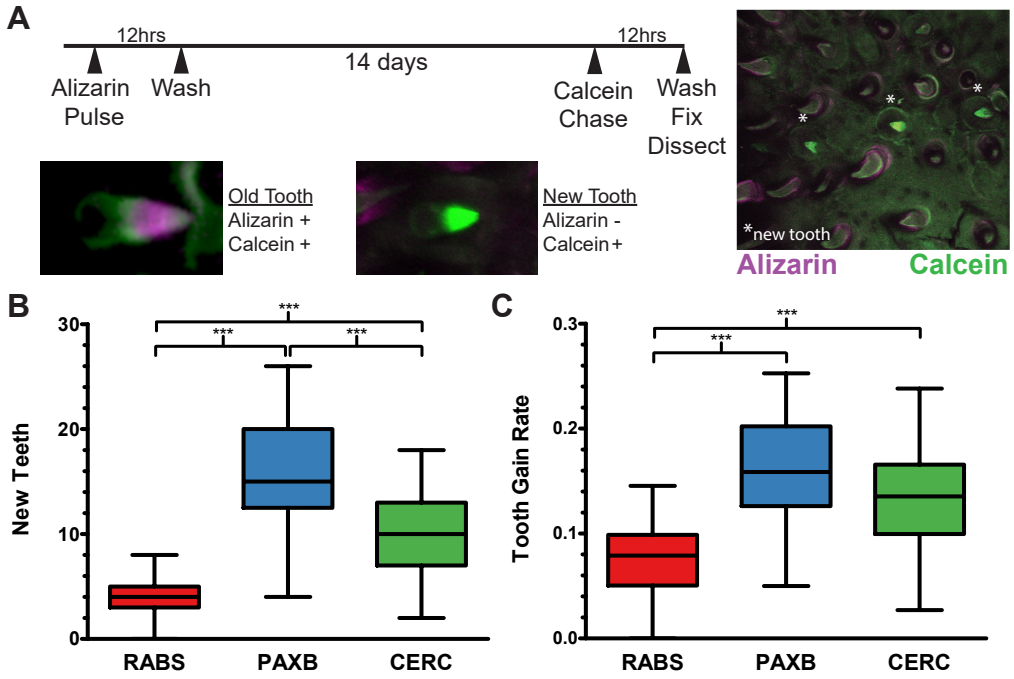

Figure 2.8: **Pulse-chase reveals that both freshwater populations have elevated rates of new tooth formation.**
(A) Schematic of pulse-chase method using Alizarin and Calcein to mark developing teeth in living fish. Examples of a field of teeth (right) and individually classified teeth (beneath) are included. Alizarin is false colored magenta. White asterisks denote new teeth. (B) Number of new teeth. (C) Normalized rates of tooth gain (new teeth divided by total teeth). $***P<0.001$ (one-way ANOVA using a Tukey-Kramer post-hoc test). (B,C) Sample size: n=33 RABS, n=25 PAXB, n=22 CERC.

plate for all three populations (Table 2.2) shows that although PAXB makes more new teeth off the tooth plate than either CERC or RABS, the number of total teeth on the tooth plate is still significantly larger in PAXB compared with CERC and RABS. Therefore, distinct developmental mechanisms in the two high-toothed freshwater populations result in different timing of tooth number divergence and different spatial patterns of new tooth formation, supporting a different mechanism of evolved tooth gain.

Unique genetic basis of evolved tooth gain

To begin to understand the genetic basis of evolved tooth gain in the CERC population, we performed genome-wide linkage mapping of tooth patterning traits. Previous work on a large PAXB x marine F2 cross identified five genomic regions controlling evolved tooth gain in PAXB fish (Miller et al., 2014). We generated a CERC x marine F2 cross and determined genome-wide genotypes using Genotyping-by-Sequencing (GBS)(Elshire et al., 2011; Glazer

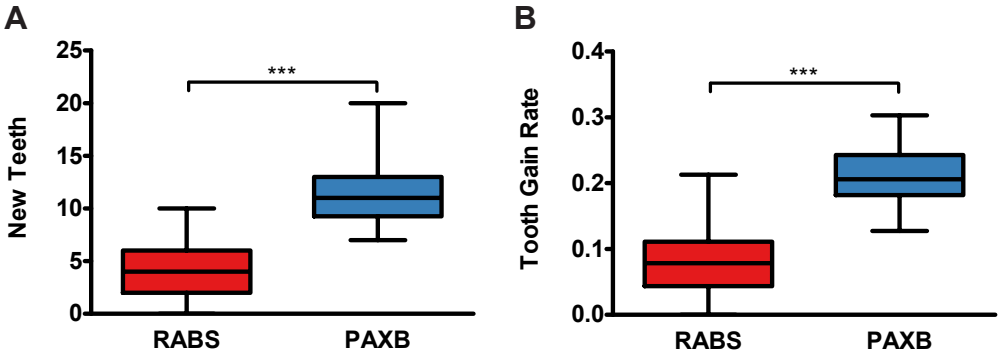

Figure 2.9: **Early pulse-chase reveals tooth gain rates are relatively fixed early in marine and freshwater sticklebacks.**
(A-B) Pulse-chase performed on two month, ~20 mm, PAXB and RABS sticklebacks show new tooth number (A) and tooth gain rate (B) differences are established early and are comparable to adult gain rates. $^{***}P<0.001$ (two-tailed t-test).

	Population		
	RABS	PAXB	CERC
20 mm average tooth number (~2 month)	51.8	54.8	55.6
40 mm average tooth number (~6 month)	54.4	98.2	75.4
Average new teeth per two weeks	3.8	16.2	10.2
Expected gain in tooth number	30.5	129.3	81.8
Actual gain in tooth number	2.6	43.4	19.8
Teeth shed (expected minus actual)	28	85.9	62.1
Inferred teeth shed per two weeks	3.5	10.7	7.8
Net gain in tooth number per two weeks	0.3	5.4	2.6
Tooth gain rate (%)	7.3	16.4	13.9
Inferred tooth shedding rate (%)	6.4	10.9	10.3
Net fain rate (%)	0.8	5.5	3.6

Table 2.1: **Tooth cycling dynamics.**
Average 20 mm tooth number sample size: RABS=31, PAXB=24, CERC=30. Average 40 mm tooth number sample size: RABS=33, PAXB=25, CERC=22 (see Figure 2.2). Average new teeth per two weeks is derived from the pulse-chase (see Figure 2.8). Expected gain in tooth number is the average new teeth per two weeks multiplied by 8 to represent the 4 month period. Actual gain in tooth number is the 20 mm tooth number minus the 40 mm tooth number. Net gain in tooth number per two weeks is the average new teeth per two weeks minus the teeth shed per two weeks. All rates are new teeth/teeth shed/net gain divided by the 40 mm tooth number to correct for overall tooth number differences.

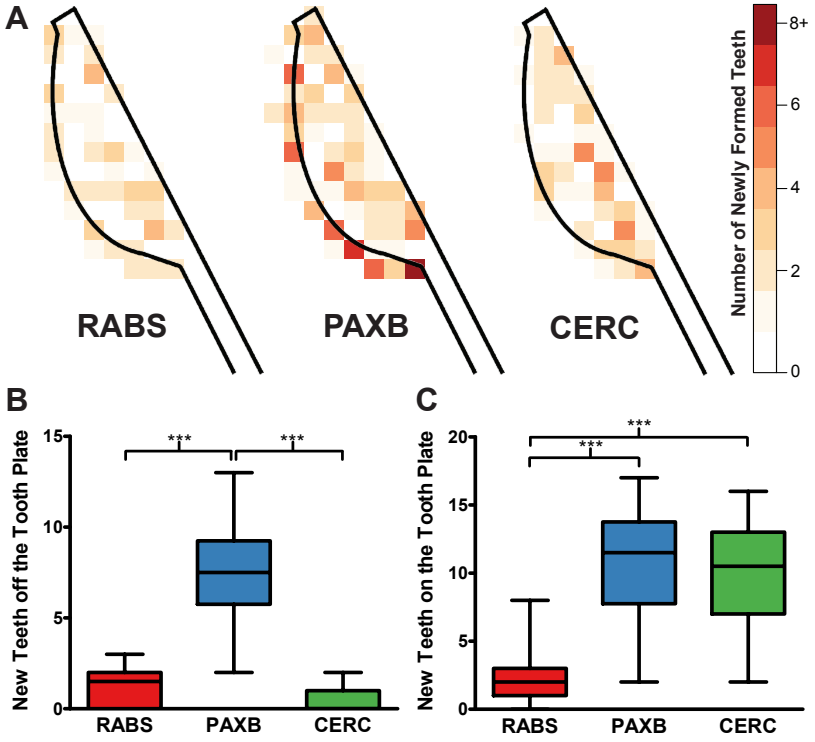

Figure 2.10: **Distinct spatial patterns of new teeth in two high-toothed freshwater populations.**
(A) Heat maps of the spatial location of newly formed teeth on an idealized tooth plate by population. (B) New teeth off the tooth plate. (C) New teeth on the tooth plate. ***P<0.001 (one-way ANOVA using a Tukey- Kramer post-hoc test). (A-C) Sample size: n=14 for each population (see Table 2.2).

Population	Total Teeth	Teeth off VTP	Teeth on VTP	New teeth off VTP	New teeth on VTP
RABS	59.4 (± 1.5)	5.6 (± 0.6)	53.7 (± 1.6)	1.2 (± 0.3)	2.4 (± 0.5)
PAXB	98.9 (± 2.6)	12.6(± 0.9)	86.3 (± 2.2)	7.5 (± 0.7)	10.6 (± 1.2)
CERC	79.3 (± 2.2)	0.9 (± 0.3)	78.4 (± 2.1)	0.5 (± 0.2)	10.1 (± 1.0)

Table 2.2: **Spatial location of teeth by population.**
Mean values are given for each trait ± standard error (VTP= Ventral Tooth Plate). All pairwise comparisons between populations for total teeth, teeth off VTP, and teeth on VTP are significantly different (P<0.001, with the exception of PAXB vs. CERC teeth on VTP being P<0.05). New teeth off and on VTP are plotted in Figure 2.10B,C (Sample size: n=14 for each population).

et al., 2015) to test whether the convergently evolved tooth gain in freshwater fish (PAXB and CERC) occurs through a similar genetic architecture. Since, during development, CERC fish gain teeth earlier than PAXB fish (Fig. 2.4) and form new teeth in adults in a different spatial pattern (Fig. 2.10), we hypothesized that the genetic basis controlling evolved tooth gain would differ in at least some respects between the two high-toothed freshwater populations.

Supporting this hypothesis, we identified six genomic regions (quantitative trait loci, or QTL) controlling ventral pharyngeal tooth patterning in the CERC cross (Figs. 2.11 and 2.13, Tables 2.3 and 2.4), including five tooth number QTL, two intertooth spacing QTL, and no area QTL. One tooth number and one spacing QTL map to the same region on chromosome 18. In these CERC x marine F2 fish, as was found for a PAXB x marine F2 (~6 months) tooth plate area and intertooth spacing, yet tooth plate area and intertooth spacing were not significantly correlated with each other (Fig. 2.12), further supporting the idea that tooth plate area and intertooth spacing are genetically separable. We also detected two DTP1 tooth number QTL and a single DTP2 tooth number QTL (Fig. 2.14, Tables 2.3 and 2.4). Of all identified CERC cross QTL, only one QTL on chromosome 21 overlaps the QTL previously identified in the PAXB cross (Miller et al., 2014; Cleves et al., 2014) (Fig. 2.11). However, the peak marker for the PAXB QTL is not in the CERC interval, suggesting that these might be two distinct loci.

Trait	Chr	Peak position (cM)	LOD score	PVE	1.5 LOD interval (cM)	1.5 LOD interval (Mb)	Mean Phenotype ± Standard Error		
							MM	MF	FF
VTP Tooth Number	4	7.7	4.2	6.8	0-15.4	0-3.1	50.7 (± 1.4)	55.1 (± 0.8)	54.8 (± 1.4)
VTP Tooth Number	13	0	4.8	7.8	0-8	1.0-1.9	52.5 (± 1.4)	53.5 (± 0.8)	58.4 (± 1.4)
VTP Tooth Number	17	51	4.5	7.3	32.8-71.7	3.7-11.7	52.2 (± 1.2)	53.6 (± 0.8)	58.9 (± 1.4)
VTP Tooth Number	18	32.7	5.5	9.0	13.8-38.2	2.9-11.2	57.6 (± 1.2)	54.7 (± 0.8)	50.4 (± 1.1)
VTP Tooth Number	21	19	8.0	13.5	14.6-31.3	3.7-9.0	49.3 (± 1.2)	55.4 (± 0.8)	56.8 (± 1.2)
VTP Intertooth Spacing	9	27.7	4.7	11.3	21.2-35.9	6.7-16.4	0.105 (± 0.001)	0.108 (± 0.001)	0.114 (± 0.002)
VTP Intertooth Spacing	18	28.7	4.1	9.9	17.8-49.4	4.8-13.2	0.104 (± 0.002)	0.108 (± 0.001)	0.113 (± 0.001)
DTP1 Tooth Number	18	2.5	4.1	9.3	1.1-13.8	0-3.4	23.2 (± 0.5)	20.8 (± 0.4)	20.7 (± 0.5)
DTP1 Tooth Number	19	140.6	5.7	13.1	102.4-140.6	2.4-17.8	19.7 (± 0.6)	21.9 (± 0.4)	25.3 (± 1.8)
DTP2 Tooth Number	16	61	5.7	14.2	47.1-72.0	13.2-17.6	59.5 (± 1.3)	64.3 (± 0.9)	69.2 (±1.3)

Table 2.3: **Summary of CERC tooth patterning QTL.**
Genotypic classes of F2 fish are abbreviated: MM=homozygous marine, MF=heterozygous, FF=homozygous freshwater. LOD is the logarithm of the odds and PVE is the percentage of phenotypic variance explained (cM=centiMorgans, Mb=megabases, VTP=Ventral Tooth Plate, DTP1=Dorsal Tooth Plate 1, DTP2=Dorsal Tooth Plate 2). Intertooth spacing is measured in mm.

The QTL on chromosome 21 has the largest effect on tooth number in each cross, and the PAXB QTL has recently been associated with cis-regulatory changes in an excellent candidate gene, *Bmp6* (Cleves et al., 2014). Candidate genes within the CERC cross QTL include another BMP pathway member, *Bmp7a*, and a downstream effector of BMP signaling, *Msxe*, both located on chromosome 17. The mammalian homologs of *Bmp7a* and *Msxe* cause tooth agenesis when deleted in mice (Satokata and Maas, 1994; Zouvelou et al., 2009). Another candidate gene, *Pitx2*, maps near the peak marker of the chromosome 4

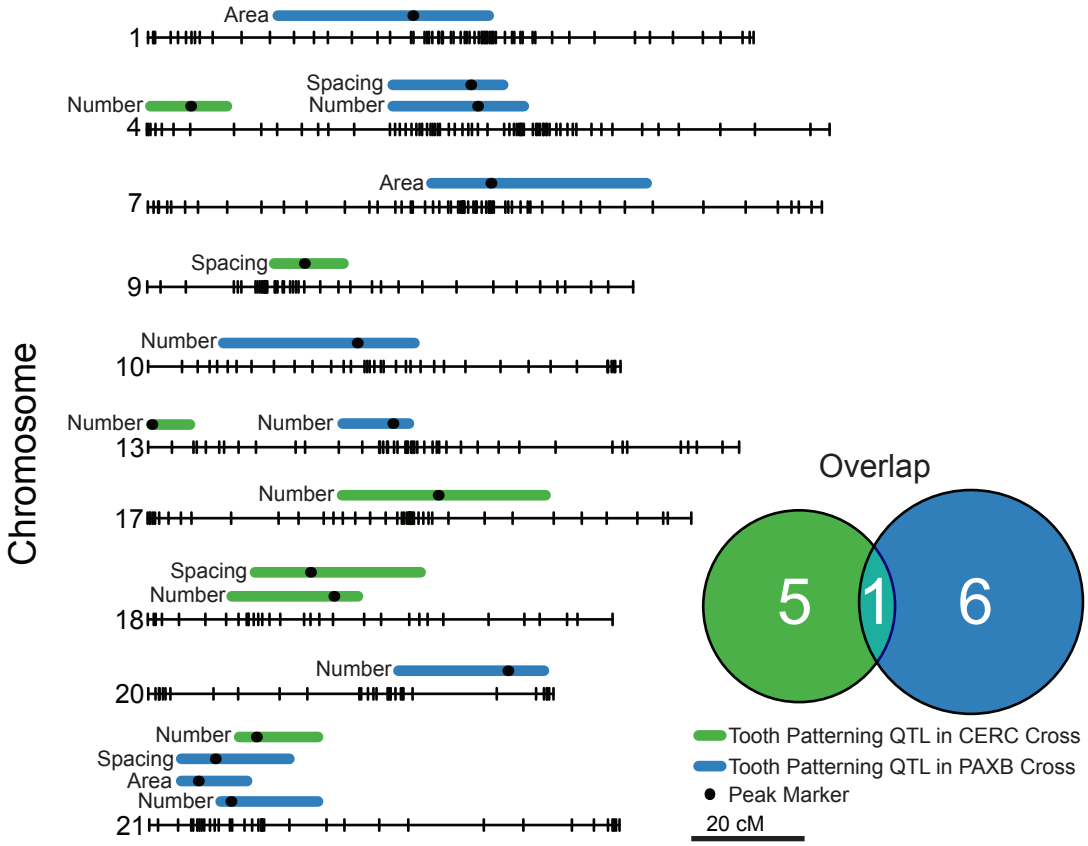

Figure 2.11: **Largely distinct genetic bases underlie evolved tooth gain in two high-toothed freshwater populations.**
Summary of identified tooth patterning QTL from a CERC x marine F2 cross (this study) compared with a PAXB x marine F2 cross (Cleves et al., 2014; Miller et al., 2014). Each black horizontal line represents a chromosome and each vertical line is a genetic marker. Each colored bar represents the 1.5 LOD interval with the black dot denoting the peak marker. The overlap between CERC and PAXB QTL is depicted in the Venn diagram.

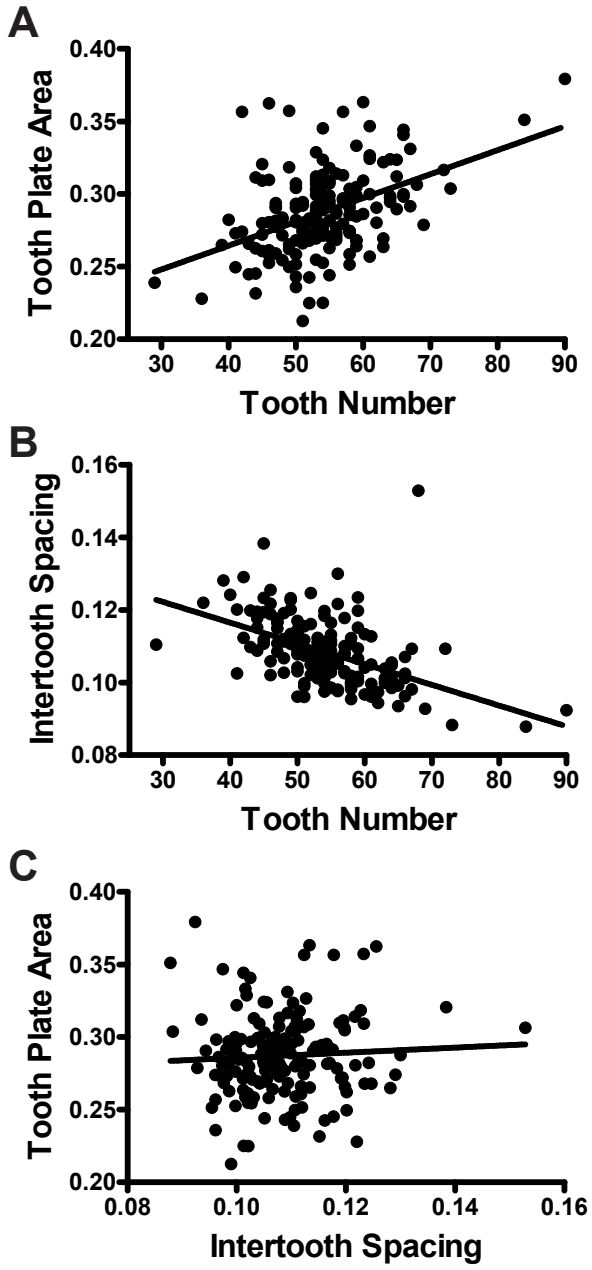

Figure 2.12: **Correlation of tooth number, tooth plate area, and intertooth spacing phenotypes in F2 cross.**
(A-C) Pairwise correlations of three ventral pharyngeal tooth patterning traits from CERC x marine F2 cross. (A) Tooth plate area and tooth number are positively correlated (P<0.001, r^2=0.20). (B) Intertooth spacing and tooth number are negatively correlated (P<0.001, r^2=0.23). (C) Tooth plate area and intertooth spacing are not correlated (P=0.47, r^2=0.003). (linear regression).

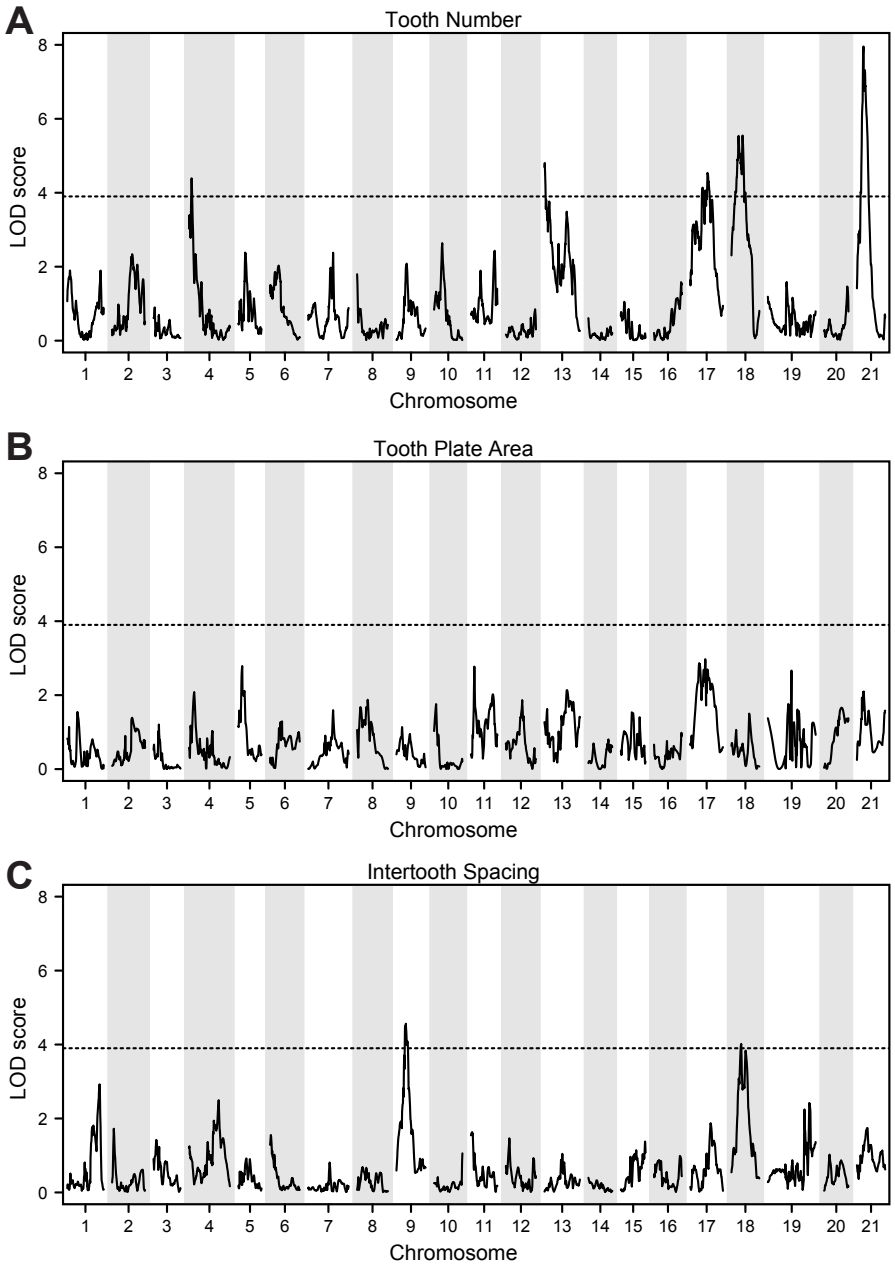

Figure 2.13: **Genome wide QTL scans for tooth number, area, and intertooth spacing.**
(A-C) Manhattan plots for tooth number (A), tooth plate area (B), and intertooth spacing (C). The y-axis is the logarithm of the odds (LOD) score of the association between genotype and phenotype. The dotted line is the genome wide significance threshold of alpha=0.05 determined by permutation tests.

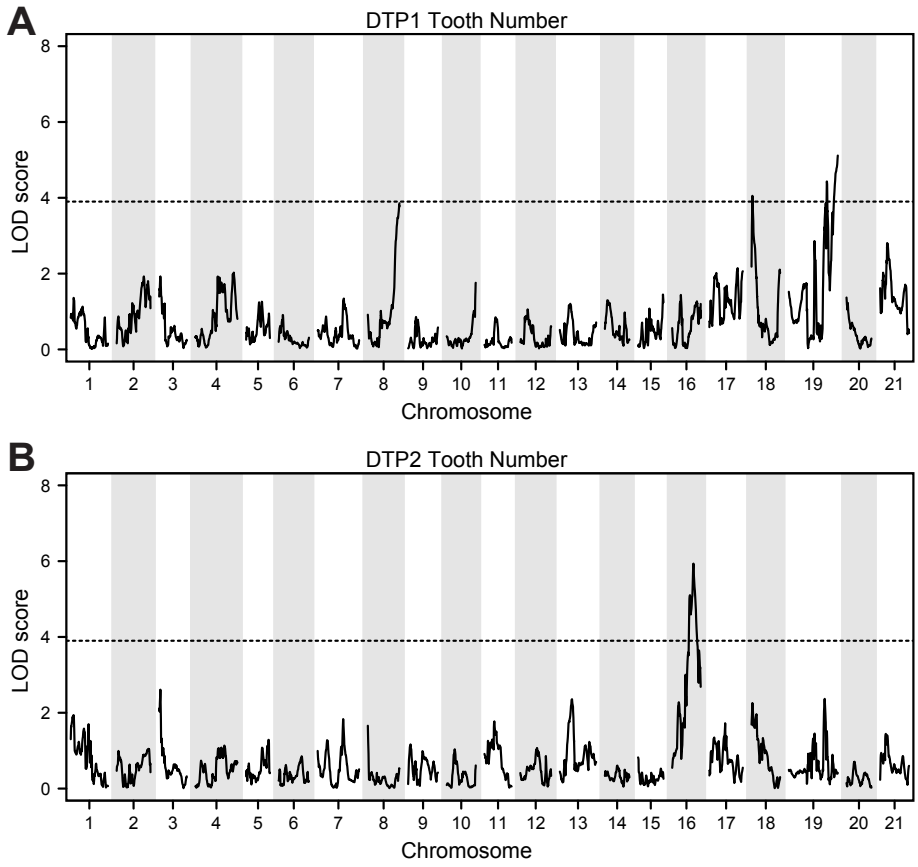

Figure 2.14: **Genome wide QTL scans for dorsal pharyngeal tooth number.** (A-B) Manhattan plots for dorsal pharyngeal tooth number on DTP1 (A) and DTP2 (B). The y-axis is the logarithm of the odds (LOD) score of the association between genotype and phenotype. The dotted line is the genome wide significance threshold of alpha=0.05 determined by permutation tests.

QTL and is expressed early in the tooth field and later in the epithelium of both primary and replacement teeth in other fish (Smith et al., 2009b).

Overall, the largely non-overlapping sets of genomic regions controlling dental patterning in PAXB and CERC suggest that the convergent evolution of tooth gain in these two freshwater populations is controlled by largely distinct genetic mechanisms.

2.5 Discussion

Evolved tooth gain occurs through a developmentally late increased rate of new tooth formation in two independently derived freshwater populations

Here we identify a second derived freshwater stickleback population (Cerrito Creek, CERC)

Trait	Chr	Peak position (cM)	Peak Marker	Peak LOD score	Left 1.5 LOD			Right 1.5 LOD			FDR *P*-value
					Marker	Position (cM)	Score	Marker	Position (cM)	Score	
VTP Tooth Number	4	7.7	20_3	4.2	65_1	0	3.0	20_4	15.4	1.6	0.026
VTP Tooth Number	13	0	51_3	4.8	51_3	0	4.7	52_1	8.0	3.3	0.0076
VTP Tooth Number	17	51	18_7	4.5	25_7	32.8	3.0	18_11	71.7	1.9	0.014
VTP Tooth Number	18	32.7	21_12	5.5	29_7	13.8	4.0	21_13	38.2	3.7	0.0024
VTP Tooth Number	21	19	16_11	8.0	16_8	14.6	5.9	16_18	31.3	5.4	0.0001
VTP Intertooth Spacing	9	27.7	8_9	4.7	8_25	21.2	2.6	8_6	35.9	2.8	0.010
VTP Intertooth Spacing	18	28.7	21_10	4.1	21_1	17.8	2.1	32_2	49.4	2.3	0.035
DTP1 Tooth Number	18	2.5	29_3	4.1	29_1	1.1	2.6	29_7	13.8	1.9	0.036
DTP1 Tooth Number	19	140.6	3_28	5.7	34_5	102.4	3.2	3_28	140.6	5.1	0.0021
DTP2 Tooth Number	16	61	44_4	5.7	14_17	47.1	3.5	44_3	72.0	3.8	0.0017

Table 2.4: **CERC QTL interval details.**
LOD is the logarithm of the odds and FDR is the false discovery rate (cM=centiMorgans, VTP=Ventral Tooth Plate, DTP1=Dorsal Tooth Plate 1, DTP2=Dorsal Tooth Plate 2).

that has evolved more teeth than ancestral marine fish. This increase in tooth number, like the increased tooth number in the Canadian Paxton benthic (PAXB) population (Cleves et al., 2014), occurs at least in part through an expansion of the tooth plate area (tooth field) as well as a decrease in intertooth spacing. In both freshwater populations, the increased tooth number occurs late in development, is associated with an increased number of tooth germs in juveniles and adults, and an increased rate of new tooth formation in adults. Thus, evolved differences have resulted in the convergent evolution of changes in dental patterning in the two independently derived freshwater populations. In freshwater x marine F2 crosses from both freshwater populations, tooth number is highly correlated with tooth plate area (field size) and intertooth spacing, whereas tooth plate area and intertooth spacing are not correlated. This lack of correlation between tooth plate area and intertooth spacing suggests separable mechanisms for specifying the area of the tooth plate and the spacing of the teeth, which is supported by findings in mice that tooth field size is specified by *Osr2* without any reported tooth spacing phenotype (Zhang et al., 2009).

Both freshwater populations have an increased number of teeth through an increase in tooth germ number, ruling out the possibility that the differences in adult tooth number arise solely through differential shedding dynamics. Despite having more developing tooth germs, the germs are not smaller in area in the high-toothed freshwater populations, arguing against an increase in tooth number via reduced lateral inhibition signals due to a smaller tooth germ. Unlike in cichlids, where developing tooth germ size has been shown to correlate with intertooth spacing (Fraser et al., 2008), we found no significant difference in germ sizes between populations despite different intertooth spacing. However, this cichlid study measured spacing of the first few *Shh*-expressing germs in the oral jaws of wholemount embryos, whereas we measured pharyngeal tooth germ size in histological sections and pharyngeal tooth spacing in juveniles and adults by ossified tooth pattern. Nevertheless, both freshwater populations have adult teeth that are narrower than marine teeth, which could result in a reduced zone of inhibition from adult teeth, perhaps consistent with the observed

activation of the tooth replacement process in alligators upon adult tooth removal (Wu et al., 2013). The increased number of tooth germs combined with the increased new tooth formation rates in adults support a model (Fig. 2.15) whereby the tooth replacement program has been sped up in the two independently derived freshwater populations, and this increased replacement rate underlies evolved tooth gain.

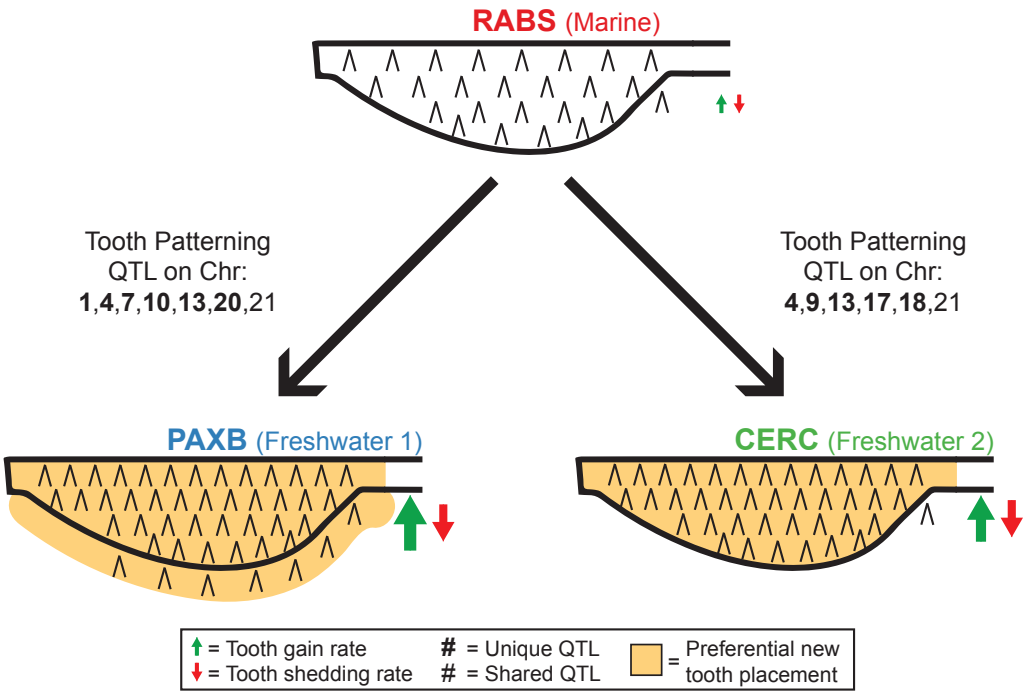

Figure 2.15: **Model for convergent evolution of tooth gain in two freshwater populations.**
Evolved tooth gain in two independently derived freshwater stickleback populations (PAXB and CERC) occurs through increased tooth replacement rates and multiple distinct mechanisms, such as the different spatial placement of new teeth and a largely non-overlapping genetic basis. Shading indicates preferred regions of new tooth placement. Green and red arrow size is representative of the relative levels of tooth gain and shedding rates between populations. The PAXB and CERC QTL on chromosome 21 overlap, whereas the PAXB and CERC QTL on chromosome 4 do not.

Most polyphyodonts, unlike diphyodont humans, have replacement teeth adjacent to the functional teeth they replace and that do not physically dislodge the older primary tooth. In basal polyphyodont vertebrates, like sharks, tooth replacement occurs in tooth families, where discrete tooth positions contain a developmentally staggered series of replacement teeth (Reif, 1984; Smith et al., 2009a). Although a few fish species, such as zebrafish, medaka and gobies, have been reported to have tooth families (Abduweli et al., 2014; Huysseune,

2006; Huysseune et al., 1998; Moriyama et al., 2010; Van der heyden and Huysseune, 2000), most teleosts lack obvious multigerm tooth families, instead appearing to replace teeth on an individual basis as has been termed one-for-one replacement, such as in rainbow trout, Lake Malawi cichlids, Mexican tetra, among others (Atukorala and Franz-Odendaal, 2014; Bemis et al., 2005; Fraser et al., 2006, 2013; Kerr, 1960; Motta, 1984; Wakita et al., 1977). In both cases, replacement teeth can be present on the tooth plate before the previous tooth is shed and can contribute to the functional dentition. Recently, Tucker and Fraser (2014) proposed that dental diversity could arise in a system of continuous tooth replacement by shifting the replacement program to produce an adaptive advantage. Supporting that proposal, here we find that the rate of new tooth formation is significantly higher in both freshwater populations than in their marine counterpart, resulting in increased tooth number late in development. Although it is formally possible that newly formed teeth in adults could be late-forming primary teeth, we interpret the majority of late-forming new teeth to be replacement teeth based on their frequent proximity to large old teeth or craters of recently shed teeth.

Distinct developmental bases underlie convergently evolved tooth gain

A second main finding of this study is that despite converging on the same adult phenotype of increased tooth number through an increased rate of new tooth formation late in development, two independently derived freshwater stickleback populations have increased tooth number via distinct developmental mechanisms, with different timing of divergence and spatially different patterns of new tooth formation.

First, comparing the developmental timecourse trajectories shows that although both high-toothed freshwater populations increase tooth number late, but not early, the increase in tooth number appears to occur earlier in development in CERC (10-15 mm) than in PAXB (20-25 mm) fish. Second, although both freshwater populations add new teeth on and off the tooth plate late, many new teeth in PAXB fish form medially off the edge of the tooth plate whereas most new teeth in CERC fish form on the tooth plate. We hypothesize that newly formed teeth off the tooth plate in the PAXB population function to expand the area of the tooth plate, which is larger in PAXB than in marine or CERC fish, which add fewer teeth off the tooth plate. The different spatial patterns of new tooth formation could result from different programs of primary tooth placement (e.g. the PAXB population but not the CERC population might add a medial row of primary teeth late during development). Arguing against this model is the lack of any difference in the distribution of germ sizes in the three populations, instead suggesting a model of altered replacement dynamics. Together, our findings suggest that some features of tooth development appear more constrained (e.g. the size of early tooth germs, early larval tooth number) than others (e.g. the rate and the spatial pattern of new tooth formation in adults).

Distinct genetic bases underlie convergently evolved tooth gain

A third main finding of this study is that two independently derived freshwater stickleback populations have evolved more teeth via largely distinct genetic mechanisms. These different

genetic mechanisms are perhaps surprising as previous work in sticklebacks has shown that the genetic basis of many derived traits, including loss of armored plates (Colosimo et al., 2005), reduced pelvis (Chan et al., 2010; Shapiro et al., 2004), reduced pigmentation (Miller et al., 2007), reduced gill raker number (Glazer et al., 2014) and increased branchial bone length (Erickson et al., 2014), have similar genetic bases in multiple freshwater populations. Largely distinct genetic bases of evolved tooth gain could result from differences in available genetic variation in the two freshwater populations, pleiotropy of tooth patterning with other traits that differ in the two freshwater populations, and/or different diets in the two freshwater niches being better processed by differently patterned pharyngeal jaws. Additionally, serially repeated structures, such as teeth, that might be functionally redundant could be less constrained genetically to evolve changes than previously studied traits.

Despite the polygenic nature of evolved tooth gain, our genome- wide linkage mapping using GBS identified eight unlinked genomic regions that control pharyngeal tooth patterning in the high-toothed CERC freshwater population. For ventral pharyngeal tooth patterning, we identified five tooth number QTL and two intertooth spacing QTL. Only one genomic region on chromosome 21 is shared between the two high-toothed freshwater populations. This QTL also has the largest effect on tooth number in each cross. However, the peak marker for the PAXB QTL is not included in the CERC QTL interval, suggesting the two chromosome 21 QTL might have distinct genetic bases as well. Thus, it appears that similar changes in morphology (more teeth) have evolved via largely distinct developmental genetic mechanisms, as has been found in sex comb patterning (Tanaka et al., 2009) and wing size (Zwaan et al., 2000) in Drosophila, trunk elongation in salamanders (Parra-Olea and Wake, 2001) and eye loss in different cavefish species (Stemmer et al., 2015).

A largely distinct genetic basis of evolved tooth gain was also detected for dorsal pharyngeal tooth number. We detected two genomic regions controlling tooth number on DTP1 and only a single genomic region controlling tooth number on DTP2, although DTP2 tooth number was not significantly different between marine and freshwater fish. However, CERC freshwater fish trended towards having more DTP2 teeth than marine fish (P=0.09). Also, detecting QTL does not require phenotypic differences between populations, as different populations can have the same quantitative phenotype due to different combinations of positive and negative allelic effects. None of the three detected QTL from the CERC cross had any significant effect on dorsal pharyngeal tooth number in the PAXB cross.

The genetic basis of dorsal and ventral tooth patterning is also largely modular, as two of the three dorsal tooth number QTL have no significant effects on ventral pharyngeal tooth number in either the CERC or PAXB cross. Similar modularity for evolved differences in dorsal and ventral pharyngeal tooth number was also previously reported in sticklebacks (Miller et al., 2014). Thus, tooth number is highly modular at a genetic level, with different loci controlling dorsal and ventral pharyngeal tooth number in both crosses. Modularity of the dentition can be seen across vertebrate lineages, as in *Cypriniformes* such as zebrafish, which have uncoupled tooth patterning in the dorsal and ventral pharynx, completely losing dorsal pharyngeal teeth while retaining ventral pharyngeal teeth (Stock, 2007). In zebrafish, the addition of a single transgene driving ubiquitous *Ectodysplasin* is sufficient to drive the

formation of ancestrally lost dorsal pharyngeal teeth (Aigler et al., 2014). In mice, strong support for genetic modularity of the dentition has also been found. *Dlx1/Dlx2* double mutants lack dorsal (maxillary) molars but other teeth are unaffected (Qiu et al., 1997; Thomas et al., 1997), and *activin A* mutants lack incisors and ventral (mandibular) molars whereas dorsal molars are unaffected (Ferguson et al., 1998). Similarly, in *Gli2*$-/-$; *Gli3*$+/-$ mice dorsal (maxillary) incisors are more severely affected than ventral (mandibular) incisors (Hardcastle et al., 1998).

Several outstanding candidate genes lie within the QTL detected in the CERCmarine cross. *Pitx2* lies close to the peak marker on the chromosome 4 QTL and is required for tooth development in mice (Lu et al., 1999) and humans (Childers and Wright, 1986; Semina et al., 1996). *Pitx2* is also expressed in the epithelium connecting the primary tooth to the replacement tooth in some polyphyodonts (Fraser et al., 2013; Smith et al., 2009b) and has been hypothesized to be important for the tooth replacement process. Pitx homeodomain proteins have been shown to bind a mouse *Bmp4* tooth enhancer, with this binding site required for *Bmp4* enhancer activity (Jumlongras et al., 2012). *Pitx2* has also been shown to inhibit the BMP antagonists *Bmper* and *Nog* through miR200c in dental epithelium in mice (Cao et al., 2013) and to regulate the Wnt signaling pathway (Vadlamudi et al., 2005). *Msxe*, on chromosome 17, is a downstream effector of BMP signaling, and mutations in the mammalian ortholog, *Msx1*, cause tooth agenesis in mice (Satokata and Maas, 1994) and humans (Nieminen, 2009; Vastardis et al., 1996). *Bmp7a*, a close paralog of *Bmp6*, also lies on chromosome 17 in a region controlling tooth number in CERC, and has been shown to promote dental ossification when added exogenously (Sloan et al., 2000) and to be required for tooth development in mice (Zouvelou et al., 2009).

Although convergent evolution of increased tooth number has occurred using largely distinct sets of genes, different components of the same genetic circuitry might be altered in the two high-toothed populations (e.g. *Bmp6*, *Bmp7*, *Msx1*). Future work will test the hypothesis that the convergently evolved tooth gain presented here occurs through modulating different components of the BMP signaling pathway to alter tooth replacement stem cell dynamics.

2.6 Acknowledgments

We thank Emily Killingbeck for generating CERC cross sequencing libraries; Priscilla Erickson for helpful suggestions and generating a subset of the PAXB animals; Marvalee Wake for sectioning advice; Alisha Ellis for pulse-chase assistance; and Anthony Lee for excellent fish husbandry and phenotyping assistance.

This work was supported in part by the National Institutes of Health (NIH) [R01-DE021475 to C.T.M.]; National Science Foundation (NSF) Graduate Research Fellowships (N.A.E., A.M.G., P.A.C.); an Achievement Rewards for College Scientists (ARCS) Fellowship (N.A.E.); and NIH Genetics Training Grant [5T32GM007127 to A.M.G., P.A.C.]. The

Vincent J. Coates Genomics Sequencing Laboratory at UC Berkeley is generously supported by NIH S10 Instrumentation Grants [S10RR029668 and S10RR027303].

2.7 References

Abduweli, D., Baba, O., Tabata, M. J., Higuchi, K., Mitani, H. and Takano, Y. (2014). Tooth replacement and putative odontogenic stem cell niches in pharyngeal dentition of medaka (*Oryzias latipes*). *Microscopy* 63, 141-153.

Ahn, Y. (2015). Signaling in tooth, hair, and mammary placodes. Curr. Top. Dev. Biol. 111, 421-459. Aigler, S. R., Jandzik, D., Hatta, K., Uesugi, K. and Stock, D. W. (2014). Selection and constraint underlie irreversibility of tooth loss in cypriniform fishes. *Proc. Natl. Acad. Sci. USA* 111, 7707-7712.

Aigler, S. R., Jandzik, D., Hatta, K., Uesugi, K. and Stock, D. W. (2014). Selection and constraint underlie irreversibility of tooth loss in cypriniform fishes. *Proc. Natl. Acad. Sci. USA* 111, 7707-7712.

Anker, G. C. H. (1974). Morphology and kinetics of the head of the stickleback, *Gasterosteus aculeatus. Trans. Zool. Soc. Lond.* 32, 311-416.

Atukorala, A. D. S. and Franz-Odendaal, T. A. (2014). Spatial and temporal events in tooth development of Astyanax mexicanus. *Mech. Dev.* 134, 42-54.

Atukorala, A. D. S., Inohaya, K., Baba, O., Tabata, M. J., Ratnayake, R. A. R. K., Abduweli, D., Kasugai, S., Mitani, H. and Takano, Y. (2011). Scale and tooth phenotypes in medaka with a mutated ectodysplasin-A receptor: implications for the evolutionary origin of oral and pharyngeal teeth. *Arch. Histol. Cytol.* 73, 139-148.

Bei, M. (2009). Molecular genetics of tooth development. *Curr. Opin. Genet. Dev.* 19, 504-510.

Bell, M. A. and Foster, S. A. ed. (1994). *The Evolutionary Biology of the Threespine Stickleback*. New York: Oxford University Press.

Bemis, W. E., Giuliano, A. and McGuire, B. (2005). Structure, attachment, replacement and growth of teeth in bluefish, *Pomatomus saltatrix* (Linnaeus, 1776), a teleost with deeply socketed teeth. *Zoology* 108, 317-327.

Biggs, L. C. and Mikkola, M. L. (2014). Early inductive events in ectodermal appendage morphogenesis. Semin. *Cell Dev. Biol.* 25-26, 11-21.

Broman, K. W. and Sen, S. (2009). *A Guide to QTL Mapping with R/qtl*. New York: Springer.

Cao, H., Jheon, A., Li, X., Sun, Z., Wang, J., Florez, S., Zhang, Z., McManus, M. T., Klein, O. D. and Amendt, B. A. (2013). The Pitx2:miR-200c/141:noggin pathway regulates Bmp signaling and ameloblast differentiation. *Development* 140, 3348-3359.

Chan, Y. F., Marks, M. E., Jones, F. C., Villarreal, G., Jr, Shapiro, M. D., Brady, S. D., Southwick, A. M., Absher, D. M., Grimwood, J., Schmutz, J. et al. (2010). Adaptive evolution of pelvic reduction in sticklebacks by recurrent deletion of a Pitx1 enhancer. Science 327, 302-305.

Childers, N. K. and Wright, J. T. (1986). Dental and craniofacial anomalies of Axenfeld-Rieger syndrome. *J. Oral Pathol.* Med. 15, 534-539.

Chuong, C.-M., Yeh, C.-Y., Jiang, T.-X. and Widelitz, R. (2013). Module-based complexity formation: periodic patterning in feathers and hairs. *Wiley Interdiscip. Rev. Dev. Biol.* 2, 97-112.

Cleves, P. A., Ellis, N. A., Jimenez, M. T., Nunez, S. M., Schluter, D., Kingsley, D. M. and Miller, C. T. (2014). Evolved tooth gain in sticklebacks is associated with a cis-regulatory allele of Bmp6. *Proc. Natl. Acad. Sci. USA* 111, 13912-13917.

Colosimo, P. F., Hosemann, K. E., Balabhadra, S., Villarreal, G., Jr, Dickson, M., Grimwood, J., Schmutz, J., Myers, R. M., Schluter, D. and Kingsley, D. M. (2005). Widespread parallel evolution in sticklebacks by repeated fixation of ectodysplasin alleles. *Science* 307, 1928-1933.

Elshire, R. J., Glaubitz, J. C., Sun, Q., Poland, J. A., Kawamoto, K., Buckler, E. S. and Mitchell, S. E. (2011). A robust, simple Genotyping-by-Sequencing (GBS) approach for high diversity species. *PLoS ONE* 6, e19379.

Erickson, P. A., Glazer, A. M., Cleves, P. A., Smith, A. S. and Miller, C. T. (2014). Two developmentally temporal quantitative trait loci underlie convergent evolution of increased branchial bone length in sticklebacks. *Proc. R. Soc. B Biol. Sci.* 281, 20140822.

Ferguson, C. A., Tucker, A. S., Christensen, L., Lau, A. L., Matzuk, M. M. and Sharpe, P. T. (1998). Activin is an essential early mesenchymal signal in tooth development that is required for patterning of the murine dentition. *Genes Dev.* 12, 2636-2649.

Fraser, G. J., Berkovitz, B. K., Graham, A. and Smith, M. M. (2006). Gene deployment for tooth replacement in the rainbow trout (*Oncorhynchus mykiss*): a developmental model for evolution of the osteichthyan dentition. *Evol. Dev.* 8, 446-457.

Fraser, G. J., Bloomquist, R. F. and Streelman, J. T. (2008). A periodic pattern generator for dental diversity. *BMC Biol.* 6, 32.

Fraser, G. J., Hulsey, C. D., Bloomquist, R. F., Uyesugi, K., Manley, N. R. and Streelman, J. T. (2009). An ancient gene network is co-opted for teeth on old and new jaws. *PLoS Biol.* 7, e1000031.

Fraser, G. J., Bloomquist, R. F. and Streelman, J. T. (2013). Common developmental pathways link tooth shape to regeneration. *Dev. Biol.* 377, 399-414.

Gaete, M. and Tucker, A. S. (2013). Organized emergence of multiple-generations of teeth in snakes is dysregulated by activation of Wnt/beta-catenin signalling. *PLoS ONE* 8, e74484.

Glazer, A. M., Cleves, P. A., Erickson, P. A., Lam, A. Y. and Miller, C. T. (2014). Parallel developmental genetic features underlie stickleback gill raker evolution. *Evodevo* 5, 19.

Glazer, A. M., Killingbeck, E. E., Mitros, T., Rokhsar, D. S. and Miller, C. T. (2015). Genome assembly improvement and mapping convergently evolved skeletal traits in sticklebacks with Genotyping-by-Sequencing. *G3* (in press).

Handrigan, G. R. and Richman, J. M. (2010). A network of Wnt, hedgehog and BMP signaling pathways regulates tooth replacement in snakes. *Dev. Biol.* 348, 130-141.

Handrigan, G. R., Leung, K. J. and Richman, J. M. (2010). Identification of putative dental epithelial stem cells in a lizard with life-long tooth replacement. *Development* 137, 3545-3549.

Hardcastle, Z., Mo, R., Hui, C. and Sharpe, P. T. (1998). The Shh signalling pathway in tooth development: defects in Gli2 and Gli3 mutants. *Development* 125, 2803-2811.

Harris, M. P., Rohner, N., Schwarz, H., Perathoner, S., Konstantinidis, P. and Nusslein-Volhard, C. (2008). Zebrafish eda and edar mutants reveal conserved and ancestral roles of ectodysplasin signaling in vertebrates. *PLoS Genet.* 4, e1000206.

Hulsey, C. D., Fraser, G. J. and Streelman, J. T. (2005). Evolution and development of complex biomechanical systems: 300 million years of fish jaws. *Zebrafish* 2, 243-257.

Humason, G. (1962). *Animal Tissue Techniques*. San Francisco: W. H. Freeman and Company.

Huysseune, A. (2006). Formation of a successional dental lamina in the zebrafish (Danio rerio): support for a local control of replacement tooth initiation. *Int. J. Dev. Biol.* 50, 637-643.

Huysseune, A. and Thesleff, I. (2004). Continuous tooth replacement: the possible involvement of epithelial stem cells. *Bioessays* 26, 665-671.

Huysseune, A., Van der heyden, C. and Sire, J.-Y. (1998). Early development of the zebrafish (Danio rerio) pharyngeal dentition (Teleostei, Cyprinidae). *Anat. Embryol.* 198, 289-305.

Jernvall, J. and Thesleff, I. (2000). Reiterative signaling and patterning during mammalian tooth morphogenesis. *Mech. Dev.* 92, 19-29.

Jernvall, J. and Thesleff, I. (2012). Tooth shape formation and tooth renewal: evolving with the same signals. *Development* 139, 3487-3497.

Jumlongras, D., Lachke, S. A., OConnell, D. J., Aboukhalil, A., Li, X., Choe, S. E., Ho, J. W. K., Turbe-Doan, A., Robertson, E. A., Olsen, B. R. et al. (2012). An evolutionarily conserved enhancer regulates Bmp4 expression in developing incisor and limb bud. *PLoS ONE* 7, e38568.

Jung, H.-S., Francis-West, P. H., Widelitz, R. B., Jiang, T.-X., Ting-Berreth, S., Tickle, C., Wolpert, L. and Chuong, C.-M. (1998). Local inhibitory action of BMPs and their relationships with activators in feather formation: implications for periodic patterning. *Dev. Biol.* 196, 11-23.

Jussila, M., Crespo Yanez, X. and Thesleff, I. (2014). Initiation of teeth from the dental lamina in the ferret. *Differentiation* 87, 32-43.

Juuri, E., Jussila, M., Seidel, K., Holmes, S., Wu, P., Richman, J., Heikinheimo, K., Chuong, C.-M., Arnold, K., Hochedlinger, K. et al. (2013). Sox2 marks epithelial competence to generate teeth in mammals and reptiles. *Development* 140, 1424-1432.

Kerr, T. (1960). Development and structure of some actinopterygian and urodele teeth. *Proc. Zool. Soc. Lond.* 133, 401-422.

Kimmel, C. B., DeLaurier, A., Ullmann, B., Dowd, J. and McFadden, M. (2010). Modes of developmental outgrowth and shaping of a craniofacial bone in *zebrafish*. *PLoS ONE* 5, e9475.

Lan, Y., Jia, S. and Jiang, R. (2014). Molecular patterning of the mammalian dentition. *Semin. Cell Dev. Biol.* 25-26, 61-70.

Lauder, G. (1983). Functional design and evolution of the pharyngeal jaw apparatus in euteleostean fishes. *Zool. J. Linn. Soc.* 77, 1-38.

Lu, M.-F., Pressman, C., Dyer, R., Johnson, R. L. and Martin, J. F. (1999). Function of Rieger syndrome gene in leftright asymmetry and craniofacial development. *Nature* 401, 276-278.

Mikkola, M. L. and Thesleff, I. (2003). *Ectodysplasin* signaling in development. *Cytokine Growth Factor Rev.* 14, 211-224.

Miller, C. T., Beleza, S., Pollen, A. A., Schluter, D., Kittles, R. A., Shriver, M. D. and Kingsley, D. M. (2007). cis-Regulatory changes in *kit ligand* expression and parallel evolution of pigmentation in sticklebacks and humans. *Cell* 131, 1179-1189.

Miller, C. T., Glazer, A. M., Summers, B. R., Blackman, B. K., Norman, A. R., Shapiro, M. D., Cole, B. L., Peichel, C. L., Schluter, D. and Kingsley, D. M. (2014). Modular skeletal evolution in sticklebacks is controlled by additive and clustered quantitative trait loci. *Genetics* 197, 405-420.

Moriyama, K., Watanabe, S., Iida, M. and Sahara, N. (2010). Plate-like permanent dental laminae of upper jaw dentition in adult gobiid fish, *Sicyopterus japonicus*. *Cell Tissue Res.* 340, 189-200.

Motta, P. J. (1984). Tooth attachment, replacement, and growth in the butterfly fish, *Chaetodon miliaris* (Chaetodontidae, Perciformes). *Can. J. Zool.* 62, 183-189.

Mou, C., Pitel, F., Gourichon, D., Vignoles, F., Tzika, A., Tato, P., Yu, L., Burt, D. W., Bedhom, B., Tixier-Boichard, M. et al. (2011). Cryptic patterning of avian skin confers a developmental facility for loss of neck feathering. *PLoS Biol.* 9, e1001028.

Nieminen, P. (2009). Genetic basis of tooth agenesis. *J. Exp. Zool. B Mol. Dev. Evol.* 312B, 320-342.

Noramly, S. and Morgan, B. A. (1998). BMPs mediate lateral inhibition at successive stages in feather tract development. *Development* 125, 3775-3787.

OConnell, D. J., Ho, J. W. K., Mammoto, T., Turbe-Doan, A., OConnell, J. T., Haseley, P. S., Koo, S., Kamiya, N., Ingber, D. E., Park, P. J. et al. (2012). A Wnt-bmp feedback circuit controls intertissue signaling dynamics in tooth organogenesis. *Sci. Signal.* 5, ra4.

Osborn, J. (1971). The ontogeny of tooth succession in *Lacerta vivipara Jacquin* (1787). *Proc. R. Soc. B Biol. Sci.* 179, 261-289.

Osborn, J. (1978). Morphogenetic gradients: fields versus clones. In *Development, Function, and Evolution of Teeth* (ed. P. Butler and K. Joysey), pp. 171-201. London: Academic Press.

Parra-Olea, G. and Wake, D. B. (2001). Extreme morphological and ecological homoplasy in tropical salamanders. *Proc. Natl. Acad. Sci. USA* 98, 7888-7891.

Qiu, M., Bulfone, A., Ghattas, I., Meneses, J. J., Christensen, L., Sharpe, P. T., Presley, R., Pedersen, R. A. and Rubenstein, J. L. R. (1997). Role of the Dlx homeobox genes in proximodistal patterning of the branchial arches: mutations of Dlx-1, Dlx-2, and Dlx-1

and -2 alter morphogenesis of proximal skeletal and soft tissue structures derived from the first and second arches. *Dev. Biol.* 185, 165-184.

Reif, W.-E. (1984). Pattern regulation in shark dentitions. In Pattern Formation (ed. G. M. Malacinski and S. V. Bryant), pp. 603-621. New York: Macmillan Publishing Company.

Satokata, I. and Maas, R. (1994). Msx1 deficient mice exhibit cleft palate and abnormalities of craniofacial and tooth development. *Nat. Genet.* 6, 348-356.

Schluter, D. and McPhail, J. D. (1992). Ecological character displacement and speciation in sticklebacks. *Am. Nat.* 140, 85-108.

Schneider, C. A., Rasband, W. S. and Eliceiri, K. W. (2012). NIH Image to ImageJ: 25 years of image analysis. *Nat. Methods* 9, 671-675.

Schulte-Merker, S. (2002). Looking at embryos. In *Zebrafish* (ed. C. Nusslein- Volhard and R. Dahm), pp. 54-55. New York: Oxford University Press.

Semina, E. V., Reiter, R., Leysens, N. J., Alward, W. L. M., Small, K. W., Datson, N. A., Siegel-Bartelt, J., Bierke-Nelson, D., Bitoun, P., Zabel, B. U. et al. (1996). Cloning and characterization of a novel bicoid-related homeobox transcription factor gene, RIEG, involved in Rieger syndrome. *Nat. Genet.* 14, 392-399.

Shapiro, M. D., Marks, M. E., Peichel, C. L., Blackman, B. K., Nereng, K. S., Jonsson, B., Schluter, D. and Kingsley, D. M. (2004). Genetic and developmental basis of evolutionary pelvic reduction in threespine sticklebacks. *Nature* 428, 717-723.

Sibbing, F. (1991). Food capture and oral processing. In *Cyprinid Fishes* (ed. I. J. Winfield and J. S. Nelson), pp. 377-412. London: Chapman and Hall.

Sloan, A. J., Rutherford, R. B. and Smith, A. J. (2000). Stimulation of the rat dentine-pulp complex by bone morphogenetic protein-7 in vitro. *Arch. Oral Biol.* 45, 173-177.

Smith, M. M., Fraser, G. J., Chaplin, N., Hobbs, C. and Graham, A. (2009a). Reiterative pattern of sonic hedgehog expression in the catshark dentition reveals a phylogenetic template for jawed vertebrates. *Proc. R. Soc. B Biol. Sci.* 276, 1225-1233.

Smith, M. M., Fraser, G. J. and Mitsiadis, T. A. (2009b). Dental lamina as source of odontogenic stem cells: evolutionary origins and developmental control of tooth generation in gnathostomes. *J. Exp. Zool. B Mol. Dev. Evol.* 312B, 260-280.

Stemmer, M., Schuhmacher, L.-N., Foulkes, N. S., Bertolucci, C. and Wittbrodt, J. (2015). Cavefish eye loss in response to an early block in retinal differentiation progression. *Development* 142, 743-752.

Stock, D. W. (2007). Zebrafish dentition in comparative context. *J. Exp. Zool. B Mol. Dev. Evol.* 308B, 523-549.

Tanaka, K., Barmina, O. and Kopp, A. (2009). Distinct developmental mechanisms underlie the evolutionary diversification of Drosophila sex combs. *Proc. Natl. Acad. Sci. USA* 106, 4764-4769.

Thesleff, I. (2003). Epithelial-mesenchymal signalling regulating tooth morphogenesis. *J. Cell Sci.* 116, 1647-1648.

Thomas, B. L., Tucker, A. S., Qui, M., Ferguson, C. A., Hardcastle, Z., Rubenstein, J. L. R. and Sharpe, P. T. (1997). Role of Dlx-1 and Dlx-2 genes in patterning of the murine dentition. *Development* 124, 4811-4818.

Tucker, A. S. and Fraser, G. J. (2014). Evolution and developmental diversity of tooth regeneration. *Semin. Cell Dev. Biol.* 25-26, 71-80.

Tucker, A. and Sharpe, P. (2004). The cutting-edge of mammalian development; how the embryo makes teeth. *Nat. Rev. Genet.* 5, 499-508.

Tummers, M. and Thesleff, I. (2009). The importance of signal pathway modulation in all aspects of tooth development. *J. Exp. Zool. B Mol. Dev. Evol.* 312B, 309-319.

Vadlamudi, U., Espinoza, H. M., Ganga, M., Martin, D. M., Liu, X., Engelhardt, J. F. and Amendt, B. A. (2005). PITX2, beta-catenin and LEF-1 interact to synergistically regulate the LEF-1 promoter. *J. Cell Sci.* 118, 1129-1137.

van den Boogaard, M.-J., Creton, M., Bronkhorst, Y., van der Hout, A., Hennekam, E., Lindhout, D., Cune, M. and Ploos van Amstel, H. K. (2012). Mutations in WNT10A are present in more than half of isolated hypodontia cases. *J. Med. Genet.* 49, 327-331.

Van der heyden, C. and Huysseune, A. (2000). Dynamics of tooth formation and replacement in the zebrafish (*Danio rerio*) (Teleostei, Cyprinidae). *Dev. Dyn.* 219, 486-496.

Vastardis, H., Karimbux, N., Guthua, S. W., Seidman, J. G. and Seidman, C. E. (1996). A human MSX1 homeodomain missense mutation causes selective tooth agenesis. *Nat. Genet.* 13, 417-421.

Wainwright, P. (2006). Functional morphology of the pharyngeal jaw apparatus. In *Fish Physiology: Fish Biomechanics* (ed. R. E. Shadwick and G. V. Lauder), pp. 77-102. San Diego: Academic Press.

Wakita, M., Itoh, K. and Kobayashi, S. (1977). Tooth replacement in the teleost fish Prionurus microlepidotus Lacepede. *J. Morphol.* 153, 129-141.

Wu, P., Wu, X., Jiang, T.-X., Elsey, R. M., Temple, B. L., Divers, S. J., Glenn, T. C., Yuan, K., Chen, M.-H., Widelitz, R. B. et al. (2013). Specialized stem cell niche enables repetitive renewal of alligator teeth. *Proc. Natl. Acad. Sci. USA* 110, E2009-E2018.

Zhang, Z., Lan, Y., Chai, Y. and Jiang, R. (2009). Antagonistic actions of Msx1 and Osr2 pattern mammalian teeth into a single row. *Science* 323, 1232-1234.

Zouvelou, V., Luder, H.-U., Mitsiadis, T. A. and Graf, D. (2009). Deletion of BMP7 affects the development of bones, teeth, and other ectodermal appendages of the orofacial complex. *J. Exp. Zool. B Mol. Dev. Evol.* 312B, 361-374.

Zwaan, B. J., Azevedo, R. B. R., James, A. C., Van T Land, J. and Partridge, L. (2000). Cellular basis of wing size variation in Drosophila melanogaster: a comparison of latitudinal clines on two continents. *Heredity* 84, 338-347

Chapter 3

Opposing roles for BMP signaling in tooth formation and replacement in sticklebacks

> "The beginning of knowledge is the discovery of something we do not understand."
> -Frank Herbert

The following chapter is a manuscript in preparation.

Nicholas A. Ellis, James C. Hart, Andrew M. Glazer, Emily E. Killingbeck, Siegen A. McKellar and Craig T. Miller

Department of Molecular and Cell Biology, University of California-Berkeley, Berkeley CA, 94720, USA

3.1 Abstract

BMP signaling plays multiple complex roles during organogenesis and regeneration. Here we test the roles of BMP signaling in tooth development and replacement in the three-spine stickleback fish, a polyphyodont vertebrate that undergoes continuous tooth replacement. Increased tooth number has evolved convergently in different freshwater stickleback populations, and in one population is associated with *cis*-regulatory reductions in *Bmp6*. Here we test the effects on tooth number and positioning by pharmacologically and genetically reducing BMP signaling. Pharmacological inhibition of BMP signaling with the small molecule inhibitor LDN-193189 and induced mutations in *Smad5* inhibited tooth formation and reduced total tooth number. However, pharmacological inhibition of BMP signaling also stimulated dose dependent premature tooth replacement events. Transcriptional profiling dental tissue from LDN-treated fish confirmed that the expression of predicted BMP effectors was reduced, while the FGF, WNT and NOTCH pathways were significantly up-regulated. Finally, late in development, we show inhibition of BMP signaling increased the number of newly forming teeth, likely through increased tooth replacement. Collectively these data support a model where BMP signaling positively regulates tooth development while negatively regulating tooth replacement.

3.2 Introduction

Ectodermal appendages such as teeth, hair, and feathers have served as classic model systems to study organogenesis in vertebrates. Both activating and inhibitory roles of BMP signaling have been identified across continuously replacing ectodermal organs including teeth (see below), feathers (Jung et al., 1998; Mou et al., 2011; Noramly and Morgan, 1998; Scaal et al., 2002), and hair (see below). Teeth are an excellent model to study this phenomenon due to the wide variation in tooth number and replacement across vertebrates. During the development of tooth placodes, BMPs appear to both inhibit and activate tooth development. *Bmp4* was initially implicated in tooth development as an inhibitory signal that positions *Pax9* in dental mesenchyme (Neubser et al., 1997). However, other data indicate BMPs also play activating roles during tooth development. A loss-of-function mutation in the *Bmpr1a* gene in the epithelium arrests mouse tooth development (Andl et al., 2004). Down regulation of BMP signaling with keratin14-*Noggin* results in the loss of the third molar (M3) and a reduction in size of the other two molars (M1 and M2) (Plikus et al., 2005) while adding BMP beads to cultured mouse molar germs can accelerate tooth formation (Kavanagh et al., 2007). Mouse *Bmp7* mutants either fail to form teeth or form malformed teeth (Zouvelou et al., 2009) while addition of *Bmp7* can induce osteoblast matrix secretion in tooth sections (Sloan et al., 2000). Depletion of *Bmp4* in the mesenchyme results in arrest of mandibular molars and smaller maxillary molars accompanied with cusp defects (Jia et al., 2013). In humans, a SNP in *BMP4* is associated with the timing of tooth eruption (Fatemifar et al., 2013). Mutations in *Msx1*, a known BMP effector during tooth development, result in tooth agenesis

in mice and humans, consistent with BMPs activating tooth development (Nieminen, 2009; Satokata and Maas, 1994; Vastardis et al., 1996). Additionally, mice deficient for *Sostdc1*, which encodes a Bmp and Wnt antagonist, have altered cusp patterns and supernumerary teeth (Kassai et al., 2005). Heat shock inducible *noggin1* causes bicuspid and supernumerary teeth in early zebrafish larvae which normally have unicuspid teeth (Jackman et al., 2013). Thus, in both mice and fish, altering levels of BMP signaling in teeth can alter tooth size and number.

However, much less is known about the role of BMP signaling during tooth replacement, in part because mice dont replace their teeth. In cichlid fish, pharmacological reduction of BMP signaling with Dorsomorphin results in missing teeth through an arrest of the replacement process in the oral jaw (Fraser et al., 2013) while treatment with LDN-193189 also results in a reduction in tooth number (Bloomquist et al., 2015).

In other continuously replacing organ systems, BMP signaling acts to both promote development and inhibit regeneration. In the hair follicle system, *Bmpr1a* loss of function mutation in the epithelium early in development results in increased follicle density from accelerated follicle morphogenesis; however, late in development the hair shafts fail to differentiate and cycle properly resulting in the lack of hair and formation follicular cysts (Andl et al., 2004; Kobielak et al., 2003). During hair regeneration, periodic expression of BMP ligands play a role cycling the hair follicle with high BMPs conferring a refractory stage and low BMPs allowing competence for regeneration (Plikus et al., 2008). Overexpression of the BMP antagonist *Noggin* shortens the refractory stage and allows follicle regeneration to occur more quickly while addition of a *Bmp4* soaked bead prevents propagation of the regenerative wave (Plikus et al., 2008). These results, among others (Genander et al., 2014; Kandyba et al., 2013; Kobielak et al., 2007; Zhang et al., 2006) suggest BMP signaling suppresses stem cell activation in the hair follicle. In the intestines, BMPs suppress stem cell activation and conditional inactivation of *Bmpr1a* in mice results in overproliferation and expansion of the size and number of intestinal crypts (He et al., 2004). In humans, mutations in *SMAD4* and *BMPR1A* have been associated with juvenile polyposis syndrome characterized by abnormal growths in the gastrointestinal tract (Howe et al., 1998; Howe et al., 2001).

Threespine stickleback fish (*Gasterosteus aculeatus*) have undergone an extensive adaptive radiation, with oceanic populations migrating into coastal freshwater lakes and creeks throughout the northern hemisphere. Many morphological changes have accompanied this adaptation to freshwater including a dramatic increase in tooth number (Cleves et al., 2014; Miller et al., 2014). We have previously identified two freshwater populations with evolved tooth gain that occurs late not early in development, in part due to increased tooth replacement rates (Ellis et al., 2015). Despite a similar developmental basis for evolved tooth gain, the genetic basis is completely different (Ellis et al., 2015). The association of a *cis*-regulatory allele of *Bmp6* with evolved tooth gain in one population (Cleves et al., 2014) suggests the hypothesis that changes in different components of the BMP signaling pathway underlie convergent evolution of tooth gain and play an important role in establishing tooth number and replacement. Here we test the hypothesis that BMP signaling regulates tooth number

and replacement by pharmacologically and genetically reducing BMP signaling and assaying effects on tooth development and replacement. Collectively our data support a model where BMP signaling promotes tooth development and initiation at primary positions, while BMP signaling inhibits tooth replacement.

3.3 Materials and Methods

Stickleback husbandry
Fish were raised in 110 l aquaria at 18°C in a common brackish salinity (3.5 g/l Instant Ocean salt, 0.217 ml/l 10% sodium bicarbonate). Fish were fed a common diet of live *Artemia* as young fry, live *Artemia* and frozen Daphnia as juveniles and frozen bloodworms and *Mysis* shrimp as adults. All treatments were performed in Rabbit Slough (RABS) marine fish and Paxton Benthic (PAXB) freshwater fish. All experiments were performed with approval of the Institutional Animal Care and Use Committees of the University of California-Berkeley (protocol # R330).

Tooth patterning
Bilateral ventral pharyngeal tooth plates were scored for tooth patterning using a previously described early stickleback dental pattern (Ellis et al., 2016). Left and right side tooth plates were each scored and each position on the tooth plate was assigned a developmental stage (ex Fig. 2A-D). Position one replacement and shedding were scored as binary traits.

Small molecule treatment, skeletal staining, and pulse-chase
A stock solution of LDN-193189 (Sigma-Aldrich or BioVision) was rehydrated to 10 mM in dimethyl sulfoxide (DMSO). Fish were immersed in 1-50 μM LDN on day eight, raised in LDN for 4 days, tank water replaced on day 12, and grown until 20 days post fertilization. Fish were fixed in 10% neutral buffered formalin (NBF) overnight at 4°C, washed in water, and stained with an acid-free Alizarin Red S and Alcian blue two color protocol as described (Walker and Kimmel, 2007) using 200mM MgCl2. Fish were cleared in 50% glycerol and 0.25% KOH. Branchial skeletons were dissected and mounted as previously described (Ellis and Miller, 2016; Miller et al., 2014).

Live vital dye bone staining was adapted from Kimmel et al., (2010) and previously described (Ellis et al., 2015). Briefly, fish were pulsed with 50 μg/ml Alizarin Red S buffered with 1 mM HEPES (pH 7.0) for 6 hours, washed thoroughly, and raised in 1 μM LDN for 14 days. Fish were chased with 25 μg/ml Calcein buffered with sodium phosphate (pH 8.0) for 6 hours, washed thoroughly, fixed in 10% neutral buffered formalin overnight at 4°C, and stored in 100% ethanol in the dark at 4°C until dissection and clearing.

Histology
Fish were fixed as above, dissected, decalcified in Humasons formic acid A (Humason, 1962), and tissue processed as previously described (Ellis et al., 2015). Briefly, Histoclear (National

Diagnostics) was used in the place of xylene for clearing, tissue was embedded in Paraplast (Fisher), sectioned using a Microm HM340E (Thermo Scientific), and baked at 50°C overnight. Slides were stained with hematoxylin and eosin and cover-slipped with Permount (Fisher).

RNA isolation and library preparation

Twelve fish (3 Marine DMSO control, 3 Marine LDN, 3 Freshwater DMSO control, 3 Freshwater LDN) were treated with 20 μM LDN from day 8-12, euthanized, and immediately dissected into 0.5 ml TRI reagent (Sigma) on ice. Ventral tooth plates were ground with a pestle and stored at -80°C. All fish were PCR confirmed to be male (as previously described in Glazer et al., 2014). RNA was isolated using 0.1 ml of chloroform, centrifuged, and aqueous layer extracted. RNA was co-precipitated with 1 μl GlycolBlue (Fisher) overnight at -80°C using 250 μl of isopropanol, centrifuged, washed with 80% ethanol and re-suspended in 21 μl of water. Following a RNA quality check on an Agilent Bioanalyzer, 200 ng of RNA was used as input to the Illumina TruSeq stranded mRNA Library Prep Kit (RS-122-2101) following the manufacturer's protocol. After a library quality check on an Agilent Bioanalyzer, libraries were pooled and sequenced on an Illumina HiSeq 4000.

Gene Expression quantification and analysis

RNA-seq reads were mapped using STAR (v 2.3, Dobin et al., 2013) to the stickleback reference genome (Jones et al., 2012). Following sorting and indexing using Samtools (v 0.1.18, Li et al., 2009), PCR duplicates were removed using picard tools (v 1.15) with the options ("$AS = TrueREMOVEDUPLICATES = true$"). Gene expression was quantified with the cufflinks suite (v 2.2.1, Roberts et al., 2011a; Roberts et al., 2011b; Trapnell et al., 2010) using ENSEMBL gene predictions 81 as a reference transcriptome. Genes with a mean expression less than 0.1 FPKM were filtered from further analysis. Gene set expression change statistical enrichment was performed following Irizarry et. al., (2009) using a set of custom python scripts. Briefly, each gene was subject to a t-test to test for a difference in mean expression between the two treatments with the resulting t-values subject to a 1-sample t-test. Cutoffs were validated using a bootstrapping approach, with 10,000 replicate gene sets chosen from the same filtered expression matrix. Stickleback orthologues were determined using annotated ENSEMBL orthologues. Principal components analysis was performed using the FactorMineR (v 1.24, L et al., 2008) R package.

Statistical analysis and phenotype corrections

Data were analyzed using R and Prism 5. For comparing phenotypes between treatments, one way analysis of variance (ANOVA) using a Tukey-Kramer post hoc test was performed for statistical analyses between greater than 2 groups, a two tailed t-test was performed for analyses between 2 groups, and ratios were compared with Fishers exact test. *Smad5* TALEN tooth counts were corrected for fish size (correlation $P < 0.001$) by linear regression, then back-transforming residuals to a mean standard length of 21.5 mm.

Supplementary phenotyping

Branchiostegal ray (BSR) length and width were measured on BSR3 (closest to subopercle) and are the average of left and right side measurements. BSR3 length was measured with the segmented line tool in ImageJ while BSR3 width was measured at the widest point directly after the developing epihyal cartilage disc, perpendicular to BSR length. BSR fusion and ectopic BSRs are combined left and right measurements. The ascending process of the premaxilla was measured along the medial edge of the process (midline) using the segmented line tool in ImageJ and is the average of left and right side measurements. Oral tooth counts are combined premaxillary and dentary. Tooth plate area was measured as previously described (Cleves et al., 2014). All tooth counts are combined left and right side.

Mutating *Smad5* with TALENs

TALENs targeting exon 2 of Smad5 were designed using the TALENT online tool (https://talent.cac.cornell.edu/, Doyle et al., 2012). The Smad5 TALENs NN NN NI NN NN NI HD HD NG NN NN NI NN NI NI NN NN HD HD HD NG and NN NN NG NG NI HD NN HD NI HD NG NG NN HD NG NN NN were designed to bind to the DNA sequences GGAGGACCTGGAGAAGGCCCT and GGTTACGCACTTGCTGG, respectively. The TALENs were cloned as described in (Cermak et al., 2011), digested with NotI, RNA transcribed from each TALEN plasmid using a SP6 transcription kit (New England Biolabs), and cleaned up with an RNeasy Mini kit (Qiagen). A mixture containing 400 ng TALEN 1 RNA, 400 ng TALEN 2 RNA and 1 μl phenol red injection dye in a total volume of 10 μl water was made and 5-10 nl of this mixture was injected into fertilized 1 cell embryos from a lab-reared Rabbit Slough marine line.

To detect TALEN-induced mutations, DNA was isolated from ground up embryos at 2 days post fertilization or from pieces of caudal fin tissue from fry. Three methods were used to detect TALEN-induced mutations: (1) The target site for the TALEN-induced double-strand break overlapped a restriction enzyme cut site. A PCR product spanning the TALEN target site was assayed for whether it could be cleaved by the restriction enzyme. PCR products were amplified using primers GTGGACCTACCAGGACTCTCC and ACAGGTCCTCCCTTTCACCT and assayed by gel electrophoresis, with cut PCR products indicating wild type alleles and uncut PCR products indicating mutant alleles. (2) Fragment analysis was used to assay the exact base pair size of a PCR product spanning the TALEN target site. A three primer genotyping reaction was used (Schuelke, 2000). The primers FAM-M13, TGTAAAACGACGGCCAGTGGTGAAAAAGCTGAAGAAGAAGA, and CGGAAGACCTTTCCTGTGAG amplified a 160 bp product for the wild-type allele. Fish heterozygous or homozygous for mutant sequences had different size amplicons that could be used to determine the insertion or deletion size by comparing the band size to the 160 bp wild-type allele. (3) Sanger sequencing of mutant heterozygotes (as assayed by approach 1 or 2) was performed to identify specific mutant sequences. The cut assay (approach 1) PCRs and digests were performed, the failed to cut (mutant) band was gel extracted (Qiagen Gel Extraction Kit) and Sanger sequenced with primer ACAGGTCCTCCCTTTCACCT.

F0 Smad5 TALEN mutants were assayed using the restriction digest assay, and fish with

a high frequency (>30%) of mutant alleles were outcrossed to lab-reared marine fish. F1 offspring were a mix of homozygous wild types and heterozygotes. F1 offspring were screened using method (2) and heterozygotes were in crossed to generate F2 clutches. The F2 cross was genotyped with methods (1) and (2).

3.4 Results/Discussion

BMP signaling promotes stickleback tooth development

To test the hypothesis that BMP signaling is required for stickleback tooth development, we treated marine and freshwater sticklebacks with a pharmacological antagonist of BMP signaling, LDN-193189 (Cuny et al., 2008; Mohedas et al., 2013, hereby referred to as LDN), and then assayed tooth number (Fig. 3.1A). Early inhibition of BMP signaling reduced total tooth number on both ventral (Fig. 3.1B-E) and dorsal pharyngeal tooth plates (Fig. 3.1G-J) and in the upper and lower oral jaw (Fig. 3.2A,B). Tooth germs established during and after the initial phases of drug treatment developed into qualitatively shorter and wider teeth on both the pharyngeal (Fig. 3.1C-D, H, L) and oral (Fig. 3.2A,B) jaw. Total length differences were not observed between treated and control fish (Table 3.1). Reduction in the size and number of molars has also been reported in mice upon downregulation of BMP signaling (Plikus et al., 2005). We also found a variety of other craniofacial skeletal defects, including a reduction in the length of the upper jaw premaxillary posterior extension (Fig. 3.2A,C), a reduction in length and increase of width of the ventral hyoid dermal bones (branchiostegal rays, BSRs) and fused and ectopic BSRs (Fig. 3.2D-H). The shorter and wider ventral BSRs resembled the nearby, more dorsal opercle bone supporting a dorsalization hypothesis consistent with phenotypes seen upon reducing ventral specifying BMP and Endothelin signals in zebrafish (Kimmel et al., 2003; Zuniga et al., 2011). To genetically reduce BMP signaling, we generated induced predicted loss-of-function mutations in *Smad5* using TALENs (Fig. 3.3). *Smad5* mutants also displayed quantitative reductions in tooth number (Fig. 3.3) further supporting the reduced tooth phenotype resulting from the reduction of BMP signaling.

RNA-seq reveals transcriptional response to LDN-193189 treatment

To determine the transcriptional response of LDN treatment and test whether expression of stickleback orthologs of known BMP signaling effectors were reduced, we performed RNAseq on ventral pharyngeal tooth plates of LDN-treated fish and DMSO-treated controls (see Fig. 3.1A, Table 3.2). Three biological replicates were included for each treatment of DMSO control or LDN treatment in both marine and freshwater sticklebacks for a total of 12 samples. Principal component analysis revealed PC1 explained 45.1% of the variance across samples while PC2 explained 17.1% of the variance, separating 5 of the 6 LDN data points from DMSO, with no trend of separating marine from freshwater (Fig. 3.4). Since LDN treatment had much greater effects than fish population and since the phenotypic effects were similar in marine and freshwater populations (see Fig. 3.1, 3.7), we pooled marine and freshwater treatment groups for increased statistical power. As expected, after 4 days of

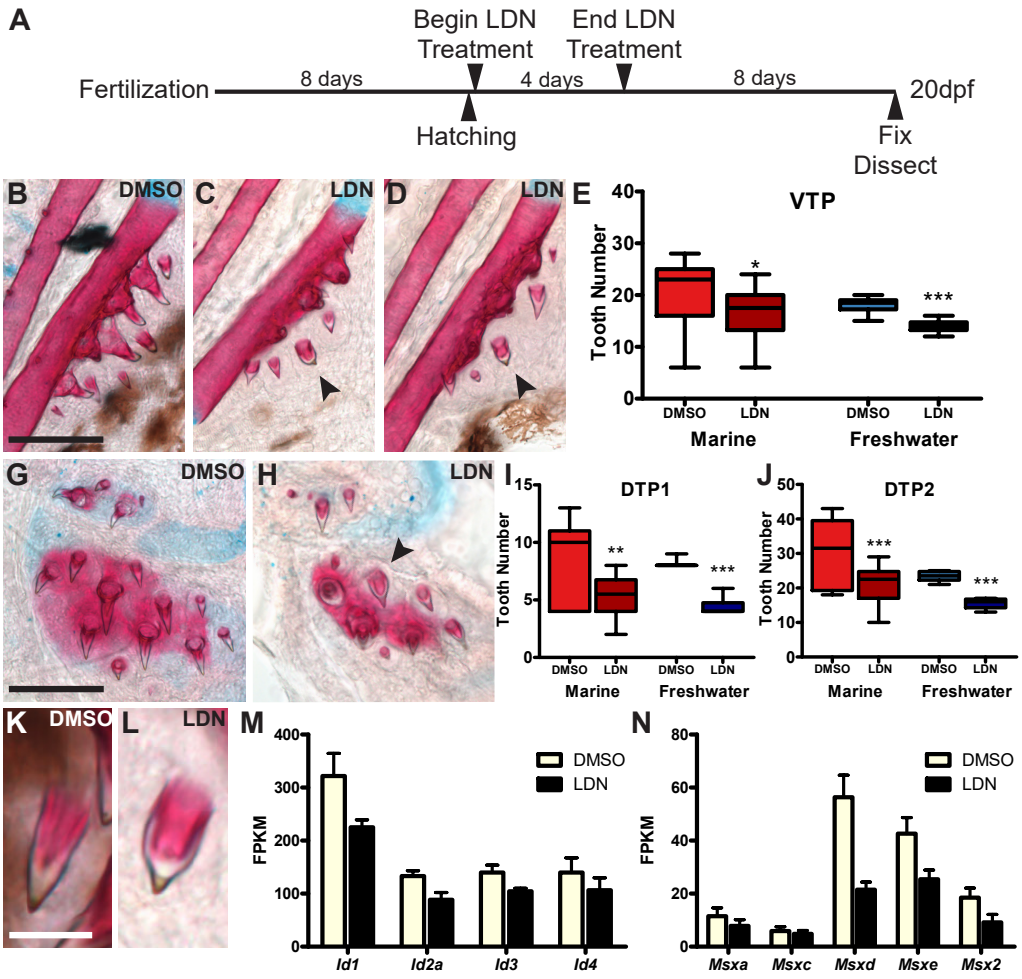

Figure 3.1: **BMP knockdown reduces pharyngeal tooth number in marine and freshwater populations.**
(A) Strategy for early pharmacological inhibition with 20 μM LDN-193189. (B-D, G-H) Representative examples of freshwater LDN treated and DMSO control larval ventral (B-D) and dorsal (G-H) pharyngeal tooth plates stained with Alcian blue and Alizarin red to label cartilage and bone/teeth, respectively. Irregular tooth shapes are noted with black arrowheads. (E, I-J) Quantification of LDN treated and DMSO control tooth numbers on ventral (E) and dorsal (I-J) tooth plates. Total length was not significantly different in drug treated versus control animals (marine $P = 0.85$, freshwater $P = 0.75$, two-tailed t-test). (K-L) Close up of irregular shaped tooth. (M-N) RNAseq expression levels (Fragments Per Kilobase of transcript per Million mapped reads, FPKM) of *Ids* ($P < 0.01$ for treatment in a two-way ANOVA, M) and *Msxs* ($P < 0.001$ for treatment in a two-way ANOVA, N) in pooled DMSO and LDN treatment. Scale bars are 100 μm (B-D,G-H) and 25 μm (K-L). Sample sizes for E,I,J are as follows: DMSO marine = 17,15,16; LDN marine = 18,16,16; DMSO freshwater = 12,11,12; LDN freshwater = 12,12,12 respectively. *** = $P < 0.001$, ** = $P < 0.01$, * = $P < 0.05$, two-tailed t-test. Additional statistics are listed in Table 3.1.

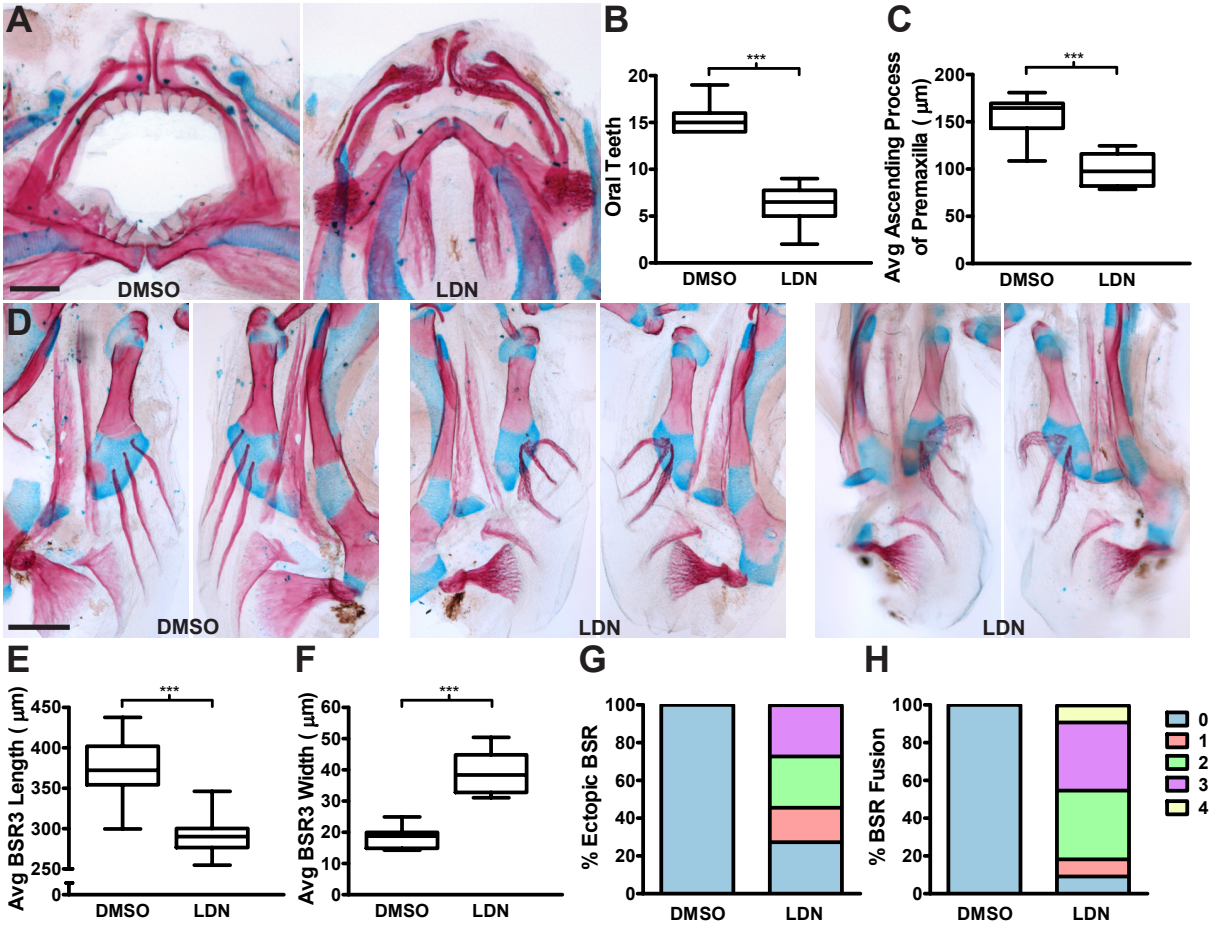

Figure 3.2: **BMP signaling is required for proper jaw and hyoid dermal skeletal development.**
(A) Representative examples of freshwater LDN-193189 treated and DMSO control oral jaw. Scale bar is 100 μm. (B-C) Quantification of oral tooth number (B) and the average length of the ascending process on the premaxilla (C) (Sample size A-C: DMSO control n=11,8 LDN treated n=12,9, respectively). (D) Representative examples of freshwater LDN treated and DMSO control branchiostegal rays (BSRs) and surrounding bones. Scale bar is 200 μm. (E-H) Quantification of average BSR3 length (E), average BSR3 width (F), ectopic BSRs (G), and BSR fusions (H). Sample size E-H: DMSO control n=11, LDN treated n=11. *** = $P < 0.001$, two-tailed t-test.

Population	Treatment Group	Total Length				Ventral Tooth Plate				Dorsal Tooth Plate 1				Dorsal Tooth Plate 2			
		n	Average TL	Within pop (*P* value)	Between pop (*P* value)	n	Average VTP	Within pop (*P* value)	Between pop (*P* value)	n	Average DTP1	Within pop (*P* value)	Between pop (*P* value)	n	Average DTP2	Within pop (*P* value)	Between pop (*P* value)
Marine	DMSO	17	8.17 (± 0.24)	ns	ns	17	20.47 (± 1.40)	<0.05	ns	15	8.07 (± 0.95)	<0.01	ns	16	29.88 (± 2.35)	<0.01	<0.05
Marine	20µM LDN	18	8.23 (± 0.25)		ns	18	16.33 (± 1.14)		ns	16	5.13 (± 0.46)		ns	16	20.69 (± 1.33)		<0.01
Freshwater	DMSO	12	7.88 (± 0.04)	ns		12	18.08 (± 0.42)	<0.001		11	8.18 (± 0.12)	<0.001		12	23.33 (± 0.41)	<0.001	
Freshwater	20µM LDN	12	7.91 (± 0.08)			12	13.92 (± 0.34)			12	4.42 (± 0.23)			12	15.50 (± 0.38)		

Table 3.1: **LDN treatment causes reduced tooth number in both marine and freshwater populations.**
Trait averages and statistics are listed for total length (mm), ventral, and dorsal tooth numbers. Averages include ± the standard error of the mean. Tooth counts are the sum of left and right sides. P values from two tailed t-tests are listed for pairwise comparisons. Data from Figure 3.1 and 3.7.

LDN treatment, the expression of stickleback orthologs of BMP downstream effectors *Ids* (Hollnagel et al., 1999; Miyazono and Miyazawa, 2002; Yang et al., 2013) and *Msxs* (Barlow and Francis-West, 1997; Suzuki et al., 1997; Vainio et al., 1993) were both significantly lower compared to DMSO control (Fig. 3.1M-N). Individual treatment groups follow the same overall trend of reduced expression in LDN treated fish and were not driven solely by one population (Fig. 3.5A-B).

Surprisingly, despite forming fewer teeth overall and the reduced *Id* and *Msx* expression, LDN treated fish had significantly upregulated stickleback orthologs of known tooth markers from three different sets: BiteIt (mice, http://bite-it.helsinki.fi), ToothCode (mice, http://compbio.med.harvard.edu/ToothCODE/, OConnell et al., 2012), and a hand annotated Teleost Tooth Gene set (fish) that we generated from published papers and the zfin.org database (Fig. 3.6A). This increased expression may arise from arrested germs which attempt to continue to signal, but fail to overcome the developmental arrest. Alternatively, despite fewer overall calcified teeth, this upregulated tooth marker expression might reflect a wave of induced precocious replacement teeth (see Figs. 3.7, 3.10). By sorting tooth marker genes by signaling pathway (OConnell et al., 2012) we found some, but not all common signaling pathways are affected (Fig. 3.6B). Despite the decreased expression of downstream BMP effector genes, genes in the BMP signaling pathway were significantly upregulated, including both BMP ligands and BMP receptors (Fig 3.5C). Additionally, expression of genes in the FGF, WNT, and NOTCH pathways were significantly upregulated, while genes in the SHH, ACTIVIN, TGF-B, and EDA pathways were not significantly affected.

BMP signaling inhibits stickleback tooth replacement early

In addition to a reduction of tooth number, we noticed a change in the positions of teeth in LDN treated fish. In early stages of stickleback development, teeth erupt in a stereotypic order and location (Ellis et al., 2016). We tested whether there were positioning differences in drug treated fish at a stage where the dental pattern is relatively invariant and individual

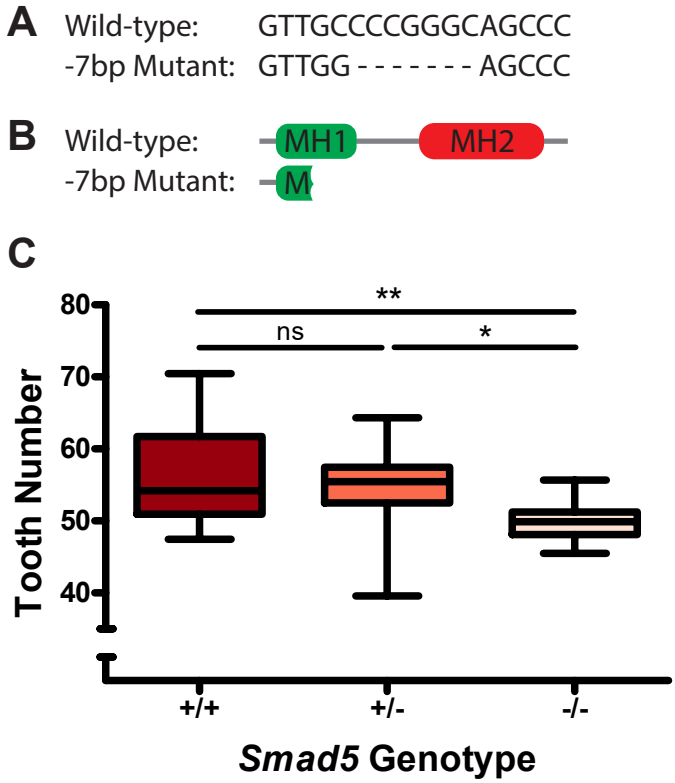

Figure 3.3: ***Smad5* mutant fish exhibit reduced tooth number.**
(A) Sequence of wildtype and a 7 base pair deletion allele generated using TALENs. (B) Schematic of predicted truncated protein resulting from 7 base pair deletion allele. (C) Homozygous mutant fish have fewer teeth than heterozygotes and wildtype fish. Sample size = 54. ** $P < 0.01$, * $P < 0.05$ one-way ANOVA using a Tukey-Kramer post hoc test, ns is not significant.

tooth positions are identifiable. Despite the overall reductions in tooth number in LDN treated fish resulting from a failure to form later medial tooth positions, multiple ectopic teeth close to the oldest, established positions on the tooth plate developed, which we interpret to be precocious replacement teeth (Fig. 3.7A-E, 3.8A-B). No ectopic teeth were detected in any of the vehicle controls. The ectopic teeth forming near the first tooth to form (position 1) developed in the same location as the first replacement tooth in section (above the fifth ceratobranchial, CB5, Fig. 3.7F) further suggesting these ectopic teeth are premature replacement teeth. Additionally, no primary teeth normally develop in any of these positions. Similarly, in the hair follicle system, reduction of BMP signaling through overexpression of the BMP antagonist *Noggin* causes sped up, premature follicle regeneration (Plikus et al., 2008). In both mice and zebrafish, reduction of BMP signaling has been reported to result in ectopic teeth through placode splitting, where one tooth germ splits

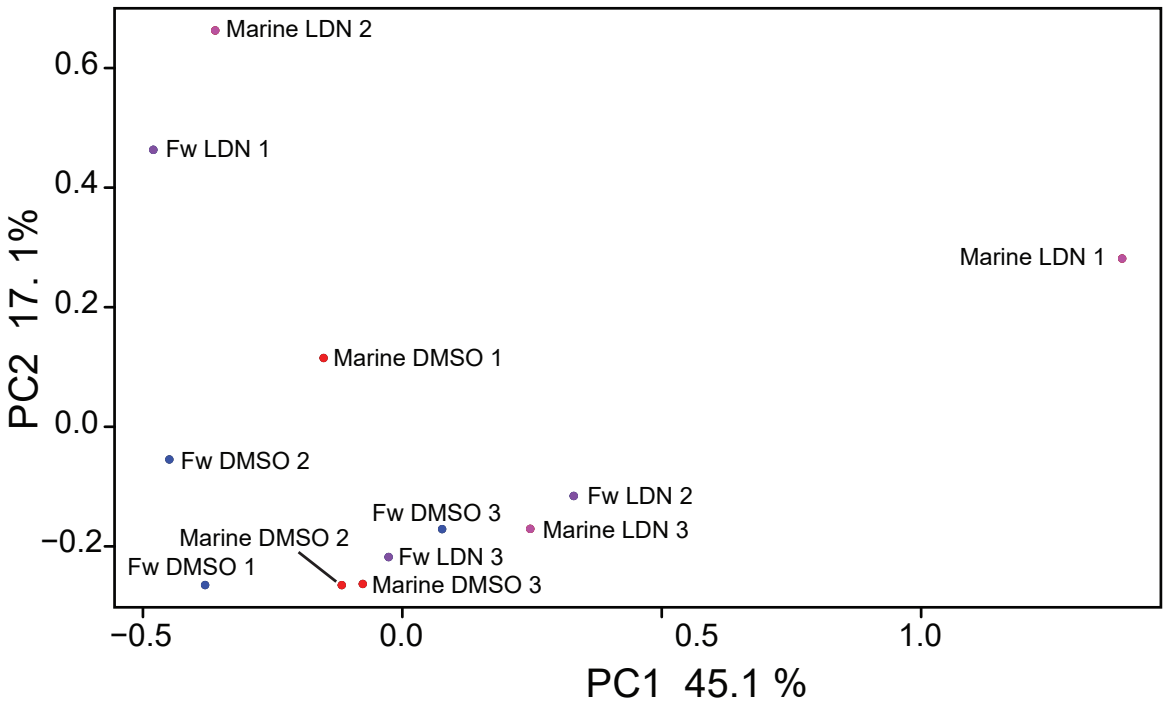

Figure 3.4: **Principal component analysis for LDN RNAseq.**
Principal component analysis on marine and freshwater LDN-193189 and DMSO treated fish using combined BiteIt and ToothCode tooth marker gene sets. Principal component one explains 45.1% of the variance while principle component two explains 17.1% of the variance. Marine DMSO treated fish are in red, marine LDN treated fish in magenta, freshwater DMSO treated fish in blue, and freshwater LDN treated fish in purple

and forms two teeth (Jackman et al., 2013; Munne et al., 2010). If BMP signaling inhibition caused newly forming placodes to split in our treatments, we would expect to detect ectopic teeth along the medial edge of the tooth plate, where newly born tooth placodes are developing in new positions (Ellis et al., 2016). Instead, we detected ectopic teeth near the base of the earliest forming fully calcified teeth, positions that have already specified prior to LDN treatment, supporting an accelerated replacement event rather than a split placode.

Notably, we detected no evidence of tooth shedding in histological sections and detected no osteoclast activity eroding the bone of attachment between the predecessor tooth and the replacement typical of normal tooth replacement. We measured replacement and shedding rates of the first pioneer tooth and detected no increase in tooth shedding in LDN treated fish despite increased rates of replacement (Fig. 3.9). This suggests a decoupling of replacement and shedding, a mechanism that could be exploited to achieve naturally evolved increased tooth number (Cleves et al., 2014; Ellis et al., 2015).

Next, we tested if the response to LDN treatment was dose dependent in marine fish

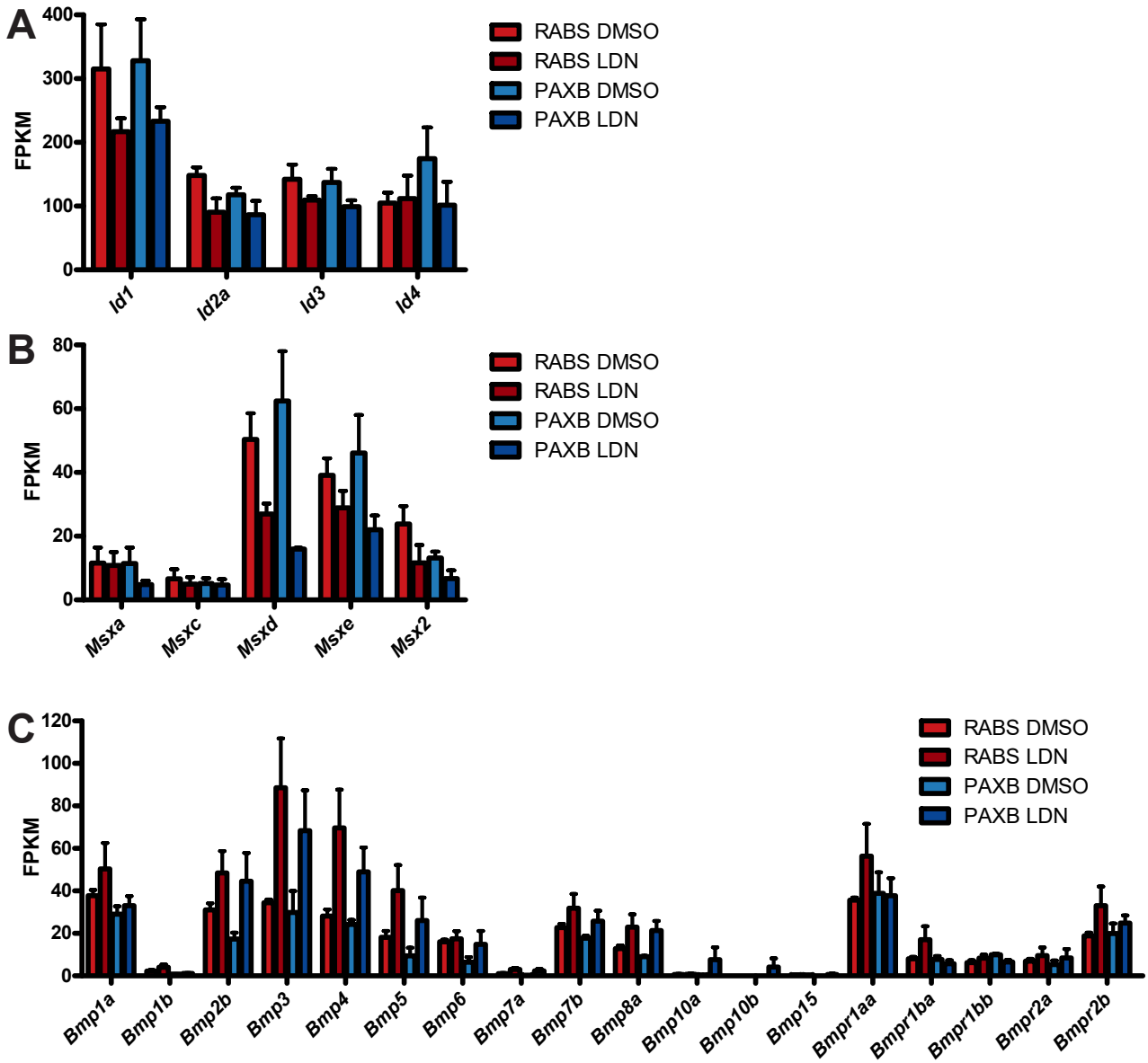

Figure 3.5: **Expression of *Ids*, *Msxs*, and BMP ligands and receptors.**
(A-B) Expression levels (Fragments Per Kilobase of transcript per Million mapped reads, FPKM) for downstream effectors of BMP signaling; *Id* (A) and *Msx* genes (B). (C) Expression level (FPKM) for BMP ligands and receptors.

Library	Sequenced Reads	Primary Mapped Reads	Primary Filtered Mapped Reads
Fw_DMSO_1	29635931	15560247	2205638
Fw_DMSO_2	36186145	26125920	6683284
Fw_DMSO_3	36093974	13817329	2703784
Marine_DMSO_1	26666453	13061478	2819776
Marine_DMSO_2	27651662	13633712	3385282
Marine_DMSO_3	26589150	19954370	5140460
Fw_LDN_1	17881360	21640832	3243880
Fw_LDN_2	38319873	24972587	6039749
Fw_LDN_3	23936155	16130974	3954785
Marine_LDN_1	28110525	27873303	6597898
Marine_LDN_2	30777934	21420996	7038659
Marine_LDN_3	26751955	18619266	4196771

Table 3.2: **Mapped reads for RNAseq of individual DMSO control and LDN treated fish.**
Mapped reads for RNAseq of individual DMSO control and LDN treated fish. Sequenced reads refer to the number of reads with a matching index obtained from the HiSeq4000. Primary mapped reads counts the most likely position where the read maps, with multi-mapping reads counted only once. Primary filtered mapped reads counts primary mapped reads that pass filtering (see materials and methods for filtering details).

Population	Treatment Group	n	Average TL	DMSO vs treatment (*P* value)	Average VTP	DMSO vs treatment (*P* value)
Marine	DMSO	17	8.02 (± 0.07)		21.47 (± 0.88)	
Marine	1 µM LDN	12	8.12 (± 0.12)	ns	19.08 (± 1.07)	ns
Marine	5 µM LDN	10	8.18 (± 0.16)	ns	19.20 (± 1.01)	ns
Marine	10 µM LDN	13	8.16 (± 0.21)	ns	17.85 (± 0.97)	ns
Marine	20 µM LDN	12	8.00 (± 0.27)	ns	16.25 (± 0.91)	<0.01
Marine	50 µM LDN	7	8.26 (± 0.24)	ns	16.29 (± 1.04)	<0.05

Table 3.3: **Increasing LDN dosage decreases tooth number without affecting size.**
Trait averages and pairwise P values are listed. Averages include ± the standard error of the mean. *P* values are from a one-way ANOVA using a Tukey-Kramer post hoc test. Data from Figure 3.10.

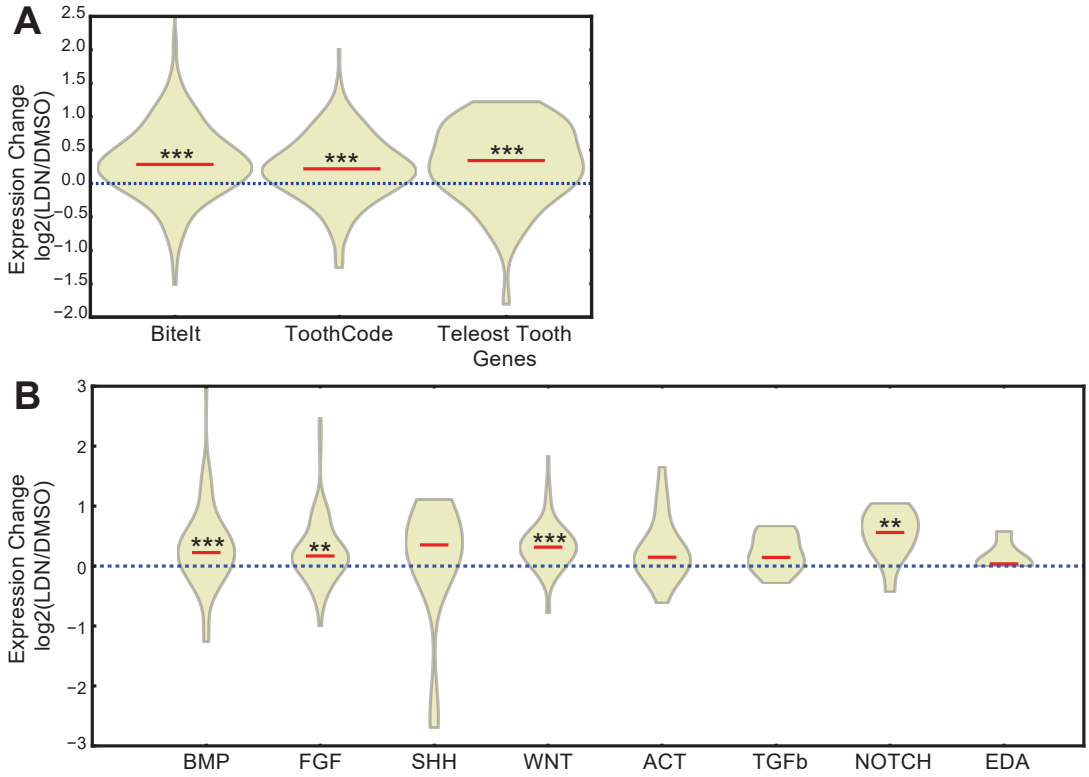

Figure 3.6: **BMP knockdown results in up-regulation of tooth development markers.**
(A) Expression change (ratio of LDN/DMSO) of two published sets of genes expressed in mouse teeth (BiteIt, ToothCode) and one hand annotated set of genes expressed in teleost fish teeth. (B) Expression change (ratio of LDN/DMSO) for signaling pathways as defined by ToothCode. Red line indicates the median expression for each gene set. *** = $P < 0.001$, ** = $P < 0.01$, * = $P < 0.05$ (gene set enrichment analysis, see Methods)

where the phenotype was slightly more severe (see Fig 3.7E). Treating with a range of different doses (1-50 μM) revealed that the extent of both the reduction of overall tooth number and the induction of premature replacement teeth (Fig. 3.10A-B, Table 3.3) was largely dose dependent. As the level of BMP knockdown increased, fewer later positions developed while more premature replacements were initiated (Fig. 3.10B-C). Overall tooth number declined (Fig. 3.10D) while the rate of replacement at the first position increased (Fig. 3.10E) with increased dosage. We also detected no increase in shedding at the first position with increasing dosage (Fig. 3.10F) further supporting the decoupling of replacement and shedding. Notably, the 10 μM dose did not significantly affect overall tooth number (Fig. 3.10B), however significantly affected the position of teeth on the tooth plate and frequency of replacement at position one (Fig. 3.10D,E). The dose response dropped off at 50 μM.

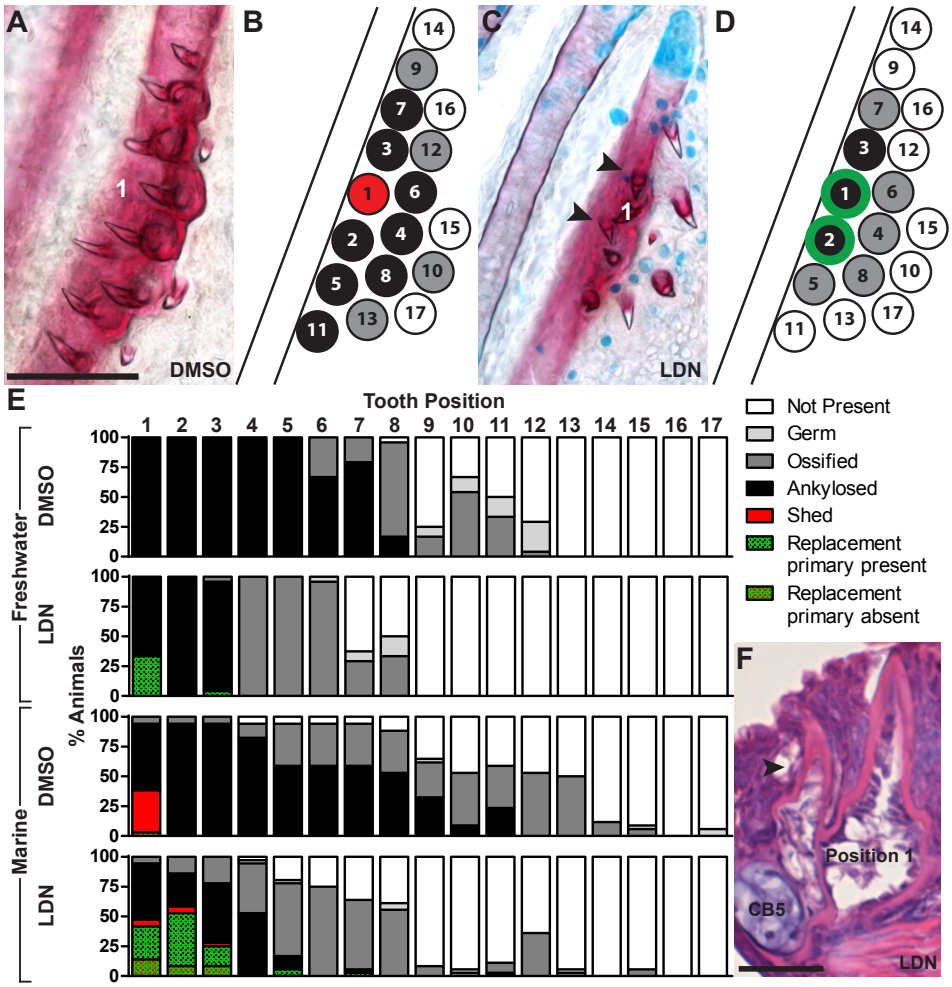

Figure 3.7: **BMP knockdown inhibits formation of primary positions, but stimulates early tooth replacement.**
(A-D) Left: representative examples of marine LDN-193189 treated (A) and DMSO control (C) ventral pharyngeal tooth plates stained with Alcian blue and Alizarin red to label cartilage and bone/teeth, respectively. Right: position scoresheet of example tooth plates (B,D). Each circle represents a tooth position with each number corresponding to the order the teeth typically arise on the tooth plate. Open circles have no tooth present at that position while colored in circles signify a tooth at one of the various stages of development (see key in E). The number 1 on the images corresponds to position 1 in the schematic to the right. Black arrowheads indicate ectopic, apparent precocious replacement teeth. See Ellis et al. (2016) for description of early tooth sequence. (E) Tooth patterning in freshwater and marine, LDN treated and DMSO control data sets from Figure 3.1. Each tooth position is a column and the y-axis is the percent of fish with that position occupied. Key to right lists developmental stages and corresponding colors in graph. (F) Hematoxylin and eosin stained 6 micron section of the first tooth position with an early replacement tooth (black arrowhead). cb5 = ceratobranchial 5. Scale bars = 100 μm (A,C), 25 μm (F).

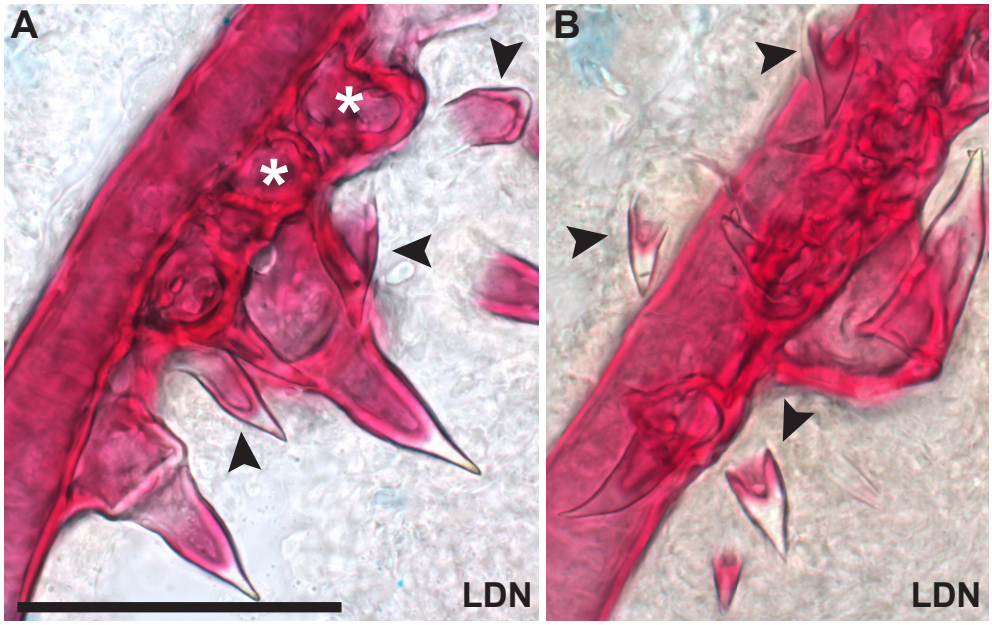

Figure 3.8: **Examples of mis-patterned LDN-193189 treated tooth plates.** (A-B) Additional examples of LDN-193189 treated. White asterisks mark positions where teeth have been shed and black arrowheads mark ectopic, apparent precocious replacement teeth. Scale bar = 100 μm (A-B)

BMP knockdown late in development results in more newly forming teeth across the tooth plate

To test whether an extended low dose of LDN can increase tooth replacement in marine sticklebacks, we coupled LDN treatment with pulse chase using vital dyes. We previously used this assay to track tooth replacement rates late in development at a stage where tooth number is different between populations and individual tooth positions are difficult to track. Tooth replacement rates late in development are significantly different between marine and freshwater sticklebacks (Ellis et al., 2015). While marine and freshwater sticklebacks respond similarly to BMP knockdown early, marine fish induced replacements beyond the first tooth position and were slightly more affected (Fig. 3.7, 3.10).

To test the effect of BMP inhibition upon new tooth formation in older fish, we pulsed with Alizarin, treated with LDN, then 14 days later chased with Calcein (Fig. 3.11A). At this late stage, overall tooth number was unaffected in LDN treated fish, likely due to a combination of the opposing roles blocking late forming primary teeth and increasing tooth replacement (Fig. 3.11B). Interestingly, when using our pulse chase assay, we detected an upward trend in the number of new teeth and new tooth formation rate (Fig. 3.11C), and significantly more small, newly erupted teeth upon LDN treatment (Fig. 3.11F). This

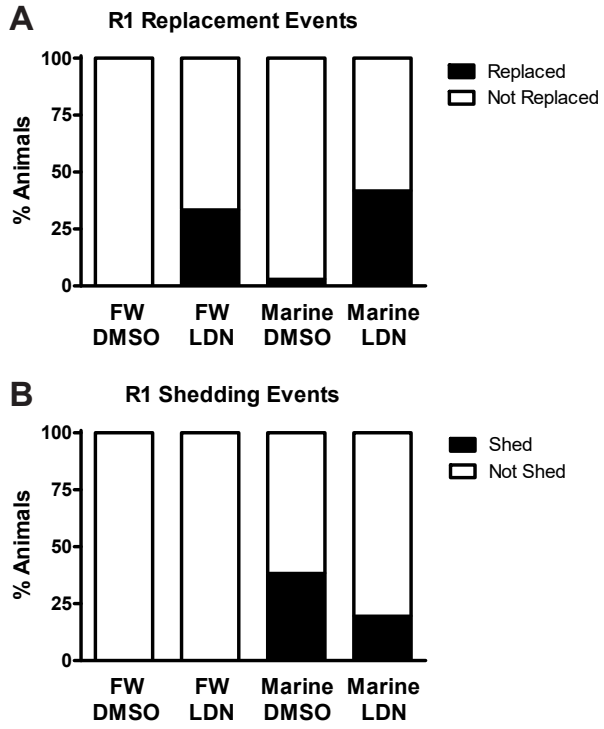

C

Phenotype	Comparison	Fisher's exact test p-value
Replacement	FW DMSO vs FW LDN	**0.0039**
Replacement	Marine DMSO vs Marine LDN	**0.0001**
Replacement	Marine DMSO vs FW DMSO	1
Replacement	Marine LDN vs FW LDN	0.59
Shedding	FW DMSO vs FW LDN	1
Shedding	Marine DMSO vs Marine LDN	0.19
Shedding	Marine DMSO vs FW DMSO	**0.0008**
Shedding	Marine LDN vs FW LDN	**0.035**

Figure 3.9: **BMP knockdown induces early replacements independent of tooth shedding at the first tooth position.**
(A-B) Frequency of replacement (A) and shedding (B) events at the first tooth position in LDN-193189 treated and DMSO control fish. (C) Fishers exact test P-values for replacement and shedding frequency. Bold P values are significant ($P < 0.05$). FW = freshwater. Samples from Figures 3.1 and 3.7.

suggests that increased tooth replacement is occurring upon BMP knockdown as the majority of teeth forming on the tooth plate at this late stage are replacement teeth. To test whether the increased number of new teeth were alternatively a wave of newly forming primary teeth, we tested whether LDN treated fish affected the size of the tooth field by measuring tooth plate area, as primary teeth form off the tooth plate, mineralize around their base, and contribute to a larger tooth plate. We found the opposite trend, where tooth plate size was smaller, although not significantly so, upon LDN treatment suggesting changes in tooth number are likely accompanied by changes to intertooth spacing to maintain the size of the tooth plate (DMSO = $0.15 \pm 0.006\ mm^2$, LDN = $0.13 \pm 0.009\ mm^2$, $P = 0.06$, two tailed t-test). Alternatively, two weeks may not be enough time to detect significant changes to the size of the tooth field.

Collectively, our data support a model where during tooth formation and replacement, BMP signaling positively regulates tooth development while negatively regulating tooth replacement. This apparent inhibitory effect of BMP signaling on tooth replacement could

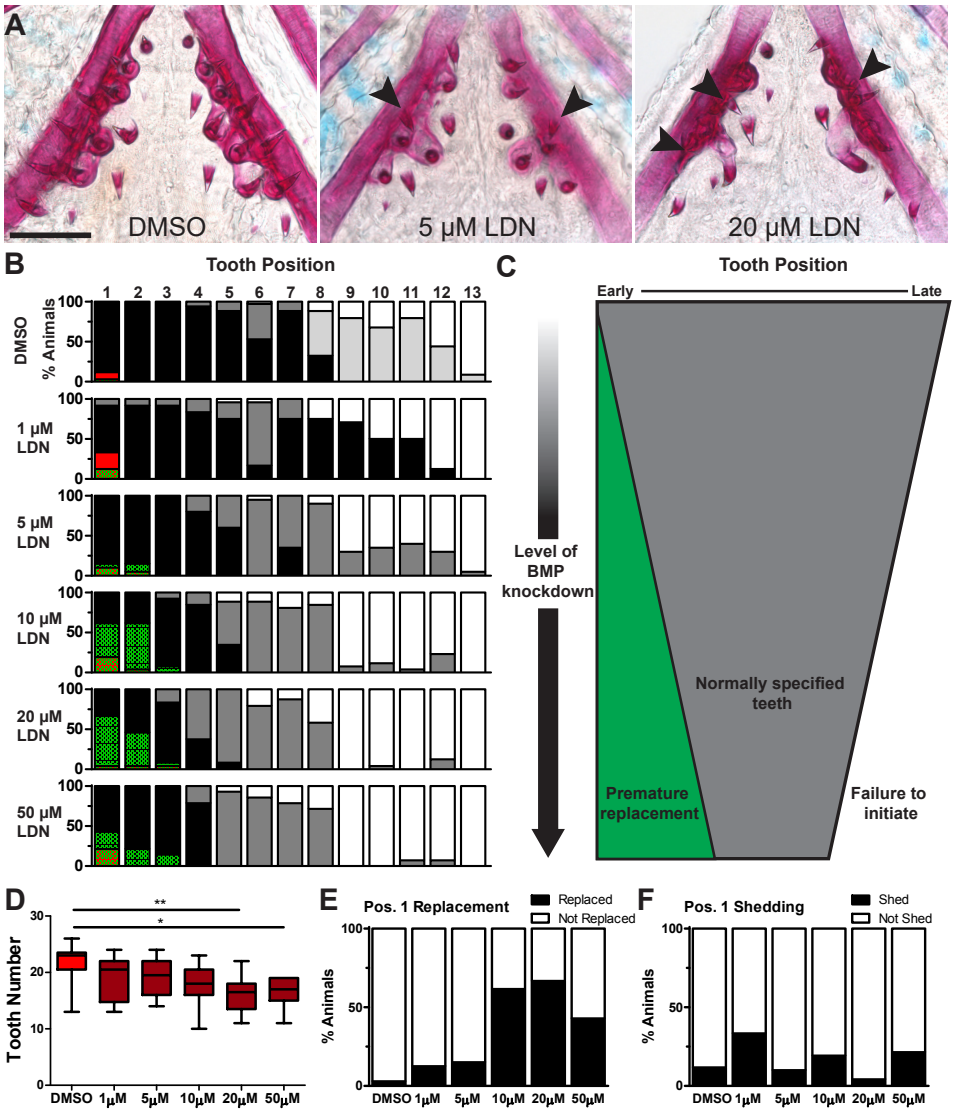

Figure 3.10: **Effects on tooth number and replacement are dose dependent with replacement events independent of tooth shedding.**
(A) Examples of ventral tooth plates of DMSO control and two LDN-193189 dosage levels. Black arrowheads point out premature replacement teeth. Scale bar is 100 μm. (B) Tooth patterning across increasing dosage of LDN. Columns are individual tooth positions and the y-axis is the percent of fish with each position occupied. See Fig. 3.7 for key. (C) Summary of data in (B). As LDN concentration increase, early positions appear to replace more frequently and late positions are less likely to initiate. (D) Tooth number decreases as dosage increases. (E) Replacement events at the first tooth position generally increase in frequency as dosage increases. (F) No increase in tooth shedding at the first tooth position is detected with increasing dosage. Sample size in B,D-F from DMSO->50 μM = 17,12,10,13,12,7 respectively. * $P < 0.05$, ** $P < 0.01$, one-way ANOVA using a Tukey-Kramer post hoc test. Additional statistics are listed in Table 3.3.

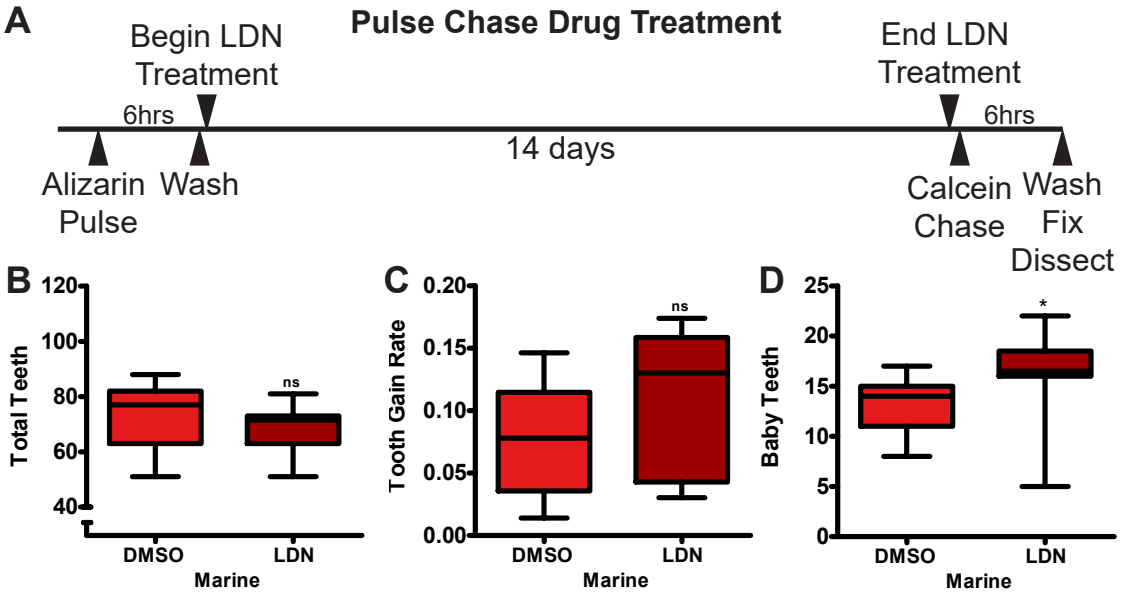

Figure 3.11: **Low level BMP knockdown late in development increases replacement in marine sticklebacks.**
(A) Diagram of pulse chase experiment using the vital dyes Alizarin and Calcein to mark growing bone and dosing with 1 μM LDN-193189. (B-D) Total teeth (B), tooth gain rate (Alizarin negative, Calcein positive/total teeth; C), and baby teeth (small, newly erupted teeth; D) are listed for drug treated and control marine fish. Sample sizes are n = 11 DMSO, 12 LDN. ns is not significant, * $P < 0.05$, two-tailed t-test.

explain how decreased *Bmp6* expression is associated with an increased tooth replacement rate in derived high-toothed freshwater fish (Cleves et al., 2014; Ellis et al., 2015). Support for (Abduweli et al., 2014; Gaete and Tucker, 2013; Handrigan et al., 2010; Huysseune and Thesleff, 2004; Juuri et al., 2013; Smith et al., 2009; Wu et al., 2013) the involvement of stem cells contributing to continuously replacing teeth have been proposed across various polyphyodont systems. However, in some fish species little support for slow-cycling label-retaining cells has been found (Vandenplas et al., 2014; Vandenplas et al., 2016). Future work will attempt to identify the cell populations and dynamics responding to different levels of BMP signaling and underlying the complex process of organ development and regeneration.

3.5 Acknowledgments

Acknowledgements We thank Nick Donde for assistance sectioning and the He lab for assistance H&E staining.

This work was supported by the National Institutes of Health (NIH) [R01-DE021475 to

C.T.M.]; National Science Foundation (NSF) Graduate Research Fellowship (N.A.E.) and an Achievement Rewards for College Scientists (ARCS) Fellowship (N.A.E.). The Vincent J. Coates Genomics Sequencing Laboratory at UC Berkeley is generously supported by NIH S10 Instrumentation Grants [S10RR029668 and S10RR027303].

3.6 References

Abduweli, D., Baba, O., Tabata, M. J., Higuchi, K., Mitani, H. and Takano, Y. (2014). Tooth replacement and putative odontogenic stem cell niches in pharyngeal dentition of medaka (*Oryzias latipes*). *Microscopy* 1-13.

Andl, T., Ahn, K., Kairo, A., Chu, E. Y., Wine-Lee, L., Reddy, S. T., Croft, N. J., Cebra-Thomas, J. a, Metzger, D., Chambon, P., et al. (2004). Epithelial *Bmpr1a* regulates differentiation and proliferation in postnatal hair follicles and is essential for tooth development. *Development* 131, 2257-68.

Barlow, A. J. and Francis-West, P. H. (1997). Ectopic application of recombinant BMP-2 and BMP-4 can change patterning of developing chick facial primordia. *Development* 124, 391-398.

Bloomquist, R. F., Parnell, N. F., Phillips, K. A., Fowler, T. E., Yu, T. Y., Sharpe, P. T. and Streelman, J. T. (2015). Coevolutionary patterning of teeth and taste buds. *Proc. Natl. Acad. Sci.* E5954-62.

Cermak, T., Doyle, E. L., Christian, M., Wang, L., Zhang, Y., Schmidt, C., Baller, J. A., Somia, N. V., Bogdanove, A. J. and Voytas, D. F. (2011). Efficient design and assembly of custom TALEN and other TAL effector-based constructs for DNA targeting. *Nucleic Acids Res.* 39, e82.

Cleves, P. A., Ellis, N. A., Jimenez, M. T., Nunez, S. M., Schluter, D., Kingsley, D. M. and Miller, C. T. (2014). Evolved tooth gain in sticklebacks is associated with a *cis*-regulatory allele of *Bmp6*. *Proc. Natl. Acad. Sci.* 111, 13912-17.

Cuny, G. D., Yu, P. B., Laha, J. K., Xing, X., Liu, J.-F., Lai, C. S., Deng, D. Y., Sachidanandan, C., Bloch, K. D. and Peterson, R. T. (2008). Structure-activity relationship study of bone morphogenetic protein (BMP) signaling inhibitors. *Bioorg. Med. Chem. Lett.* 18, 4388-92.

Dobin, A., Davis, C. A., Schlesinger, F., Drenkow, J., Zaleski, C., Jha, S., Batut, P., Chaisson, M. and Gingeras, T. R. (2013). STAR: Ultrafast universal RNA-seq aligner. *Bioinformatics* 29, 15-21.

Doyle, E. L., Booher, N. J., Standage, D. S., Voytas, D. F., Brendel, V. P., Vandyk, J. K. and Bogdanove, A. J. (2012). TAL Effector-Nucleotide Targeter (TALE-NT) 2.0: Tools for TAL effector design and target prediction. *Nucleic Acids Res.* 40, 117-122.

Ellis, N. A. and Miller, C. T. (2016). Dissection and flat-mounting of the threespine stickleback branchial skeleton. *J. Vis. Exp.* e54056.

Ellis, N. A., Glazer, A. M., Donde, N. N., Cleves, P. A., Agoglia, R. M. and Miller, C. T. (2015). Distinct developmental and genetic mechanisms underlie convergently evolved

tooth gain in sticklebacks. *Development* 142, 2442-2451.

Ellis, N. A., Donde, N. N. and Miller, C. T. (2016). Early development and replacement of the stickleback pharyngeal dentition. *J. Morphol.* in press.

Fatemifar, G., Hoggart, C. J., Paternoster, L., Kemp, J. P., Prokopenko, I., Horikoshi, M., Wright, V. J., Tobias, J. H., Richmond, S., Zhurov, A. I., et al. (2013). Genome-wide association study of primary tooth eruption identifies pleiotropic loci associated with height and craniofacial distances. *Hum. Mol. Genet.* 22, 3807-3817.

Fraser, G. J., Bloomquist, R. F. and Streelman, J. T. (2013). Common developmental pathways link tooth shape to regeneration. *Dev. Biol.* 377, 399-414.

Gaete, M. and Tucker, A. S. (2013). Organized emergence of multiple-generations of teeth in snakes is dysregulated by activation of Wnt/beta-catenin signalling. *PLoS One* 8, e74484.

Genander, M., Cook, P. J., Ramskld, D., Keyes, B. E., Mertz, A. F., Sandberg, R. and Fuchs, E. (2014). BMP Signaling and Its *pSMAD1/5* Target Genes Differentially Regulate Hair Follicle Stem Cell Lineages. *Cell Stem Cell* 15, 619-633.

Glazer, A. M., Cleves, P. A., Erickson, P. A., Lam, A. Y. and Miller, C. T. (2014). Parallel developmental genetic features underlie stickleback gill raker evolution. *Evodevo* 5, 19.

Handrigan, G. R., Leung, K. J. and Richman, J. M. (2010). Identification of putative dental epithelial stem cells in a lizard with life-long tooth replacement. *Development* 137, 3545-9.

He, X. C., Zhang, J., Tong, W.-G., Tawfik, O., Ross, J., Scoville, D. H., Tian, Q., Zeng, X., He, X., Wiedemann, L. M., et al. (2004). BMP signaling inhibits intestinal stem cell self-renewal through suppression of Wnt-beta-catenin signaling. *Nat. Genet.* 36, 1117-21.

Hollnagel, A., Oehlmann, V., Heymer, J., Rther, U. and Nordheim, A. (1999). *Id* Genes Are Direct Targets of Bone Morphogenetic Protein Induction in Embryonic Stem Cells. *J. Biol. Chem.* 274, 19838-19845.

Howe, J. R., Roth, S., Ringold, J. C., Summers, R. W., Jrvinen, H. J., Sistonen, P., Tomlinson, I. P., Houlston, R. S., Bevan, S., Mitros, F. A., et al. (1998). Mutations in the *SMAD4/DPC4* gene in juvenile polyposis. *Science* 280, 1086-1088.

Howe, J. R., Bair, J. L., Sayed, M. G., Anderson, M. E., Mitros, F. a, Petersen, G. M., Velculescu, V. E., Traverso, G. and Vogelstein, B. (2001). Germline mutations of the gene encoding *bone morphogenetic protein receptor 1A* in juvenile polyposis. *Nat. Genet.* 28, 184-7.

Humason, G. (1962). *Animal Tissue Techniques*. San Francisco: W. H. Freeman and Company.

Huysseune, A. and Thesleff, I. (2004). Continuous tooth replacement: the possible involvement of epithelial stem cells. *Bioessays* 26, 665-71.

Irizarry, R. a, Wang, C., Zhou, Y. and Speed, T. P. (2009). Gene set enrichment analysis made simple. *Stat. Methods Med. Res.* 18, 565-75.

Jackman, W. R., Davies, S. H., Lyons, D. B., Stauder, C. K., Denton-Schneider, B. R., Jowdry, A., Aigler, S. R., Vogel, S. a. and Stock, D. W. (2013). Manipulation of Fgf and

Bmp signaling in teleost fishes suggests potential pathways for the evolutionary origin of multicuspid teeth. *Evol. Dev.* 15, 107-118.

Jia, S., Zhou, J., Gao, Y., Baek, J.-A., Martin, J. F., Lan, Y. and Jiang, R. (2013). Roles of *Bmp4* during tooth morphogenesis and sequential tooth formation. *Development* 140, 423-32.

Jones, F. C., Grabherr, M. G., Chan, Y. F., Russell, P., Mauceli, E., Johnson, J., Swofford, R., Pirun, M., Zody, M. C., White, S., et al. (2012). The genomic basis of adaptive evolution in threespine sticklebacks. *Nature* 484, 55-61.

Jung, H.-S., Francis-West, P. H., Widelitz, R. B., Jiang, T.-X., Ting-Berreth, S., Tickle, C., Wolpert, L. and Chuong, C.-M. (1998). Local inhibitory action of BMPs and their relationships with activators in feather formation: implications for periodic patterning. *Dev. Biol.* 196, 11-23.

Juuri, E., Jussila, M., Seidel, K., Holmes, S., Wu, P., Richman, J., Heikinheimo, K., Chuong, C.-M., Arnold, K., Hochedlinger, K., et al. (2013). *Sox2* marks epithelial competence to generate teeth in mammals and reptiles. *Development* 140, 1424-32.

Kandyba, E., Leung, Y., Chen, Y.-B., Widelitz, R., Chuong, C.-M. and Kobielak, K. (2013). Competitive balance of intrabulge BMP/Wnt signaling reveals a robust gene network ruling stem cell homeostasis and cyclic activation. *Proc. Natl. Acad. Sci. U. S. A.* 110, 1351-6.

Kassai, Y., Munne, P., Hotta, Y., Penttil, E., Kavanagh, K., Ohbayashi, N., Takada, S., Thesleff, I., Jernvall, J. and Itoh, N. (2005). Regulation of mammalian tooth cusp patterning by *ectodin*. *Science* 309, 2067-70.

Kavanagh, K. D., Evans, A. R. and Jernvall, J. (2007). Predicting evolutionary patterns of mammalian teeth from development. *Nature* 449, 427-32.

Kimmel, C. B., Ullmann, B., Walker, M., Miller, C. T. and Crump, J. G. (2003). *Endothelin 1*-mediated regulation of pharyngeal bone development in zebrafish. *Development* 130, 1339-1351.

Kimmel, C. B., DeLaurier, A., Ullmann, B., Dowd, J. and McFadden, M. (2010). Modes of developmental outgrowth and shaping of a craniofacial bone in zebrafish. *PLoS One* 5, e9475.

Kobielak, K., Pasolli, H. A., Alonso, L., Polak, L. and Fuchs, E. (2003). Defining BMP functions in the hair follicle by conditional ablation of *BMP receptor IA*. *J. Cell Biol.* 163, 609-623.

Kobielak, K., Stokes, N., de la Cruz, J., Polak, L. and Fuchs, E. (2007). Loss of a quiescent niche but not follicle stem cells in the absence of bone morphogenetic protein signaling. *Proc. Natl. Acad. Sci. U. S. A.* 104, 10063-8.

L, S., Josse, J. and Husson, F. (2008). FactoMineR: An R package for multivariate analysis. *J Stat Softw* 25, 1-18.

Li, H., Handsaker, B., Wysoker, A., Fennell, T., Ruan, J., Homer, N., Marth, G., Abecasis, G. and Durbin, R. (2009). The Sequence Alignment/Map format and SAMtools. *Bioinformatics* 25, 2078-2079.

Miller, C. T., Glazer, A. M., Summers, B. R., Blackman, B. K., Norman, A. R., Shapiro, M. D., Cole, B. L., Peichel, C. L., Schluter, D. and Kingsley, D. M. (2014). Modular skeletal evolution in sticklebacks is controlled by additive and clustered quantitative trait loci. *Genetics* 197, 405-20.

Miyazono, K. and Miyazawa, K. (2002). *Id*: a target of BMP signaling. *Sci. STKE* 2002, pe40.

Mohedas, A. H., Xing, X., Armstrong, K. A., Bullock, A. N., Cuny, G. D. and Yu, P. B. (2013). Development of an *ALK2*-biased BMP type i receptor kinase inhibitor. *ACS Chem. Biol.* 8, 1291-1302.

Mou, C., Pitel, F., Gourichon, D., Vignoles, F., Tzika, A., Tato, P., Yu, L., Burt, D. W., Bedhom, B., Tixier-Boichard, M., et al. (2011). Cryptic patterning of avian skin confers a developmental facility for loss of neck feathering. *PLoS Biol.* 9, e1001028.

Munne, P. M., Felszeghy, S., Jussila, M., Suomalainen, M., Thesleff, I. and Jernvall, J. (2010). Splitting placodes: effects of *bone morphogenetic protein* and *Activin* on the patterning and identity of mouse incisors. *Evol. Dev.* 12, 383-92.

Neubser, A., Peters, H., Balling, R. and Martin, G. (1997). Antagonistic interactions between FGF and BMP signaling pathways: a mechanism for positioning the sites of tooth formation. *Cell* 90, 247-255.

Nieminen, P. (2009). Genetic basis of tooth agenesis. *J. Exp. Zool. B. Mol. Dev. Evol.* 312B, 32042.

Noramly, S. and Morgan, B. A. (1998). BMPs mediate lateral inhibition at successive stages in feather tract development. *Development* 125, 3775-87.

OConnell, D. J., Ho, J. W. K., Mammoto, T., Turbe-Doan, A., OConnell, J. T., Haseley, P. S., Koo, S., Kamiya, N., Ingber, D. E., Park, P. J., et al. (2012). A Wnt-bmp feedback circuit controls intertissue signaling dynamics in tooth organogenesis. *Sci. Signal.* 5, 1-10.

Plikus, M. V, Zeichner-David, M., Mayer, J.-A., Reyna, J., Bringas, P., Thewissen, J. G. M., Snead, M. L., Chai, Y. and Chuong, C.-M. (2005). Morphoregulation of teeth: modulating the number, size, shape and differentiation by tuning Bmp activity. *Evol. Dev.* 7, 440-57.

Plikus, M. V, Mayer, J. A., de la Cruz, D., Baker, R. E., Maini, P. K., Maxson, R. and Chuong, C.-M. (2008). Cyclic dermal BMP signalling regulates stem cell activation during hair regeneration. *Nature* 451, 340-4.

Roberts, A., Trapnell, C., Donaghey, J., Rinn, J. L. and Pachter, L. (2011a). Improving RNA-Seq expression estimates by correcting for fragment bias. *Genome Biol.* 12, R22.

Roberts, A., Pimentel, H., Trapnell, C. and Pachter, L. (2011b). Identification of novel transcripts in annotated genomes using RNA-seq. *Bioinformatics* 27, 2325-2329.

Satokata, I. and Maas, R. (1994). *Msx1* deficient mice exhibit cleft palate and abnormalities of craniofacial and tooth development. *Nat. Genet.* 6, 348-56.

Scaal, M., Prls, F., Fchtbauer, E., Patel, K., Hornik, C., Khler, T., Christ, B. and Brand-Saberi, B. (2002). BMPs induce dermal markers and ectopic feather tracts. *Mech. Dev.* 110, 51-60.

Schuelke, M. (2000). An economic method for the fluorescent labeling of PCR fragments A poor man s approach to genotyping for research and high-throughput diagnostics . *Nat. Biotechnol.* 18, 1-2.

Sloan, A. J., Rutherford, R. B. and Smith, A. J. (2000). Stimulation of the rat dentine-pulp complex by *bone morphogenetic protein-7* in vitro. *Arch. Oral Biol.* 45, 173-77.

Smith, M. M., Fraser, G. J. and Mitsiadis, T. A. (2009). Dental lamina as source of odontogenic stem cells: evolutionary origins and developmental control of tooth generation in gnathostomes. *J. Exp. Zool. B. Mol. Dev. Evol.* 312B, 260-80.

Suzuki, A., Ueno, N. and Hemmati-Brivanlou, A. (1997). Xenopus *msx1* mediates epidermal induction and neural inhibition by BMP4. *Development* 124, 3037-3044.

Trapnell, C., Williams, B. a, Pertea, G., Mortazavi, A., Kwan, G., van Baren, M. J., Salzberg, S. L., Wold, B. J. and Pachter, L. (2010). Transcript assembly and quantification by RNA-Seq reveals unannotated transcripts and isoform switching during cell differentiation. *Nat. Biotechnol.* 28, 511-515.

Vainio, S., Karavanova, I., Jowett, a and Thesleff, I. (1993). Identification of BMP-4 as a signal mediating secondary induction between epithelial and mesenchymal tissues during early tooth development. *Cell* 75, 45-58.

Vandenplas, S., De Clercq, A. and Huysseune, A. (2014). Tooth replacement without a dental lamina: the search for epithelial stem cells in *Polypterus senegalus*. *J. Exp. Zool. B. Mol. Dev. Evol.* 322, 281-93.

Vandenplas, S., Willems, M., Witten, P. E., Hansen, T., Fjelldal, P. G. and Huysseune, A. (2016). Epithelial Label-Retaining Cells Are Absent during Tooth Cycling in *Salmo salar* and *Polypterus senegalus*. *PLoS One* 11, e0152870.

Vastardis, H., Karimbux, N., Guthua, S., Seidman, J. and Seidman, C. (1996). A human *MSX1* homeodomain missense mutation causes selective tooth agenesis. *Nat. Genet.* 13, 417-21.

Walker, M. B. and Kimmel, C. B. (2007). A two-color acid-free cartilage and bone stain for zebrafish larvae. Biotech. *Histochem.* 82, 23-8.

Wise, S. B. and Stock, D. W. (2010). *Bmp2B* and *Bmp4* Are Dispensable for Zebrafish Tooth Development. *Dev. Dyn. 239*, 2534-46.

Wu, P., Wu, X., Jiang, T.-X., Elsey, R. M., Temple, B. L., Divers, S. J., Glenn, T. C., Yuan, K., Chen, M.-H., Widelitz, R. B., et al. (2013). Specialized stem cell niche enables repetitive renewal of alligator teeth. *Proc. Natl. Acad. Sci.* 1-10.

Zhang, J., He, X. C., Tong, W.-G., Johnson, T., Wiedemann, L. M., Mishina, Y., Feng, J. Q. and Li, L. (2006). Bone morphogenetic protein signaling inhibits hair follicle anagen induction by restricting epithelial stem/progenitor cell activation and expansion. *Stem Cells* 24, 2826-39.

Zouvelou, V., Luder, H.-U., Mitsiadis, T. a and Graf, D. (2009). Deletion of *BMP7* affects the development of bones, teeth, and other ectodermal appendages of the orofacial complex. *J. Exp. Zool. B. Mol. Dev. Evol.* 312B, 361-74.

Zuniga, E., Rippen, M., Alexander, C., Schilling, T. F. and Crump, J. G. (2011). *Gremlin 2* regulates distinct roles of BMP and *Endothelin 1* signaling in dorsoventral patterning

of the facial skeleton. *Development* 138, 5147-5156.

Chapter 4

Appendix: Dissection and flat-mounting of the stickleback branchial skeleton

> "Tell me and I forget. Teach me and I may remember. Involve me and I learn."
> -Benjamin Franklin

The following chapter was originally published as an article:
Journal of Visualized Experiments 2016, e54056

Nicholas A. Ellis and Craig T. Miller

Department of Molecular and Cell Biology, University of California-Berkeley, Berkeley CA, 94720, USA

The video component of this article can be found at http://www.jove.com/video/54056/

4.1 Abstract

The posterior pharyngeal segments of the vertebrate head give rise to the branchial skeleton, the primary site of food processing in fish. The morphology of the fish branchial skeleton is matched to a species' diet. Threespine stickleback fish (*Gasterosteus aculeatus*) have emerged as a model system to study the genetic and developmental basis of evolved differences in a variety of traits. Marine populations of sticklebacks have repeatedly colonized countless new freshwater lakes and creeks. Adaptation to the new diet in these freshwater environments likely underlies a series of craniofacial changes that have evolved repeatedly in independently derived freshwater populations. These include three major patterning changes to the branchial skeleton: reductions in the number and length of gill raker bones, increases in pharyngeal tooth number, and increased branchial bone lengths. Here we describe a detailed protocol to dissect and flat-mount the internal branchial skeleton in threespine stickleback fish. Dissection of the entire three-dimensional branchial skeleton and mounting it flat into a largely two-dimensional prep allows for the easy visualization and quantification of branchial skeleton morphology. This dissection method is inexpensive, fast, relatively easy, and applicable to a wide variety of fish species. In sticklebacks, this efficient method allows the quantification of skeletal morphology in genetic crosses to map genomic regions controlling craniofacial patterning.

Keywords: Branchial skeleton, pharyngeal teeth, gill raker, branchial bones, craniofacial, stickleback, *Gasterosteus aculeatus*

4.2 Introduction

An incredible amount of diversity exists in the head skeleton among vertebrates, especially among fishes. In many cases this diversity facilitates different feeding strategies (Albertson and Kocher, 2006; Cooper and Westneat, 2009; Martin and Wainwright, 2011; Wainwright et al., 2012), and can involve major changes to both external and internal craniofacial patterning. The branchial skeleton is located internally in the throat of a fish and surrounds most of the buccal cavity. The branchial skeleton is comprised of 5 serially homologous segments, the anterior four of which support the gills. Together these five segments function as an interface between fish and their food (Sibbing, 1991). Variation in a multitude of traits including gill rakers, pharyngeal teeth, and branchial bones contribute to efficient foraging on different types of food.

Sticklebacks have undergone an adaptive radiation after ancestral oceanic forms colonized freshwater lakes and creeks throughout the northern hemisphere. The shift in diet from small zooplankton in the ocean to larger prey in freshwater has resulted in dramatic trophic variation in several craniofacial traits (Bell and Foster, 1994). While many studies have focused on external craniofacial differences in sticklebacks (Berner et al., 2014; Caldecutt et al., 2001; Jamniczky et al., 2015; Kimmel et al., 2005; Mcgee and Wainwright, 2013; McGee

et al., 2013; McGuigan et al., 2010), important craniofacial changes evolve repeatedly in the internal branchial skeleton. The ability to create fertile hybrids between morphologically distinct stickleback populations provides an excellent opportunity to map the genetic basis of evolved changes to the branchial skeleton.

One trophic trait of ecological significance is the patterning of gill rakers, periodic dermal bones that line the anterior and posterior faces of the branchial bones and are used to filter prey items. Fish that typically feed on small prey items tend to have longer and more densely spaced gill rakers compared to fish that feed on larger prey (Kahilainen et al., 2011; Magnuson and Heitz, 1971). Variation in gill rakers has been reported both within and between species (Arengard et al., 2014; Gross and Anderson, 1984; Hagen and Gilbertson, 1972; Kahilainen et al., 2011; Magnuson and Heitz, 1971; McPhail, 1984), and aspects of gill raker patterning contribute to trophic niches and fitness (Arnegard et al., 2014). Decades of research have extensively documented gill raker number and length variation in threespine sticklebacks (Gross et al., 1984; Hagen and Gilbertson, 1972; McPhail, 1984; Robinson, 2000; Schluter and McPhail, 1992); however, these studies typically focus on the first row of gill rakers. Recent work has shown modularity in the genetic control of gill raker number across the branchial skeleton (Glazer et al., 2014; Miller et al., 2014) and across a single row in gill raker spacing (Miller et al., 2014) and length (Glazer et al., 2015) highlighting the importance of studying more than row one or a single gill raker to understand the developmental genetic basis of gill raker reduction.

A second trophic trait of both ecological and biomedical significance is the patterning of pharyngeal teeth. Teeth in fishes can be located in both the oral jaw and in the branchial skeleton, known as pharyngeal teeth. Oral teeth are used primarily for prey capture while pharyngeal teeth are used for mastication and prey manipulation (Hulsey et al., 2005; Lauder, 1983; Wainwright, 2006). Both sets form via shared developmental mechanisms and are considered developmentally homologous (Fraser et al., 2009). Interesting modularity occurs whereby some species, such as zebrafish, lack oral and dorsal pharyngeal teeth (Stock, 2007) while other species have multiple toothed ceratobranchials, pharyngobranchials, and sometimes toothed basihyal and hypobranchials (Liem and Greenwood, 1981). In sticklebacks, pharyngeal teeth are found ventrally on the fifth ceratobranchial and dorsally on the anterior and posterior pharyngobranchials (Anker, 1974). Kinematics on stickleback feeding show the oral jaw is used primarily for prey capture and facilitating suction feeding (McGee et al., 2013) leaving mastication to the pharyngeal jaw. In cichlids, lower pharyngeal jaw morphology varies dramatically (Huysseune, 1995; Meyer, 1990) and has been shown to be adaptive and correlated with trophic niche (Muschick et al., 2012). Multiple freshwater stickleback populations have evolved dramatic increases in ventral pharyngeal tooth number (Cleves et al., 2014; Ellis et al., 2015; Miller et al., 2014). Recent work has demonstrated that the developmental genetic basis of this evolved tooth gain is largely distinct in two independently derived populations of freshwater sticklebacks (Ellis et al., 2015). Unlike mammalian teeth, fish regenerate their teeth continuously throughout adult life (Tucker and Fraser, 2014). Both of these previously described high toothed freshwater populations have evolved an accelerated tooth replacement rate, providing a rare vertebrate system to study the genetic

basis of regeneration (Ellis et al., 2015).

A third trophic trait that has evolved repeatedly in freshwater sticklebacks is longer epibranchial and ceratobranchial bones, the branchial arch segmental homologs of the upper and lower jaw, respectively (Erickson et al., 2014). Longer branchial bones confer a larger buccal cavity and likely are adaptive for allowing larger prey items to be consumed. Furthermore, in other fish, epibranchial bones are important for depression of the dorsal pharyngeal tooth plates (Wainwright, 2006). Like gill rakers and pharyngeal teeth, the branchial bones are internal and thus, difficult to easily visualize or quantify.

Here we present a detailed protocol to dissect and flat-mount the branchial skeleton, allowing easy visualization and quantification of a variety of important craniofacial traits. While this protocol describes a stickleback dissection, this same method works on a variety of other fishes.

4.3 Protocol

All fish work was approved by the Institutional Animal Care and Use Committee of the University of California-Berkeley (protocol # R330). Euthanasia was performed using immersion in 0.025% Tricaine-S buffered with 0.1% sodium bicarbonate (Leary et al., 2013). All steps are performed at room temperature.

1. Preparation

Note: Perform steps 1.1-1.5 in conical tubes or scintillation vials that can seal tightly and be laid horizontally. Fish do not need to be constantly shaken, but try to mix the solution as often as possible by gently inverting or shaking the rack of tubes or vials to expose all sides of the fish to the staining solution and allow stain to penetrate the tissue evenly. Do not place a large batch of fish on a platform shaker, as the heavy weight of the liquid will break the shaker.

1. Fix either freshly euthanized fish or fish stored in ethanol with 10% Neutral Buffered Formalin (NBF) overnight. Alternatively, use 4% paraformaldehyde in 1x PBS solution instead of 10% NBF.

Note: If extracting DNA, clip a small portion of the caudal or pectoral fins prior to fixation and store in ethanol.

2. Dispose of fix properly in a chemical hood and replace with tap water (that is ~pH 7.0) for 2 hr. Avoid using de-ionized water as it can often be acidic and can decalcify bone.

3. Remove water and stain fish with 0.008% Alizarin Red S in 1% KOH in water for 24 hr. For fish less than 20 mm standard length, use 0.004% Alizarin Red S. (Make a 100x

(0.8%) stock solution of Alizarin Red S which can then be diluted).

4. Remove stain (putting in appropriate waste container in hood) and place fish in tap water for a few hr. Change water as needed until water rinse is mostly clear.

5. Remove water and place fish into 50% glycerol, 0.25% KOH for mild clearing and subsequent dissection. Note: This staining protocol is modified from previously described methods (Bell, 1984; Taylor and Van Dyke, 1985).

2. Dissection

Note: See Figure 4.1 for a review of relevant head skeletal morphology.

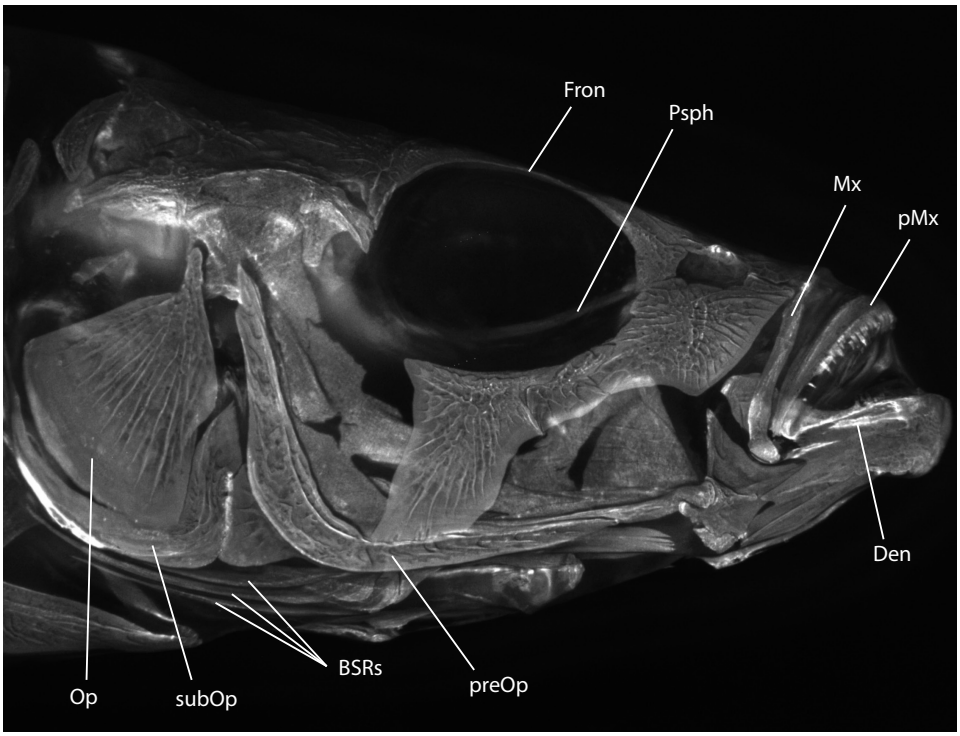

Figure 4.1: **Stickleback head skeletal morphology.**
Alizarin Red stained threespine stickleback head imaged with fluorescence under a rhodamine B filter set. Useful morphology is labeled: Op = opercle, Subop= subopercle, BSRs = branchiostegal rays, Preop = preopercle, Infraorb 1-3 = infraorbital 1-3 (also called circumorbitals or suborbitals), Dent = dentary, Premax = premaxilla, Max = maxilla, Nas = nasal, Lat. ethm = lateral ethmoid, Psph = parasphenoid, Fron = frontal bone. For a more detailed description of the stickleback head skeleton, see Anker, 1974.

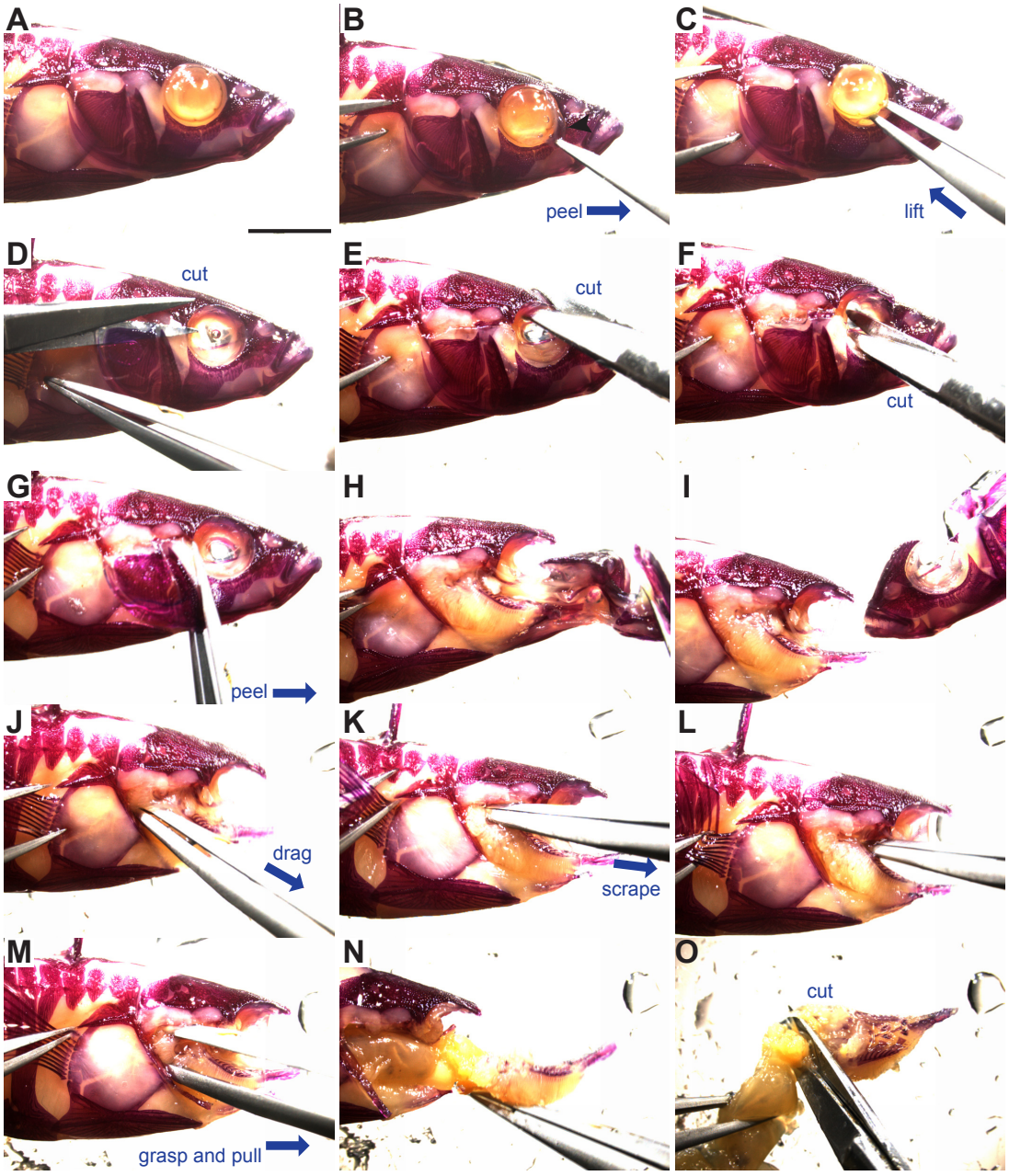

Figure 4.2: **Stickleback branchial skeleton dissection.**
Alizarin Red stained threespine stickleback fish ready for dissection. The eye is depigmented from extensive clearing. Blue arrows indicate the direction of motion. (A) Lateral view of stickleback head, anterior is to the right. (B) Removal of membrane covering the eye. (C) Removal of the eye. (D) Dorsal cut above the opercle. (E) Frontal bone cut. (F) Parasphenoid cut. (G-I) Removal of the facial skeleton. (J) Removal of ventral branchial skeleton soft tissue connections. (K-L) Removal of dorsal branchial skeleton connections. (M-N) Removal of the branchial skeleton. (O) Separate the gut tube from the branchial skeleton. See steps 2.1 through 2.16 for more details. Scale bar = 5 mm.

1. Lay the fish flat (Figure 4.1A) and insert sharp #5 watchmaker's forceps into the side of the eye at a ~45° angle to puncture the membrane covering the eye.

2. Peel the membrane away from the eye, similar to peeling a yogurt lid (Figure 4.2B).

3. Insert open forceps behind the eye, grab hold of the optic nerve behind the eye, and remove the eye (Figure 4.2C). Do not puncture the eye as it will leak melanin. If punctured, melanin can be washed away during later steps.

4. Repeat on other side.

5. Starting from the posterior, place one small dissecting scissor blade under the opercle flap, drag scissor blade dorsally above opercle, then cut soft tissue through to the eye socket (Figure 4.2D). Cut dorsal to the opercle bone.

6. Cut the frontal bone (dorsal to the eye socket) (Figure 4.2E).

7. Cut the midline parasphenoid bone around the center of the eye sockets (Figure 4.2F).

8. Repeat opercle cut on the opposing side.

9. Insert forceps under the opercle and slowly peel the face away from the body, trimming any soft tissue still attached (Figure 4.2G-H). Take care not to disrupt the first row of gill rakers.

    1. With forceps, detach the ceratohyals on both sides from the midline basihyal while peeling away and removing the anterior craniofacial skeleton (the entire jaw including the dentary, premaxilla, and maxilla; the entire hyoid skeleton including the exterior dermal opercle, preopercle, subopercle, and branchiostegal rays and the underlying dorsal and ventral endochondral elements; and the anterior part of the skull including the nasal, lateral ethmoid, and infraorbital bones, see Figures 4.1 and 4.2I).

    2. Pelvic spines can be folded out from the body, and can serve as a handle for forceps to grab hold of when present. Spines lock into place. To unlock, gently pull spine with forceps directly away from fish body, then gently bend posteriorly to press spine flat against fish.

10. Insert closed forceps posterior and ventral to the branchial skeleton (just below gut tube) and drag forceps anteriorly, teasing apart the remaining muscles and ligaments attached to the branchial skeleton (Figure 4.2J-K).

11. Using the tips of closed forceps, scrape away the muscles attaching the dorsal branchial

skeleton to the ventral braincase in a posterior to anterior direction (Figure 4.2L).

12. Repeat 2.9 and 2.10 on the opposing side.

13. Grasp the base of the gut tube and pull anteriorly to remove the branchial skeleton and gut tube (Figure 4.2M-N).

14. Separate the gut tube by making a perpendicular cut posterior to the end of the fifth ceratobranchial (Figure 4.2O).

15. After removing any remaining bone fragments from the braincase on the dorsal side of the branchial skeleton, insert scissors into the branchial basket to make a dorsal cut (cutting anterior to posterior) between the bilateral sets of dorsal tooth plates (Figure 4.3A-D). Ensure cut is centered to avoid damaging the dorsal tooth plates.

16. Make two shallow lateral cuts in the rubbery gut lumen at the posterior end of the branchial skeleton (anterior end of gut tube) to assist with opening the branchial skeleton (Figure 4.3E).

17. Place fish and all tissue pieces into a jar and place the branchial skeleton into a microcentrifuge tube with 50% glycerol, 0.25% KOH to continue gentle clearing, or 100% glycerol if no further clearing is required. Label jars and tubes with a unique identifier so they can be tracked. The amount of clearing required is largely a function of the size of the fish, large adult fish (over 40 mm in standard length) typically require additional clearing.

3. Branchial Skeleton Re-staining (if necessary)

1. To stain the branchial skeleton darker or clear tissue more, remove 50% glycerol, 0.25% KOH solution and wash with 1% KOH twice (one five minute wash followed by a second 24 hr wash while shaking horizontally on a platform shaker).

2. Remove 1% KOH and re-stain with 0.008% Alizarin Red S in 1% KOH for 24 hr.

3. Remove stain and replace with 1% KOH for 24 hr.

4. Remove KOH solution and replace with 50% glycerol, 0.25% KOH.

4. Mounting Branchial Skeleton

1. Remove branchial skeleton from 50% glycerol, 0.25% KOH or 100% glycerol and place near the bottom of a 22 mm x 60 mm glass cover slip with the dorsal side facing up (Figure 4.3F). Add a few drops of 50% glycerol, 0.25% KOH or 100% glycerol on top of branchial

skeleton. If transitioning from 50% glycerol, 0.25% KOH to 100% glycerol, change solution in a microcentrifuge tube and shake for >5 min prior to mounting to equilibrate tissue.

2. Roll out two small balls of modeling clay and place on either end of the cover slip to act as spacers.

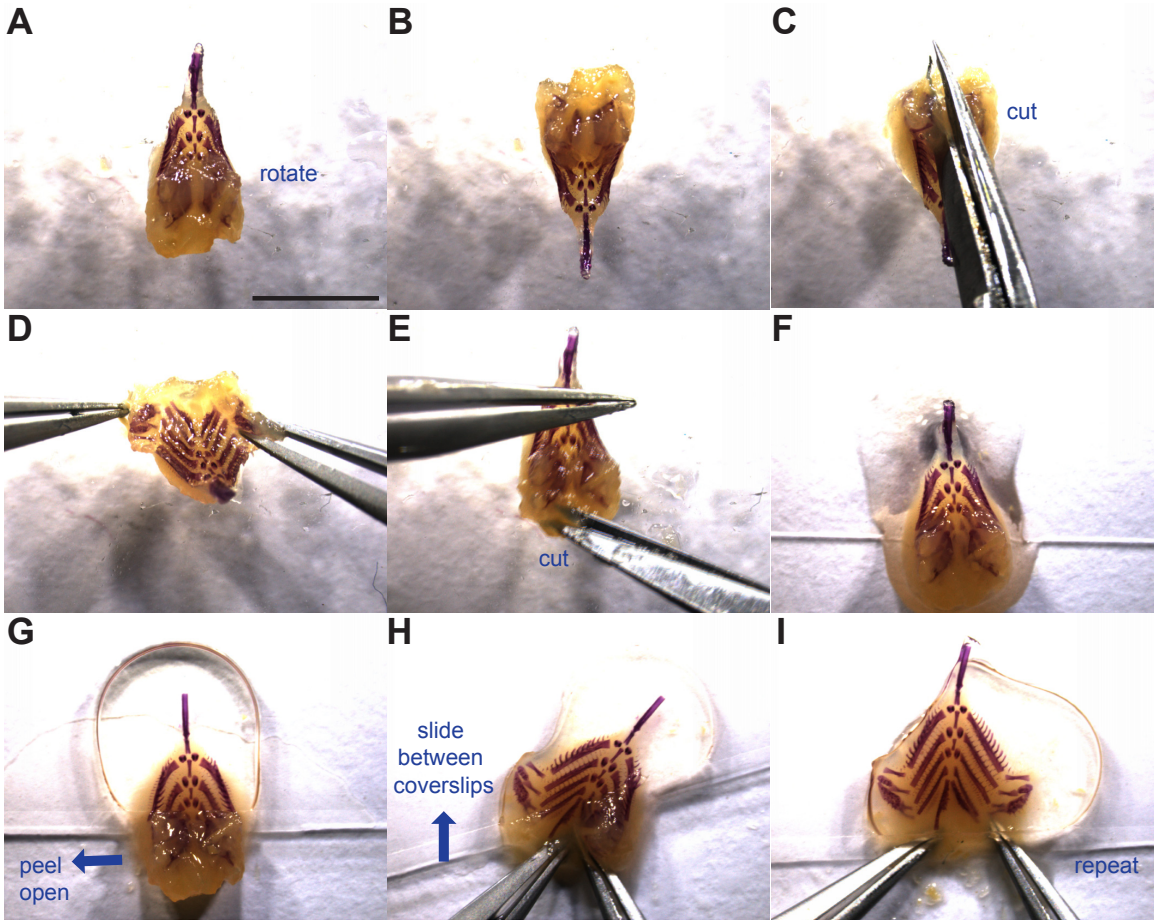

Figure 4.3: **Flat mounting the branchial skeleton.**
Manipulation and mounting of the branchial skeleton is shown. Blue arrows indicate the direction of motion. (A) Branchial skeleton dorsal side up. (B-D) Rotation and incision between the dorsal tooth plates. (E) Lateral cut in soft tissue to further open the base of the gut tube. (F) Branchial skeleton placed at the bottom of a coverslip ready for mounting. (G) Second coverslip placed on the anterior half of the branchial skeleton (above dorsal tooth plates). (H-I) Flat mounting of the branchial skeleton by opening dorsal tooth plate flaps and sliding between two cover slips. See steps 4.1 through 4.6 for more details. Scale bar = 5 mm.

3. Loosely place a second coverslip on top with enough pressure to flatten the anterior branchial skeleton (Figure 4.3G).

4. Peel open the left dorsal flap including dorsal tooth plates, flatten, and slide between the coverslips (Figure 4.3H).

5. Repeat technique with right dorsal flap and push entire branchial skeleton away from the edge of the coverslip (Figure 4.3I).

> 1. Alternatively, hold both dorsal flaps open with forceps and carefully place the coverslip on, flattening the branchial skeleton in one smooth motion.
>
> 2. Alternatively, mount the branchial skeleton upside-down on one cover slip, splaying each dorsal side out laterally so gravity does not allow the branchial skeleton to close back up. Then cover with second 22 mm x 60 mm glass cover slip and invert prep.

Note: Different mounting techniques tend to work better or worse for each individual. Try each and see what feels most comfortable.
6. Lightly press on top coverslip to flatten clay balls enough to keep the branchial skeleton mounted flat, but take care not to crush the specimen.

> 1. During the mounting process, ceratobranchials may rotate and obscure a row of rakers. Remedy this by sliding forceps between the coverslips and re-orienting the ceratobranchials or entire branchial skeleton.

7. Store preps flat in slide trays at room temperature. Mounted in 100% glycerol, preps can be stored between bridged coverslips for at least a decade. Clean forceps and scissors with isopropanol or ethanol and cover tips.

4.4 Results

This protocol results in a dissected and flat mounted branchial skeleton (Figure 4.4) where a variety of important trophic traits can be quantified. From a dorsal view, all rows of gill rakers, all pharyngeal tooth plates, and nearly all branchial bones can be easily visualized and quantified (Cleves et al., 2014; Ellis et al., 2015; Erickson et al., 2014; Erickson et al., 2015; Glazer et al., 2014; Glazer et al., 2015; Miller et al., 2014). Alizarin Red S also fluoresces on a rhodamine or similar red filter allowing double labeling with other markers (e.g., transgenic GFP, Erickson et al., 2015) and an alternative method of visualization. Fluorescence fades

quickly in light, so store preps in the dark if fluorescent imaging or phenotyping is planned. From a ventral view, the gills can be visualized and their pigmentation quantified (Miller et al., 2007). Preps can be stored in 100% glycerol for years.

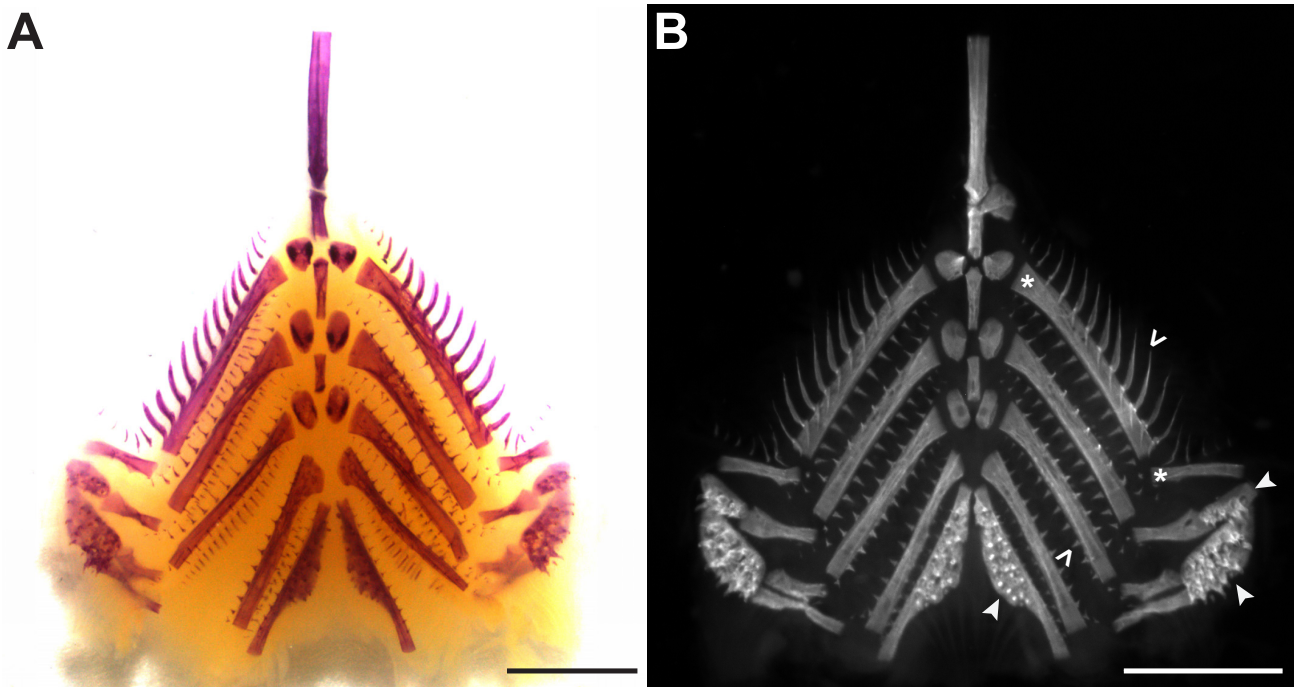

Figure 4.4: **Representative stickleback branchial skeleton.**
Two examples of stained and cleared branchial skeletons are shown. (A) Brightfield image showing bone labeled red. (B) Fluorescent image under a rhodamine B filter set. Examples of rakers, teeth, and bones are labeled with carets, arrowheads, and asterisks, respectively. Scale bars = 2 mm.

4.5 Discussion

The branchial skeleton is a complex set of bones in the throat of a fish that manipulates, filters, and masticates food items on their way to the esophagus. Many interesting trophic traits including the patterning of gill rakers, pharyngeal teeth, and branchial bones vary across and within species. The majority of these traits are difficult to near impossible to accurately measure with the branchial skeleton in situ (e.g., gill raker length, branchial bone length). This flat-mounting protocol places all branchial skeletal elements in a simple two-dimensional plane for ease of imaging and quantification of multiple traits.

One limitation of this protocol is that although teeth, gill rakers, and most endochondral bones within this flat-mounted two-dimensional prep can be easily imaged and quantified,

the second through fourth epibranchials, that have much more three-dimensional shapes, are not easily visualized and would require additional dissection to accurately measure. A second limitation of this protocol is the method is minimally destructive to the fish head. However, only two bones are damaged with a single cut each, the parasphenoid and the frontal bone. All other craniofacial skeletal elements can be returned to and measured at later points in time.

This protocol, although developed for sticklebacks, can be used in many other fish species, although sometimes modifications are necessary. For example, some fish species like zebrafish have a non-ossified dorsal chewing pad (Aigler et al., 2014) requiring the dorsal cut to be lateral, around this plate. The posterior end of the fifth ceratobranchial is curved is some species (e.g., zebrafish and other *Cypriniformes*) and must be trimmed or much larger clay spacers used to allow flat mounting. Particularly large specimens can be mounted between two pieces of glass or acrylic in the same manner. Species with a particularly thick epithelial layer covering tooth plates can be restained and cleared after dissection or more aggressively cleared with 2% KOH. Fish in this situation may also be presoaked in 1 or 2% KOH prior to Alizarin staining to increase dye penetrance. An alternative more technologically advanced method for imaging the branchial skeleton is Micro Computed Tomography (μCT) (Miller et al., 2014; Pasco-Viel et al., 2010). However, μCT requires an expensive scanner, is much more time consuming, and requires considerable training. Instead, this dissection protocol is inexpensive, quick, and amenable to high throughput studies required for quantitative studies such as quantitative trait loci (QTL) mapping genomic regions controlling evolved changes in craniofacial patterning. Additionally, these dissections can be performed at any larval or adult time point (Cleves et al., 2014; Ellis et al., 2015; Erickson et al., 2014; Glazer et al., 2014) to study skeletal development. Although fish head anatomy is complex, this simple protocol allows easy visualization of the internal branchial skeleton, a critically important component of trophic morphology.

4.6 Acknowledgments

Thanks to Craig who originally pioneered this dissection method and the countless students who tested it. Thanks to Miles Johnson for assistance with imaging and Priscilla Erickson for critical reading of the manuscript. This work was funded in part by NIH R01 #DE021475 to CTM and an NSF Graduate Research Fellowship to NAE.

4.7 References

Aigler, S. R., Jandzik, D., Hatta, K., Uesugi, K. and Stock, D. W. (2014). Selection and constraint underlie irreversibility of tooth loss in cypriniform fishes. *Proc. Natl. Acad. Sci. U. S. A.* 111, 7707-12.

Albertson, R. C. and Kocher, T. D. (2006). Genetic and developmental basis of cichlid trophic diversity. *Heredity* 97, 211-21.

Anker, G. C. (1974). Morphology and kinetics of the head of the stickleback, Gasterosteus aculeatus. *Trans. Zool. Soc. London* 32, 311-416.

Arnegard, M. E., McGee, M. D., Matthews, B., Marchinko, K. B., Conte, G. L., Kabir, S., Bedford, N., Bergek, S., Chan, Y. F., Jones, F. C., et al. (2014). Genetics of ecological divergence during speciation. *Nature* 511, 307-311.

Bell, M. A. (1984). Evolutionary Phenetics and Genetics. In *Evolutionary Genetics of Fishes* (ed. Turner, B.), pp. 431-528. New York: Plenum Press.

Bell, M. and Foster, S. (1994). *The Evolutionary Biology of the Threespine Stickleback*. (ed. Bell, M. A.) and Foster, S. A.) New York: Oxford University Press.

Berner, D., Moser, D., Roesti, M., Buescher, H. and Salzburger, W. (2014). Genetic architecture of skeletal evolution in european lake and stream stickleback. *Evolution* 68, 1792-1805.

Caldecutt, W. J., Bell, M. A. and Buckland-Nicks, J. A. (2001). Sexual Dimorphism and Geographic Variation in Dentition of Threespine Stickleback, *Gasterosteus aculeatus*. *Copeia* 4, 936-944.

Cleves, P. A., Ellis, N. A., Jimenez, M. T., Nunez, S. M., Schluter, D., Kingsley, D. M. and Miller, C. T. (2014). Evolved tooth gain in sticklebacks is associated with a cis-regulatory allele of Bmp6. *Proc. Natl. Acad. Sci.* 111, 13912-17.

Cooper, W. J. and Westneat, M. W. (2009). Form and function of damselfish skulls: rapid and repeated evolution into a limited number of trophic niches. *BMC Evol. Biol.* 9.

Ellis, N. A., Glazer, A. M., Donde, N. N., Cleves, P. A., Agoglia, R. M. and Miller, C. T. (2015). Distinct developmental and genetic mechanisms underlie convergently evolved tooth gain in sticklebacks. *Development* 2442-2451.

Erickson, P. A., Glazer, A. M., Cleves, P. A., Smith, A. S. and Miller, C. T. (2014). Two developmentally temporal quantitative trait loci underlie convergent evolution of increased branchial bone length in sticklebacks. *Proc. R. Soc. B* 281, 20140822.

Erickson, P. A., Cleves, P. A., Ellis, N. A., Schwalbach, K. T., Hart, J. C. and Miller, C. T. (2015). A 190 base pair, TGF- responsive tooth and fin enhancer is required for stickleback Bmp6 expression. *Dev. Biol.* 401, 310-323.

Fraser, G. J., Hulsey, C. D., Bloomquist, R. F., Uyesugi, K., Manley, N. R. and Streelman, J. T. (2009). An ancient gene network is co-opted for teeth on old and new jaws. *PLoS Biol.* 7, e1000031.

Glazer, A. M., Cleves, P. A., Erickson, P. A., Lam, A. Y. and Miller, C. T. (2014). Parallel developmental genetic features underlie stickleback gill raker evolution. *Evodevo* 5, 19.

Glazer, A. M., Killingbeck, E. E., Mitros, T., Rokhsar, D. S. and Miller, C. T. (2015). Genome assembly improvement and mapping convergently evolved skeletal traits in sticklebacks with Genotyping-by-Sequencing. *G3* 5, 1463-1472.

Gross, H. P., Anderson, J. M. and Gross, HP; Anderson, J. (1984). Geographic variation in the gillrakers and diet of european threespine sticklebacks, G*asterosteus aculeatus*. *Copeia* 1984, 87-97.

Hagen, D. and Gilbertson, L. (1972). Geographic Variation and Environmental Selection in *Gasterosteus aculeatus L* . in the Pacific Northwest , *America. Evolution* 26, 32-51.

Hulsey, C. D., Fraser, G. J. and Streelman, J. T. (2005). Evolution and development of complex biomechanical systems: 300 million years of fish jaws. *Zebrafish* 2, 243-57.

Huysseune, A. (1995). Phenotypic plasticity in the lower pharyngeal jaw dentition of *Astatoreochromis alluaudi* (Teleostei: Cichlidae). *Arch. Oral Biol.* 40, 1005-1014.

Jamniczky, H. a., Barry, T. N. and Rogers, S. M. (2015). Eco-evo-devo in the Study of Adaptive Divergence: Examples from Threespine Stickleback (Gasterosteus aculeatus). *Integr. Comp. Biol.* 55, 166-178.

Kahilainen, K. K., Siwertsson, A., Gjelland, K., Knudsen, R., Bhn, T. and Amundsen, P. A. (2011). The role of gill raker number variability in adaptive radiation of coregonid fish. *Evol. Ecol.* 25, 573-588.

Kimmel, C. B., Ullmann, B., Walker, C., Wilson, C., Currey, M., Phillips, P. C., Bell, M. a, Postlethwait, J. H. and Cresko, W. a (2005). Evolution and development of facial bone morphology in threespine sticklebacks. *Proc. Natl. Acad. Sci. U. S. A.* 102, 5791-5796.

Lauder, G. (1983). Functional design and evolution of the pharyngeal jaw apparatus in euteleostean fishes. *Zool. J. Linn. Soc.* 77, 1-38.

Leary, S., Underwood, W., Lilly, E., Anthony, R., Cartner, S., Corey, D., Clinic, A. V., Walla, W., Grandin, T., Collins, F., et al. (2013). AVMA Guidelines for the Euthanasia of Animals. 2013 Edition. Schaumburg, IL: American Veterinary Medical Association.

Liem, K. and Greenwood, P. (1981). A functional approach to the phylogeny of the pharyngognath teleosts. *Am. Zool.* 21, 83-101.

Magnuson, J. and Heitz, J. (1971). Gill raker apparatus and food selectivity among mackerels, tunas, and dolphins. *Fish. Bull.* 69, 361-370.

Martin, C. H. and Wainwright, P. C. (2011). Trophic novelty is linked to exceptional rates of morphological diversification in two adaptive radiations of cyprinodon pupfish. *Evolution* 65, 2197-2212.

Mcgee, M. D. and Wainwright, P. C. (2013). Convergent Evolution As a Generator of Phenotypic Diversity in Threespine Stickleback. *Evolution* 67, 1204-1208.

McGee, M. D., Schluter, D. and Wainwright, P. C. (2013). Functional basis of ecological divergence in sympatric stickleback. *BMC Evol. Biol.* 13, 277.

McGuigan, K., Nishimura, N., Currey, M., Hurwit, D. and Cresko, W. a. (2010). Quantitative genetic variation in static allometry in the threespine stickleback. *Integr. Comp. Biol.* 50, 1067-1080.

McPhail, J. D. (1984). Ecology and evolution of sympatric sticklebacks (Gasterosteus): morphological and genetic evidence for a species pair in Enos Lake, British Columbia. *Can. J. Zool.* 62, 1402-1408.

Meyer, A. (1990). Morphometrics and allometry in the trophically polymorphic cichlid fish, Cichlusomu citrinelfum: Alternative adaptations and ontogenetic changes in shape. *J. Zool., Lond.* 221, 237-260.

Miller, C. T., Beleza, S., Pollen, A. A., Schluter, D., Kittles, R. A., Shriver, M. D. and Kingsley, D. M. (2007). cis-Regulatory Changes in Kit Ligand Expression and Parallel Evolution of Pigmentation in Sticklebacks and Humans. *Cell* 131, 1179-89.

Miller, C. T., Glazer, A. M., Summers, B. R., Blackman, B. K., Norman, A. R., Shapiro, M. D., Cole, B. L., Peichel, C. L., Schluter, D. and Kingsley, D. M. (2014). Modular skeletal evolution in sticklebacks is controlled by additive and clustered quantitative trait loci. *Genetics* 197, 405-20.

Muschick, M., Indermaur, A. and Salzburger, W. (2012). Convergent Evolution within an Adaptive Radiation of Cichlid Fishes. *Curr. Biol.* 22, 2362-2368.

Pasco-Viel, E., Charles, C., Chevret, P., Semon, M., Tafforeau, P., Viriot, L. and Laudet, V. (2010). Evolutionary trends of the pharyngeal dentition in *Cypriniformes* (Actinopterygii: Ostariophysi). *PLoS One* 5, e11293.

Robinson, B. (2000). Trade Offs in Habitat-Specific Foraging Efficiency and the Nascent Adaptive Divergence of Sticklebacks in Lakes. *Behaviour* 137, 865-888.

Schluter, D. and McPhail, J. D. (1992). Ecological character displacement and speciation in sticklebacks. *Am. Nat.* 140, 85-108.

Sibbing, F. (1991). Food capture and oral processing. In *Cyprinid Fishes* (ed. Winfield, I. J.) and Nelson, J. S.), pp. 377-412. Chapman and Hall.

Stock, D. (2007). Zebrafish dentition in comparative context. *J. Exp. Zool. B. Mol. Dev. Evol.* 308B, 523-49.

Taylor, W. R. and Van Dyke, G. C. (1985). Revised Procedures For Staining and Clearing Small Fishes and Other Vertebrates For Bone and Cartilage Study. *Cybium* 9, 107-119.

Tucker, A. S. and Fraser, G. J. (2014). Evolution and developmental diversity of tooth regeneration. *Semin. Cell Dev. Biol.* 25-26, 71-80.

Wainwright, P. (2006). Functional morphology of the pharyngeal jaw apparatus. In *Fish Physiology: Fish Biomechanics* (ed. Shadwick, R. E.) and Lauder, G. V.), pp. 77-102. Academic Press.

Wainwright, P. C., Smith, W. L., Price, S. a., Tang, K. L., Sparks, J. S., Ferry, L. a., Kuhn, K. L., Eytan, R. I. and Near, T. J. (2012). The Evolution of Pharyngognathy: A Phylogenetic and Functional Appraisal of the Pharyngeal Jaw Key Innovation in Labroid Fishes and beyond. *Syst. Biol.* 61, 1001-1027.